AD-754 892

Microwave Landing System Signal Requirements for Conventional Aircraft

Transportation Systems Center

JULY 1972

REPORT NO: FAA-RD-72-86

MICROWAVE LANDING SYSTEM SIGNAL REQUIREMENTS FOR CONVENTIONAL AIRCRAFT

Maurice H. Lanman III
Transportation Systems Center
Kendall Square
Cambridge, MA. 02142

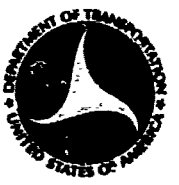

JULY 1972
FINAL REPORT

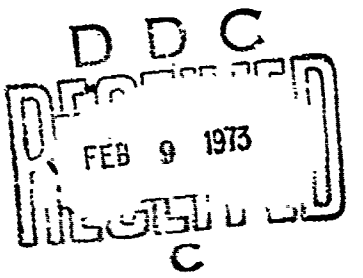

Prepared for
DEPARTMENT OF TRANSPORTATION
Federal Aviation Administration
Systems Research & Development Service
Washington, D.C. 20591

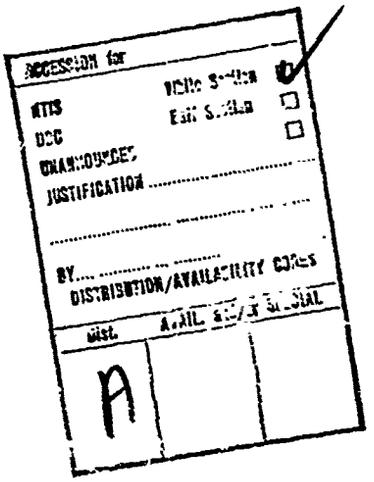

1. Report No.	2. Government Accession No.	3. Recipient's Catalog No.
FAA-RD-72-86		

4. Title and Subtitle	5. Report Date
MICROWAVE LANDING SYSTEM SIGNAL REQUIREMENTS FOR CONVENTIONAL AIRCRAFT	July 1972
	6. Performing Organization Code
7. Author(s) Maurice H. Lanman, III	8. Performing Organization Report No. DOT-TSC-FAA-72-30
9. Performing Organization Name and Address Department of Transportation Transportation Systems Center Kendall Square Cambridge, MA 02142	10. Work Unit No FA 209 11. Contract or Grant No.
12. Sponsoring Agency Name and Address Department of Transportation Federal Aviation Administration Systems Research & Development Service Washington, D.C. 20591	13. Type of Report and Period Covered Final Report FY 1971 - 1972 14. Sponsoring Agency Code
15. Supplementary Notes	

16. Abstract The results of analysis directed towards determining Microwave Landing System (MLS) signal requirements for conventional aircraft are discussed. The phases of flight considered include straight-in final approach, flareout, and rollout. A limited number of detailed problems in performance analysis are studied. Data from computer simulation, covariance propagation and system optimization, with a careful selection of variables provides a means for generalizing from the results of specific experiments to more comprehensive functional, data rate, beam noise, and control system requirements for automatic landing in turbulence.

Conclusions point toward the requirements for a re-evaluation of the MLS as sole primary landing aid; the problem arises during flareout in turbulence, when elevation information is inadequate to maintain precise sink rate control. Minimum suitable data rate and maximum allowable noise for final approach are also recommended.

17. Key Words	18. Distribution Statement
Mircowave Landing System MLS All weather landing Automatic landing	DOCUMENT IS AVAILABLE TO THE PUBLIC THROUGH THE NATIONAL TECHNICAL INFORMATION SERVICE, SPRINGFIELD, VIRGINIA 22151.

19. Security Classif. (of this report)	20. Security Classif. (of this page)	21. No. of Pages	22. Price
Unclassified	Unclassified	142	

PREFACE

The analytical methods, computer programs, and resulting data used for this study were generated by Messrs. Mukund Desai and Paul Madden of the M.I.T. Charles Stark Draper Laboratories, under Contract DOT-TSC-91.

The filtering and control system improvements described herein were also developed by these gentlemen. Many of the concepts leading to the data contained in this report represent advances in the state-of-the-art in control system design and will be formally reported on at appropriate technical conferences during the following year.

Appendices A, B, and D of this report were written by Mr. Desai and Mr. Madden.

TABLE OF CONTENTS

TABLE OF CONTENTS (CONT.)

TABLE OF CONTENTS (CONT.)

LIST OF ILLUSTRATIONS

LIST OF ILLUSTRATIONS (CONT.)

LIST OF ILLUSTRATIONS (CONT.)

LIST OF TABLES

1.0 INTRODUCTION

The National Plan for Development of the Microwave Landing System (MLS), reference 1, is well on its way toward providing a prototype system by 1977. One of the Transportation Systems Center's (TSC) assignments as part of the plan involves system requirements analysis - verifying and/or updating by analysis and simulation the preliminary system requirements as set forth by the Radio Technical Commission for Aeronautics (RTCA), Special Committee 117 (SC-117) [reference 2].

The primary operational goals of the MLS may be stated as follows:

a. Provide a signal in space of sufficient quality to allow up to Category III(c) landing.

b. Provide a signal in space of sufficient quality and over sufficient volume for terminal area navigation to aid in capacity enhancement and noise abatement.

Strong emphasis must be given in consideration of options to such concepts as:

a. Universal usage: civilian, military, VTOL, STOL.

b. Modularity: minimum system expandable to greater capability.

c. Versatility: all airborne users may use any ground facility, the combined capability being at least that of the lesser component.

d. Reliability, redundancy, freedom from unpredictable errors, etc.

From the flight performance point of view, however, it is necessary to answer four basic questions in assuring satisfaction of the primary goals:

(1) What functions need be available?

(2) Over which volume?

(3) At what data rate?

(4) With what accuracy?

This study addresses the data rate and accuracy questions, and is a continuation and extension of the work reported on in reference 3. The functional array is assumed to be that suggested by RTCA; the volume of coverage is assumed sufficient for the particular problems studied. As will be shown in Section 2.0, the matrix of possible conditions under which these questions must be answered is exceedingly large. In limiting these to a workable number, the study reports on a few detailed performance studies involving various phases of flight and aerodynamic conditions for a conventional jet transport, the Convair 880 (C-880). It is hoped that the understanding gained from the thorough examination of a few particular problems may allow the eventual generalization to system level specification.

The remainder of this report is organized as follows: Section 2.0 discusses approach and methods; Sections 3.0 and 4.0 describe the analytical models in use; Sections 5.0 and 6.0 present results and conclusions to date on final approach and flareout, respectively. Section 7.0 discusses related work on automatic rollout and planned further investigations. Section 8.0 provides a summary of the conclusions as related to MLS requirements.

2.0 PROBLEM STATEMENT AND APPROACH

In attempting to define or verify, by analytical methods, characteristics of the MLS which are necessary to the performance of all its anticipated tasks, it becomes apparent that a through treatment is not possible. There are just too many variables to consider if one expects to anticipate and conduct detailed analyses of every possible combination of MLS configuration, aircraft, terminal area situation, and weather. Table 2-1 lists, for example, a good number of the various MLS parameters and operational environments; a thorough investigation would require performance evaluation under every combination of the listed elements. If one considers only these and subsets of these, the number of specific problems from a practical viewpoint approaches infinity.

TABLE 2-1. PARAMETERS OF THE LANDING SYSTEM ANALYSIS PROBLEM

PARAMETER	OPTIONS/ENVIRONMENTS
MLS Function	Azimuth, Elevation 1, Elevation 2, DME, Back Course Azimuth
Functional Characteristics	Coverage, Distance, Scan Rate Bias, Noise, Scaling, Geometry
Flight Phase	Curved Approach, Acquisition, Final Approach, Flare, Rollout, Missed Approach
Aircraft Speed Class	1 through 5
Aircraft Equipment	Sensor Complement, Autopilot Configuration, Area Navigation, Minimum Systems, etc.
Visibility	Clear, Category I, Category II, Category III
Wind	None, Steady, Shear, Gusts
Performance Criteria	Safety Factors, Pilot Factors
Procedures	Metering, Sequencing, Spacing, Separations, Segmented GS, Variable Acquisition Point, ATC Interface

Two complementary approaches can then be taken. The first, that exercised by the RTCA Special Committee 117, involves a common sense elimination of many of the parameters, based on general operational requirements, past experience, estimates of technical feasibility and gross performance expectations. The resultant proposed configurations and specifications constitute a "strawman" or working baseline against which the second approach can be exercised.

That approach involves working in detail a performance evaluation under a specific set of assumptions, and by varying parameters in a controlled manner, determining performance sensitivity to these parameters. Hopefully, it is then possible to identify critical areas and eliminate those which are not important. Further, with a thorough understanding of the problem's assumptions and limitations, it may then be possible to bridge the gap between this particular set of conditions and overall system requirements. At the very least, however, the results of studies of this nature will tend either to reinforce or to suggest modifications to the specific recommendations of SC-117.

2.1 FLIGHT PERFORMANCE ANALYTICAL MODELS

The primary function of the MLS as currently conceived is to serve as a high integrity landing aid, the most sophisticated version of which provides sufficient information to allow a variety of aircraft to make precision curved approaches, final approaches, and in some cases touchdown and rollout in any weather or visibility condition.

To determine how well MLS accomplishes this function requires a modeling approach outlined generally by the block diagram of Figure 2-1. Most of Figure 2-1 is self-explanatory, however, a few points deserve discussion.

The purpose of the outer (MLS) control loop is to provide path following capability in the presence of deterministic and random aerodynamic disturbances (wind). The desired path is

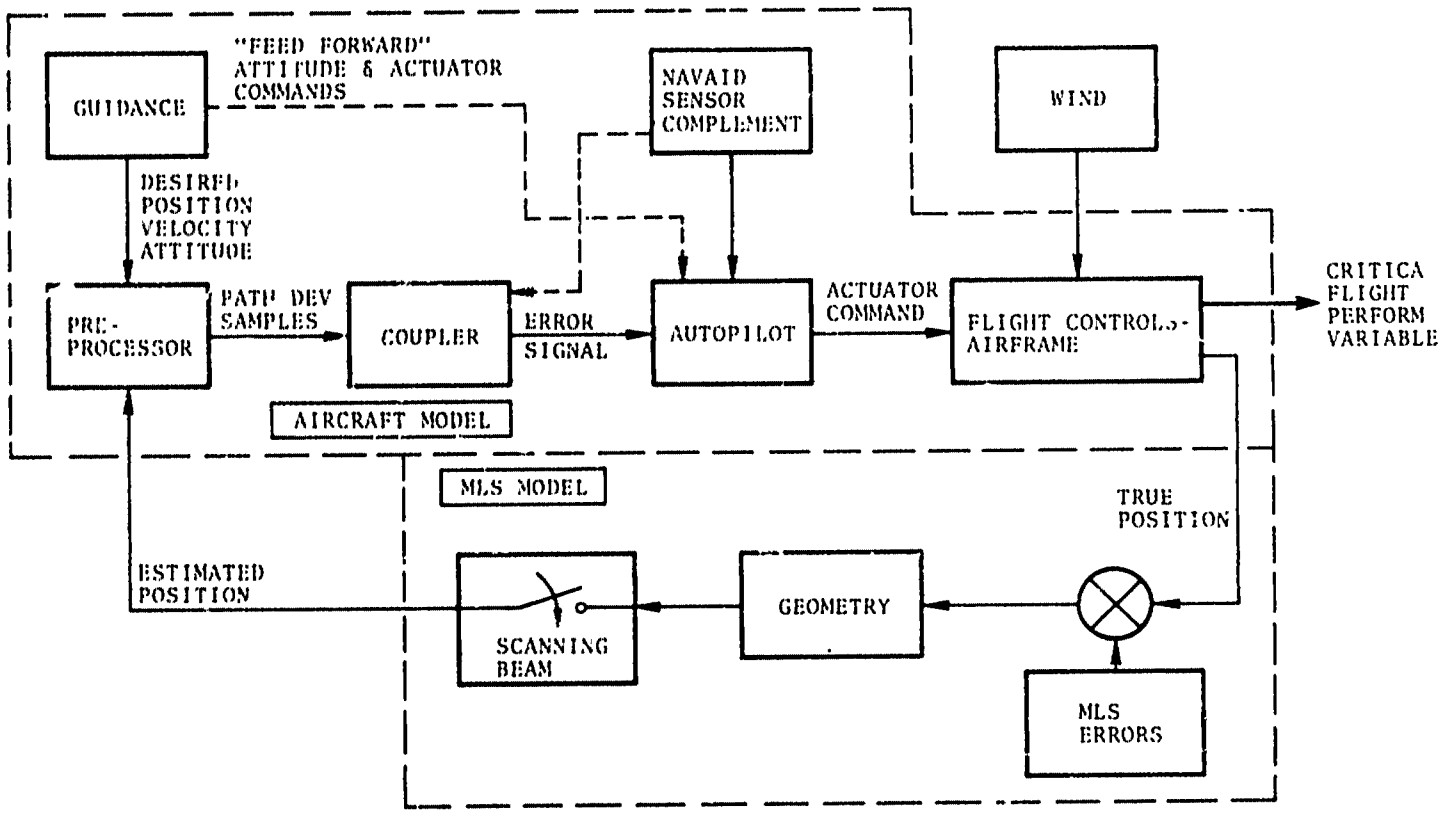

Figure 2-1. Flight Performance Analysis The General Model

generated according to some guidance law (e.g., in final approach that law simply requires maintenance of fixed azimuth and elevation angles).

The function of the coupler is the conditioning of the raw MLS angular position samples, which may be corrupted by noise, to provide a continuous linear position (and possibly higher order terms such as rate) error signal to the autopilot. It may be as simple as a zero order hold and first order filter or as a complex as a time varying Kalman filter accepting inputs from other navigation aids as well as MLS. In the most simple terms, its job is to separate and remove MLS noise from actual vehicle motion. In qualitative terms, the performance evaluation criteria require maximum path keeping ability with minimum spurious, noise-induced control actuator activity and resulting vehicle attitude activity. In the presence of a noisy signal, however, there is a definite tradeoff (accomplished by varying coupler parameters) between these two criteria.

The subsystem consisting of airborne sensors, autopilot and flight controls is the heart of the aircraft landing system, and its sophistication and complexity, or lack of it, undoubtedly has the greatest bearing on ultimate performance limitations.

The matrix of options for all of these blocks to be considered in this study are shown in Table 2-2. Not all are considered in equal detail, and in some cases work is still in progress, allowing only partial reporting of results.

The detailed characteristics of the models in use are discussed in Sections 3.0 and 4.0.

2.2 METHODS OF ANALYSIS

Three computer aided methods of analysis have been developed and used extensively in this study. Two of these are discussed in detail in a previous report (reference 3) and will be only summarized here.

TABLE 2-2: PARAMETERS OF THE TSC DATA RATE/BEAM NOISE STUDY

Airframe	Convair 880 Jet Transport
Flt. Controls	(1) Standard (2) Direct Lift Control*(DLC)
Autopilot	Modified LSI "Autoland"
Coupler	Digital Filter and Zero Order Hold
Sensors	(1) Directional and Rate Gyros, Air Data, etc. (2) Normal Accelerometer
Preprocessor	Converts MLS and Guidance into deviation from desired track at MLS data rate
Wind	See Section 4.1
MLS	See Section 3.0
Guidance	(1) Final Approach (2) Flareout (3) Rollout (4) Curved Approach*

*Work Incomplete

2.2.1 Simulation

A digital simulation which mechanizes the equation

$$\dot{x} = f(x,u,t) \qquad (2\text{-}1)$$

comprises the primary analytic tool of this study. In Equation (2-1), $\dot{x}$ represents the rate of change of the aircraft state vector; f represents the system dynamics and may be a function of the state vector, x, the disturbance inputs, u, and time, t. Linearity is not required, and limits or cross multiples may also be mechanized.

Both f and x are expandable to include any order effects (the eventual limitation is the computer size) which appear in the aircraft, control system, or measuring system models.

The simulation provides data on aircraft response to deterministic inputs, examples of response to random inputs, checks on dynamic characteristics of various systems through transient responses, and checks on simplifications made using the covariance propagation technique and the parameter optimization technique.

2.2.2 Covariance Propagation

If Equation 2-1 is expressed in a linear fashion according to Equation 2-2

$$\dot{x} = Fx + Gu \tag{2-2}$$

then it is possible under certain assumptions to write equations for the mean and variance of x as a function of time.

$$\dot{\bar{x}}(t) = F(t)\bar{x}(t) \tag{2-3}$$

$$\dot{X}(t) = F(t)X(t) + X(t)F^{T}(t) + G(t)Q(t)G^{T}(t)$$

$\bar{x}(t)$ = expected value of x at time t
$X(t)$ = covariance matrix at time t
$F(t)$ = linear system matrix
$Q(t)$ = white noise inputs
$G(t)$ = noise shaping filters and dynamics

The reader is referred to reference 3 (Section 2.0 and Appendix A) for more detailed discussion of the mechanization. The technique itself is discussed in references 4 and 5.

The obvious advantage of this method is the ability to conduct analysis using random inputs and generate statistically valid results with a single computer run. Its major disadvantage is the

linearity requirement, which for the landing problem severely degrades its usefulness below 50 feet or so due to extreme nonlinearities in ground effect.

2.2.3 Filter Optimization

Most of the results in this report are based on the use of a coupler in the form of a discrete (digital) filter for MLS information which basically provides the best combination of noise attenuation with "wind proofing". In order to select the best filter parameters for any particular set of conditions, it was necessary to perform a parameter optimization: minimizing certain elements of the covariance matrix, with particular noise and wind disturbing functions, by choosing appropriate filter parameters. Appendices A and B deal in more detail with the method used to do this. More complete treatments are available in references 4 and 5.

Some characteristics of the optimization result which are pertinent to the problem at hand include:

a. The optimization is based on minimizing path deviation and control activity; different results are obtained depending on the relative weighting each of these receive in the penalty function.

b. The optimization assumes stochastic (statistically time invariant) conditions and is highly dependent on relative values of random wind and beam noise. Therefore, each set of results may be applied properly only to those points in space along the approach trajectory which are subject to the wind/noise values assumed.

c. The system equations must be linearized as with the covariance propagation technique; further, due to the complexity of the problem, every attempt has been made to reduce the size of the state vector. However, filter parameters are transferred to the full simulation and checked to assure satisfactory performance, both transient and steady state, in the time domain.

d. The programs used for optimization also generate the variances of all the state variables for each solution. It is therefore possible to assure that these, although not explicitly included in the penalty function, are within acceptable bounds.

2.2.3.1 Typical Procedure and Format of Results - A single optimization is carried out requiring as inputs:

a. The relative weighting of root mean square (rms) path deviation versus rms control activity for the penalty function;

b. The ratio of wind gust intensity to beam noise intensity;

c. A particular data rate.

The output is a set of optimized filter parameters which provide minimum rms path deviation and control activity under this set of conditions, the rms values of these variables and the remainder of the state variables, and the wind sensitivity of the state variables to wind and to noise.

The filter parameters are inserted in the simulation and demonstration runs are made with typical random wind and MLS noise profiles. A transient response run is also made to assure satisfactory dynamic characteristics (natural frequency and damping of the control loop.

The procedure is repeated for a number of weighting factors and data rates which can then be plotted parametrically as in Figure 2-2. This figure shows minimum path deviation versus minimum control activity for a range of weighting factors with data rate as the parameter. It is also possible to plot similar curves for other state variables against weighting factor or control activity. (It should be noted, however, that the system has not been optimized with respect to these variables).

All of this data would represent only one particular ratio of wind intensity to linear noise. Since linear noise is generally variable during a particular phase of flight (angular noise assumed

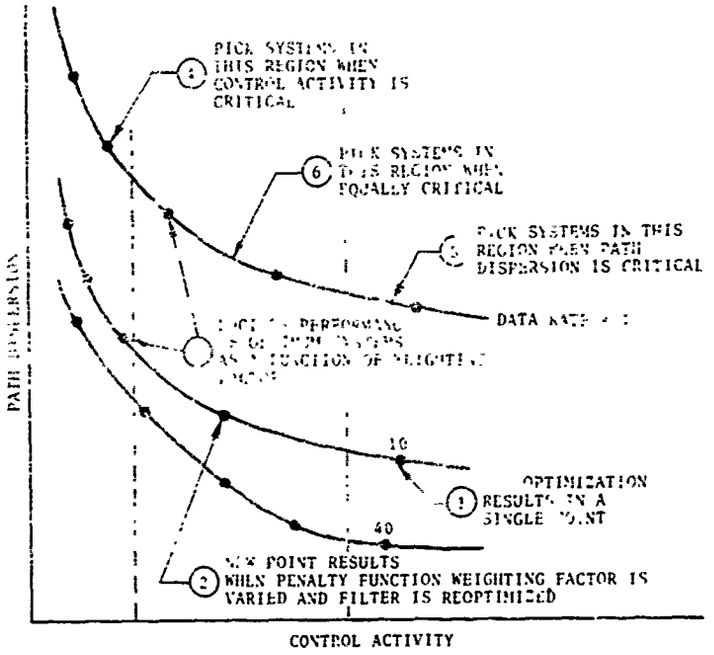

Figure 2-2. Example of Results of Filter Optimization Problem

constant), other sets of runs similar to this are required. Also, if different wind conditions are assumed, they too require another full set of runs.

Fortunately, interpolation is usually possible and full data packages for every condition of interest have not been required.

2.2.3.2 Interpretation of Results - Performance Criteria - The filter optimization results are indicative of the best possible performance that can be expected of a given aircraft and autopilot using MLS information. It provides a reliable baseline for performance analysis from two points of view:

a. If the best is not good enough to meet performance criteria, it can then be concluded that MLS parameters (data rate, noise) must be adjusted accordingly.

b. If a non-optimum filter is used, one can never be sure that poor performance is not a result of poor filter design, and the conclusions on MLS parameters cannot be as strongly drawn.

It should be clearly stated that the optimization applies only to the coupler and not to the autopilot and flight controls; autopilot design and characteristics have not, in general, been varied and nor is it contended that this is the best or optimum autopilot. It is possible that inner loop improvements could lead to better performance.

2.3 PERFORMANCE CRITERIA

Although reference 3 attempts to define a set of absolute limits on touchdown performance, it has proven impossible to generate data which may be validly statistically compared with these limits. There has also been much discussion concerning the pilot acceptability factors which appear in reference 3, as to whether they are too high or too low. For phases of flight other than touchdown and decision height, no suitable performance criteria of an absolute nature have been found. Even though general guidelines do exist, and important characteristics are recognizable, it now seems apparent that there is no clear cut absolute point at which one may say "the data rate must be no lower than N samples/sec and the noise no higher than X degrees", even for one particular aircraft in one phase of flight.

The best that can be done is the presentation of sufficient data so that performance sensitivities to data rate, noise, and other important MLS characteristics can be fully understood and critical phases of flight and performance parameters identified. Recommendations can then be made as to what exactly should be specified for MLS, whether RTCA estimates should be revised upward, revised downwards, expanded, or eliminated. However, no attempt is made to assess the costs involved and to perform the required cost-benefit analysis. Perhaps the results presented here will be useful in any such subsequent study.

3.0 MICROWAVE LANDING SYSTEM MODEL

The MLS, as conceived by the RTCA (reference 2), generates five basic functions: DME, azimuth, glide slope elevation, flare elevation, and back course azimuth. (This report will not consider operational or functional requirements for the back course). Azimuth and elevation information is in angular form referenced to the runway centerline; the angular format may be either conical or planar in nature.

In either case, x, y and z coordinates can be computed with the aid of DME and a knowledge of the geometry of the installation. Planar beams are generally assumed for MLS in this report, although it seems unlikely that the choice of conical or planar will have any ultimate effect on flight performance or airborne computational load. The particular geometry and relative location of the antennas also should not have a major impact on performance except during flare out and touchdown (assuming adequate coverage and signal visibility for all phases of flight; special siting problems and lobing due to ground reflection are not considered). The geometrical constraints associated with flare will be dealt with in Section 6.0.

From the user aircraft point of view, the MLS can be considered an airborne black box which periodically presents data on the aircraft's position in angular or linear terms with respect to some fixed, known ground reference. The black box has a number of outputs (see Figure 3-1) corresponding to the various MLS functions: azimuth, elevation #1, elevation #2, range, etc. Each function has its own data rate and is corrupted by both random and deterministic measurement errors. The coupler-processor takes the outputs for the MLS black box and computes, smoothes, filters, etc. to produce derived data such as glideslope deviation, altitude rate, etc. The processor can be as simple as a zero order hold on each function or as complex as a Kalman filter doing optimal mixing of MLS data with that of other airborne sensors.

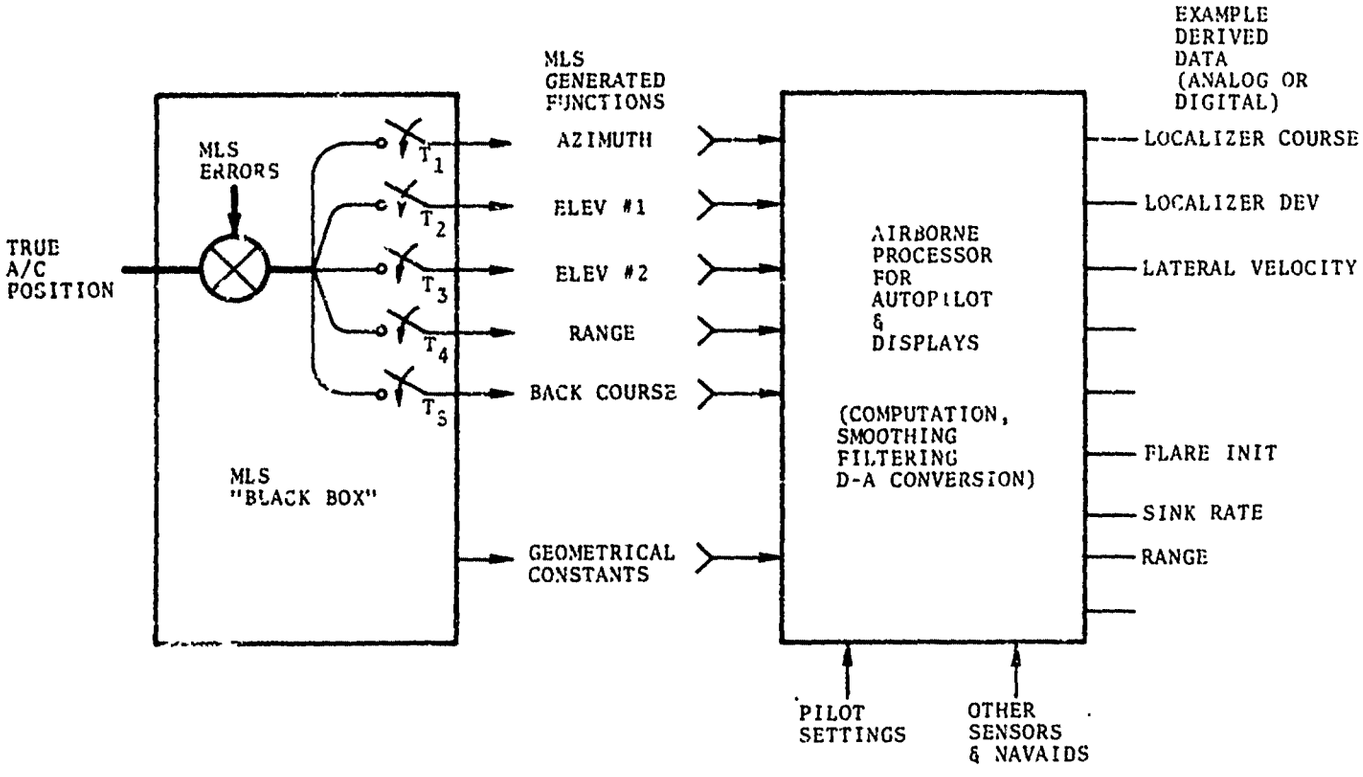

Figure 3-1. The MLS from an Airborne Point of View

Although some of the processing may in real life be done in the MLS receiver, it is convenient to consider this portion of the system as related to the aircraft guidance and autopilot functions; discussion is therefore reserved for later sections.

It remains then to model the MLS function generation and describe in an analytic sense the MLS error sources and errors.

3.1 MLS ERRORS

The most obvious first step in error modeling is to separate those errors having deterministic effects from those causing random activity. In many cases this is done for specification purposes by labeling the former "bias" and the latter "noise". Unless, however, a more precise description based on spectral composition, spatial or temporal characteristics, and statistical likelihood, especially with respect to the aircraft control system, is developed, the terms "bias" and "noise" are meaningless to the problem of flight performance analysis. For instance, a static probe may detect some level of bias at a certain point in space, but if this bias is not constant over the length of a typical flight path, it will appear as a time varying noise to the moving aircraft.

In this report the term "bias" will connote an error which is constant over the entire time of the flight phase considered. Its effects on flight performance under this definition are easy to determine, (again, except for the flare maneuver) namely a pure displacement of flight path.

Errors which exhibit a time varying property can be lumped under the generic term "noise". Even though they may in fact be deterministic (e.g., a well defined in beam reflection) in space, it will be assumed that the aircraft has neither knowledge nor compensation for it.

For statistical analysis of flight performance under random disturbing functions, it is necessary to model the disturbances as random processes with certain probability density functions. It

almost goes without saying that the better the noise model statistically, the more reliable the resultant performance statistics will be. At present, unfortunately, insufficient data is available to do much more than qualitatively describe possible error sources.

Some of these are described below for the angular function:

1. Receiver and propagation noise: can be considered gaussian distributed and uncorrelated from sample to sample.
2. Quantization, granularity, or resolution errors: of itself can be considered uniform and uncorrelated; however, if the cumulative magnitude of other noise sources is greater than the quantization level, it merely modifies these sources' probability density functions; its effect on performance is minimal. It is also the most easily adjustable of all error sources - requiring only clock and timing modifications.
3. Spatially distributed errors due to coding scale factor inaccuracy: will look like low frequency noise only if flight path is crossing lines of constant angle; on a constant angle path (e.g., glide slope) it will appear as a bias. Probability distribution correlation characteristics and magnitude dependent upon flight path and air speed as well as basic error mechanism.
4. Spatially distributed errors due to reflections and interference causing in-beam multipath: errors generated at output depend on threshold detection and decoding mechanisms; no statistical estimates are currently available.
5. Delays due to actual receiver and decoder processing time.
6. Effective noise due to missed samples.
7. Errors due to receiver inability to reject out of beam reflections and multipath; may cause receiver to track wrong signal; likely to be a problem only with lower cost airborne configurations.

Of these, items (2), (5), (6) and (7) are considered to be second order or improbable effects and have not been precisely modeled for his study (see Appendix B). Items (3) and (4), although probable major sources of system errors have not been modeled due to the lack of data, of detailed investigation on multipath environments, effects, and rejection techniques.

The net result is that to date the TSC MLS error model for angular functions has included only gaussian white noise. Since TSC investigations have been limited to CTOL operations at relatively low glide slope angles, little effort has been expended on noise models for range information from the DME (as shown in the following section, when flying constant azimuth low glide slope approach, errors in computed path deviation tend to be insensitive to range errors and noise).

3.2 MODEL FORMULATION FOR FLIGHT PERFORMANCE EVALUATION

In a physical sense, aircraft are flown in x-y-z space rather than R-θ-Φ (range, azimuth, elevation) space, that is, an aircraft control system understands a command in terms of change in altitude (z) but not a command in terms of elevation angle (Φ). It is therefore necessary to perform on board computations to convert MLS R-θ-Φ information into x-y-z for use by the control system.

On a constant localizer-glide slope, this represents nothing more than gain scheduling with range or altitude:

$$Y = R\Delta\theta \quad ; \quad Z = R\Delta\Phi \tag{3-1}$$

The control system of the aircraft in its outer loop acts to maintain a path in space and required deviation from that desired path as an input. In later sections path deviation in linear terms will generally be considered as the input to the aircraft autopilot and coupler. We, therefore, consider as part of the MLS a pre-processor which converts range, azimuth, elevation information including desired, actual and error components into path deviation signals suitable for an autopilot coupler. Figures 3-2 and 3-3 illustrate basically how this is done for

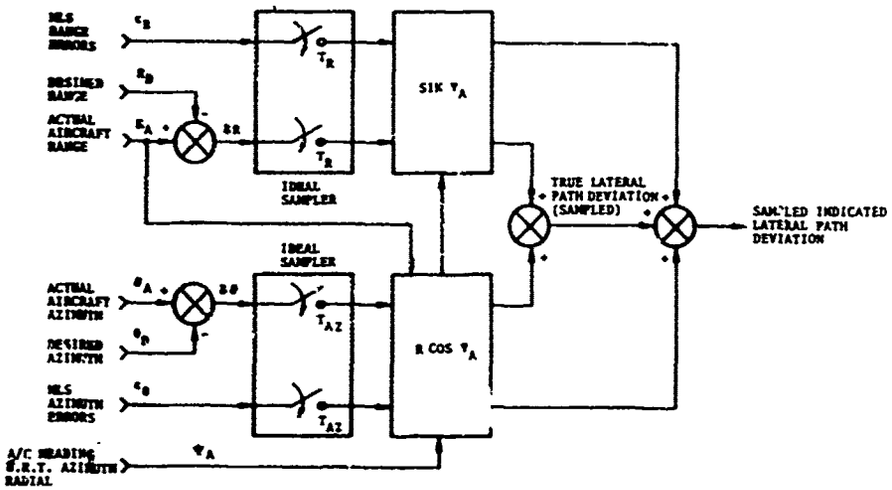

Figure 3-2. Lateral Path Deviation as Derived from MLS

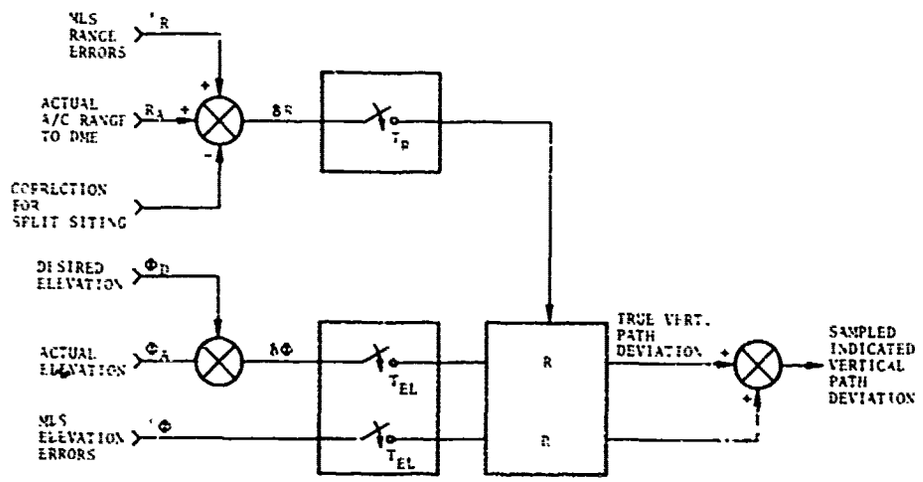

Figure 3-3. Vertical Path Deviation as Derived from MLS

the lateral and vertical channels (longitudinal path deviation, if used, is computed in a manner similar to lateral deviation except for interchange of $\sin\Psi_A$ and $\cos\Psi_A$ terms). It should be noted that these are conceptual illustrations and do not represent in detail the actual model mechanization for simulation (for instance, they do not include relative geometry of the antennas). The outputs of the preprocessor then are two (or three) sampled signals representing deviation from some desired flight path in aircraft coordinates. The job of conditioning these signals for use in the aircraft control system will be considered as a function of the MLS coupler and will be discussed in detail in later sections.

3.3 ERROR MAGNITUDES

The purpose of this study is to develop performance sensitivities to MLS errors and data rate. Although specific noise and bias values, which are related to RTCA recommended specifications, have been used to generate results reported on, they have not been considered firm, fixed numbers and are treated more as parameters of the study. In order to avoid confusion which may result if specific numbers are included as part of the TSC error model, magnitudes or rms values will not be discussed except in sections dealing with results.

3.4 SUMMARY

It has been assumed that the MLS is a "black box" which periodically emits data in azimuth (θ), elevation (Φ) and range (R). The azimuth and elevation angular data are corrupted by gaussian white noise which is also angular in nature. No error model has been developed for range data. An airborne pre-processor converts the R-θ-Φ information into path deviation samples in aircraft coordinates for use in path control. No fixed values for the various errors are assumed since these are considered parameters of the study.

4.0 WIND, AIRCRAFT, AND OTHER MODELS

In addition to discussing the MLS and pre-processor of the previous section, it is necessary to model the remainder of the blocks appearing in Figure 2-1. This has been done for some of these in adequate detail by a previous study (Reference 3) but all will be briefly reviewed in this section.

4.1 WIND MODELS

4.1.1 The Importance of Wind

Wind is defined for our purposes as the movement of the atmosphere with respect to the earth. An airplane flies in the atmosphere but attempts to maintain a path with respect to the earth. The effects of uncompensated wind then are the primary disturbing force affecting an aircraft's ability to fly a path in space oriented with respect to earth, such as a final approach and landing.

An aircraft control system, autopilot, and Navaids have two basic functions: (1) provide smooth, satisfactory transition from one phase of flight to another, and (2) maintain desired path and altitude in the presence of atmospheric disturbances.

The second becomes particularly critical during final approach and landing, and under high wind conditions will require adequate sensing and control devices for the aircraft involved in order to successfully accomplish the objective of safe, acceptable automatic landing.

If there were no wind or turbulence, the design of a ground based automatic landing aid and aircraft autopilot would be trivial indeed since all effects would be predictable and invariant with time.

4.1.2 Parameters of the TSC Model

The TSC wind model uses steady winds up to 25 kt headwind, 15 kt crosswind at reference altitude (50 ft.); wind shear of 8 kts per 100 ft. from 200 ft. to 0 ft.; and wind gusts, according to the Dryden Spectra, with rms intensity of 5 fps vertical and 10 fps horizontal. Scale lengths and corresponding gust bandwidths vary with airspeed and altitude. A thorough treatment of the development and form of this model appears in Section 3 and Appendix B of Reference 3.

4.2 AIRFRAME AND FLIGHT CONTROLS

The jet transport Convair 880 has been used exclusively during this study. It is thought to be typical of conventional aircraft in its dynamic characteristics and particularly representative of the commercial jet transport in its response to aerodynamic disturbances. Its aerodynamic characteristics are fully described in Reference 3 and Appendices D and E.

4.3 MLS COUPLER AND AUTOPILOT

Previous work done at TSC with the CV-880 simply replaced ILS localizer and glide slope with MLS azimuth and elevation functions, with insignificant coupler filter or autopilot modifications. However, in order to test ultimate performance limitations and their sensitivity to MLS parameters, it has been necessary to anticipate the design of an MLS coupler, which accounts and compensates for MLS noise and data rate as well as offering adequate signal quality for "wind proofing".

It would be trivial to eliminate the effects of MLS sampling and noise at any data rate by choosing a filter with a large enough time constant. This, however, directly affects path following ability in wind through added lag in the error signal and subsequent sluggish response to path offsets.

4.3.1 Lateral Channel Autopilot

The lateral channel autopilot is similar to one designed for use with an inertially augmented landing system (Reference 5) except that MLS information is used in place of the inertially generated lateral position and velocity. Figure 4-1 shows the resultant configuration for final approach and touchdown. (Transitional control from one phase to another has not in general been shown since the primary goal is not the design of a fully operable control system, but a testing of performance sensitivity to MLS.)

4.3.2 Lateral Channel Coupler

The lateral channel coupler, comprised of a first order digital recursive filter, zero order hold, and first order analog filter, converts lateral position deviation samples into a properly compensated analog roll angle command. The actual form of the filter is shown in Figure 4-2(a); however, its equivalent in Figure 4-2(b) is perhaps more readily understood. The term K_y represents an effective position gain; $K_{\dot{y}}$ represents effective rate gain and the filter $s/(s+a)$ provides low-passed rate from the position signal. The relationship between the digital filter parameters and the equivalent circuit parameters is also given. Numerical values associated with the filters are the subject of the optimization program and depend on data rate, wind, beam noise. (In future autopilots the gain and time constants will undoubtedly be automatically scheduled according to range, noise, phase of flight, wind condition, etc. in order to provide best flying performance for each particular environment.)

4.3.3 Longitudinal Autopilot

The longitudinal autopilot (Figure 4-3) used for this study is identical with the Lear Siegler Autoland autopilot of Reference 3 with the following exceptions:

a. The coupler has been redesigned.

b. Altitude and altitude rate are generated from MLS information.

c. In some cases, the normal accelerometer has been eliminated to test performance using only MLS information for wind suppression.

The format for the longitudinal channel remainsthe same for all phases of flight. Note also that this configuration includes an autothrottle.

4.3.4 Longitudinal Coupler

The longitudinal coupler is composed of a second order digital filter and zero order hold; it converts vertical position deviation samples (or altitude rate deviation, during flare) into a properly compensated altitude rate command. Figure 4-4(a) presents the filter in recursive form while 4-4(b) again shows the equivalent in analog terms. A number of various configurations of the filter were attempted (all of second order), including an option to insert the derived altitude rate signal into the autopilot at a point prior to the normal accelerometer complementary filter (an exact parallel of the autoland mechanization). Performance seemed relatively insensitive to these changes in mechanization, however, and the configuration of Figure 4-4(b) was chosen. Again, numerical values for gains and filter time constraints are subject to optimization depending on phase of flight, wind, noise, etc.

4.4 OTHER CONSIDERATIONS

Guidance laws, special modifications to the MLS pre-processor and couplers, and specific performance criteria will be discussed in sections dealing with each considered phase of flight.

As stated in Section 2.3, however, development of performance criteria in an absolute sense has in general not been undertaken. Rather, for each phase of flight important variables are identified, and comparative performance with respect to these variables evaluated as a function of data rate, noise, wind, and control system complexity.

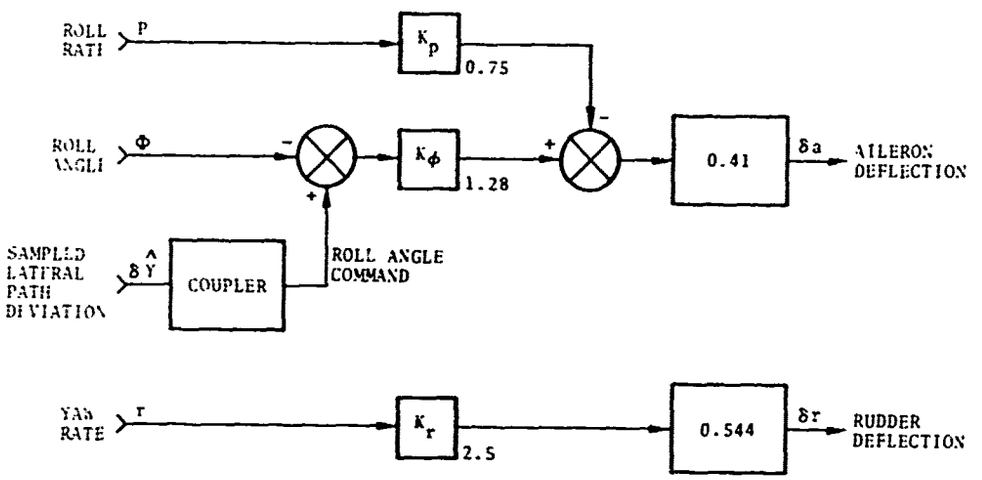

Figure 4-1. Simplified Lateral Autopilot CV-880 Final Approach

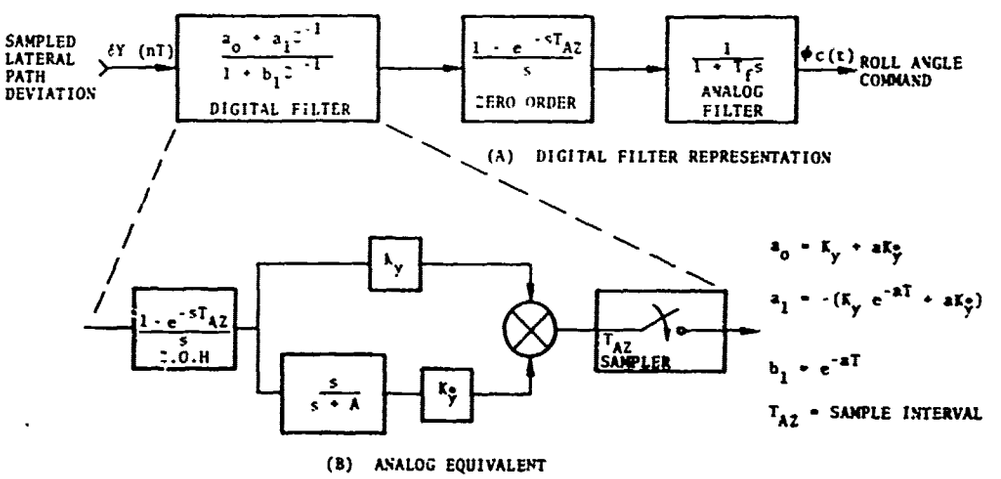

Figure 4-2. Lateral Coupler Block Diagram

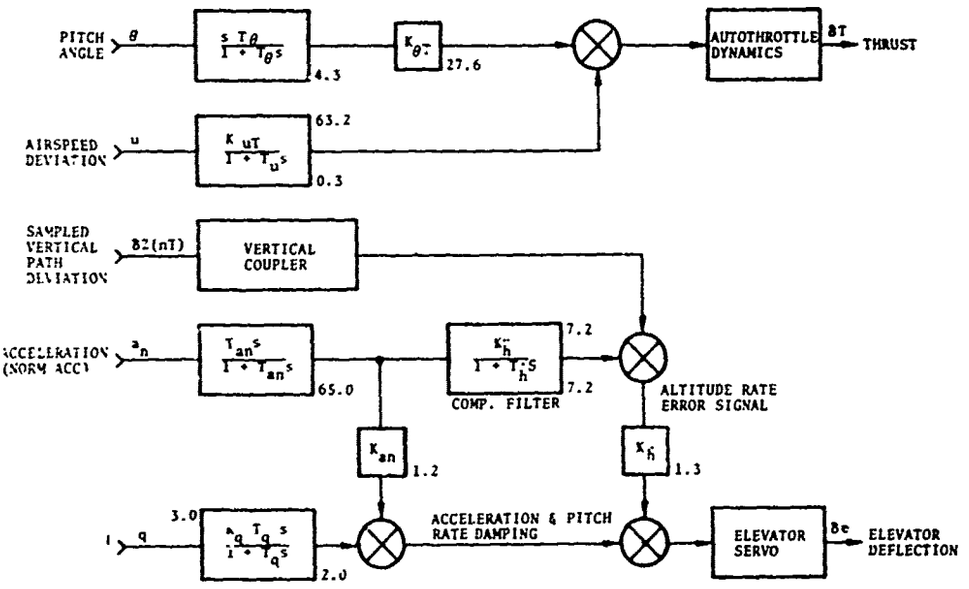

Figure 4-3. Simplified Longitudinal Autopilot CV-880 Final Approach

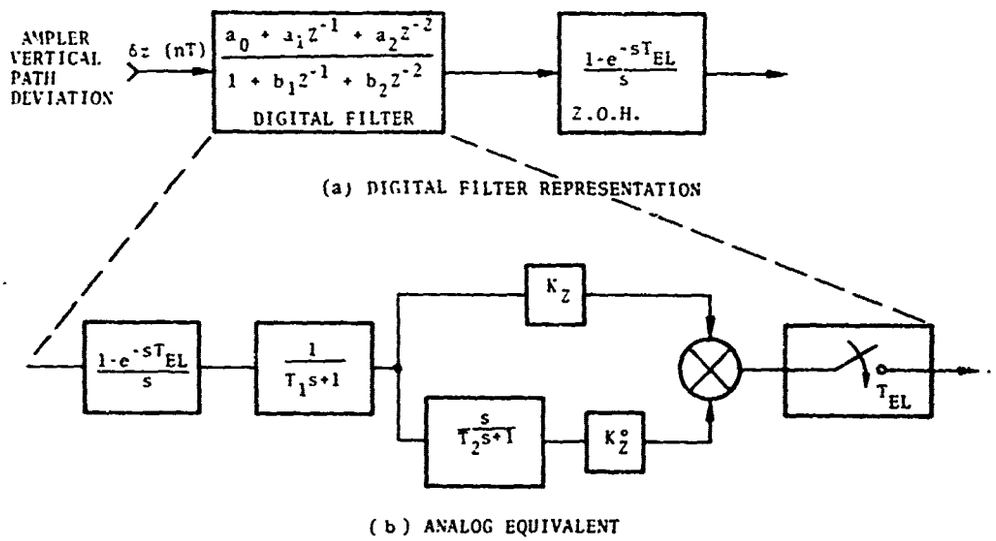

Figure 4-4. Vertical Coupler Block Diagram

5.0 REQUIREMENTS FOR FINAL APPROACH

Final approach is defined as any straight-in segment of flight from acquisition of final glidepath to flare initiation. With MLS, it could be as long as 20 nautical miles, or in some hypothetical future operational environments using curved approach to touchdown, may not exist at all. Currently the final approach phase for ILS operations is between 5 and 10 nautical miles long.

During this phase, the aircraft is attempting to maintain a fixed path in space with MLS information as reference and possible wind shear and turbulence as disturbances. For CTOL operations the glidepath angle varies between 2° and 4° with respect to elevation #1; azimuth reference is assumed to be coincident with the runway centerline.

5.1 ASSUMED CONDITIONS AND GEOMETRY

Wind gust strength and angular noise intensity from both the elevation #1 (EL1) and the azimuth (AZ) functions is assumed constant during final approach. However, linear noise and not angular noise is the true driving function for the autopilot, and it grows proportionately with distance from the antenna.

5.1.1 The Geometry of Final Approach

Figures 5-1 and 5-2 illustrate the linear and angular quantities to be dealt with in terms of desired position, actual position and measured position for the lateral and longitudinal cases, respectively [the assumption is made that range (or time) is not controlled].

For the lateral case, exact expressions for Δy (actual deviation) and δ_y (measurement error) are given by Equation 5-1.

$$\Delta y = R\sin\Delta\theta \qquad (5\text{-}1)$$

$$\delta_y = R\sin\delta\theta + \delta r \sin(\Delta\theta+\delta\theta)$$

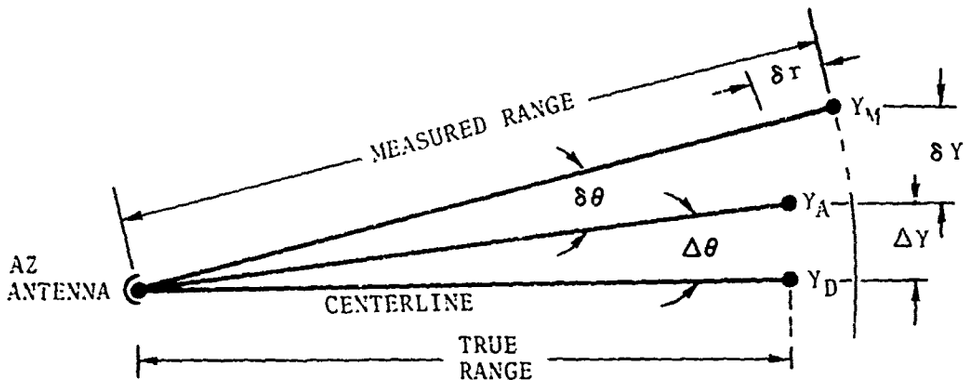

δr=range meas. error
δθ= az angle meas error
δY= resultant linear meas. error
Y_D= desired position Y_A = actual position Y_M=measured position
Δθ =az angle deviation
ΔY=Linear deviation from C.L.

Figure 5-1. Lateral Geometry for Final Approach

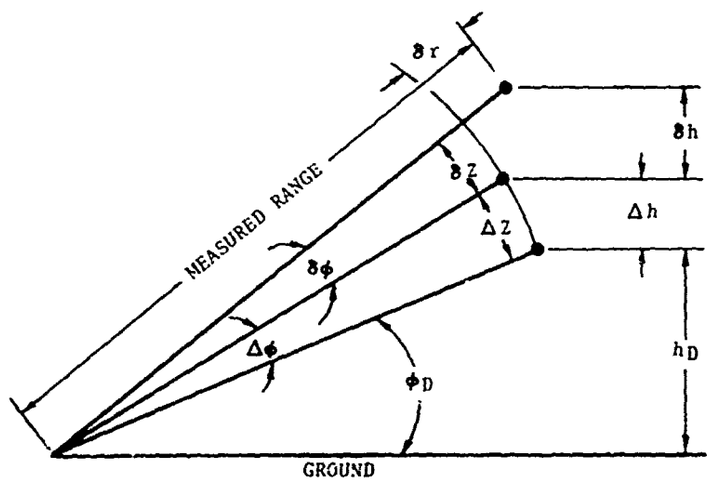

ϕ_D = desired glideslope
$\phi_D+\Delta\phi$ = actual glideslope
$\phi_D+\Delta\phi+\delta\phi$ = measured glideslope
ΔZ = actual glideslope eleviation
ΔZ + δZ = measured glideslope deviation
h_D = desired altitude
Δh = actual deviation
δ h = measurement error

Figure 5-2. Vertical Geometry for Final Approach

Using small angle approximation leads to Equation 5-2.

$$\Delta y = R\Delta\theta \qquad (5\text{-}2)$$

$$\delta y \approx R\delta\theta + \delta r(\Delta\theta+\delta\theta)$$

If $\delta r \ll R$,

then $\delta y \approx R\delta\theta$

It can therefore be concluded that range errors may be ignored for this case.

The longitudinal case is slightly different since there is a nominal glideslope angle. This, however, affects only the knowledge of absolute altitude (h) and not the controlled quantity linear glideslope deviation ($\Delta z, \delta z$).

Again,

$$\Delta z = R\Delta\Phi \quad \text{(actual)} \qquad (5\text{-}3)$$

$$\delta z = R\delta\Phi \quad \text{(measured)}$$

However

$$\Delta h \approx \Delta z \approx R\Delta\phi$$

$$\delta h \approx R\delta\phi + \delta r \sin(\phi_D - \delta\phi + \Delta\phi) \qquad (5\text{-}4)$$

$$\approx R\delta\phi + \delta_r \sin\phi_D$$

Therefore, according to Equation 5-4 errors in knowledge of altitude are dependent on range measurement errors especially as the desired glideslope angle (ϕ) becomes large. It should be re-emphasized however that Δz, the deviation perpendicular to the glideslope, is the quantity being controlled during final approach and that neither Δz nor δz are primarily sensitive to glideslope angle or to range measurement errors.

Figure 5-3 presents examples of the dependence of linear path deviation measurement error on absolute range from the transmitting antenna for various typical values of angular error.

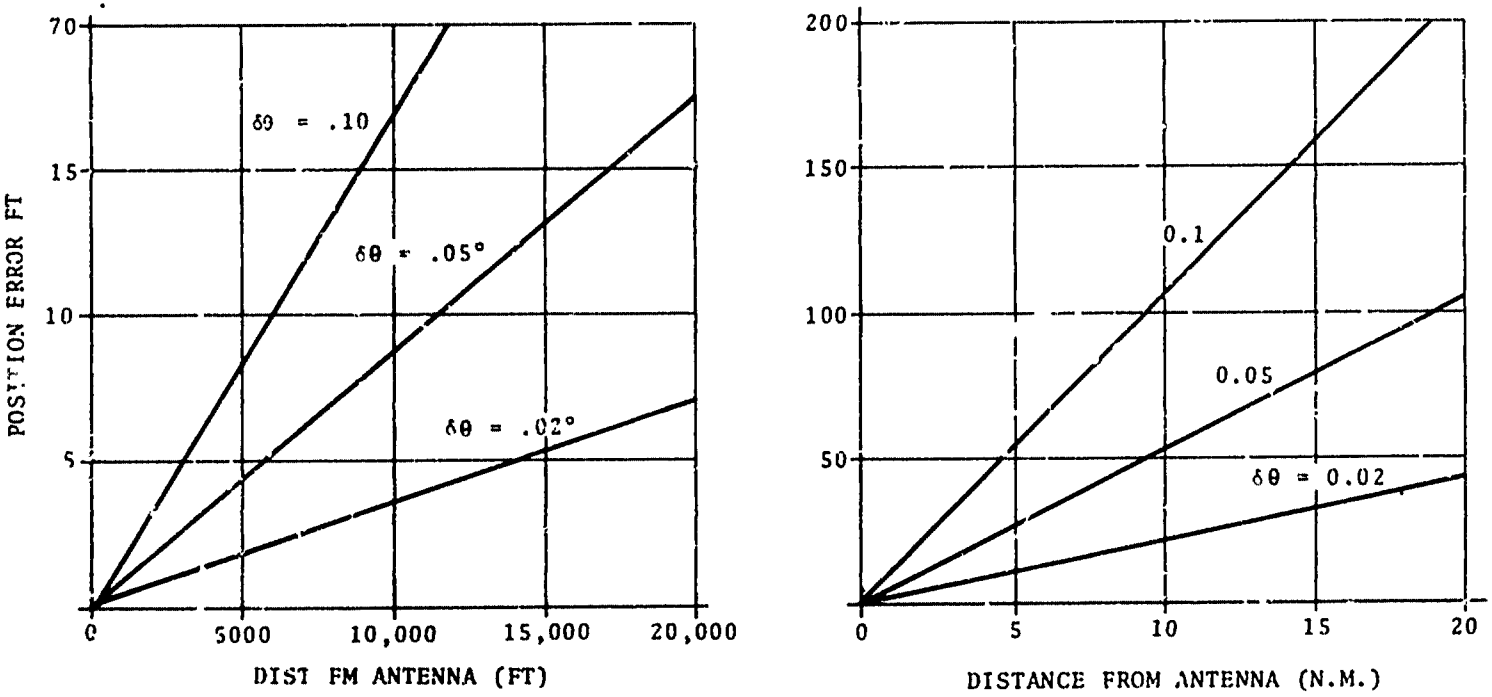

Figure 5-3. Linear Error Versus Distance from Antenna

5.2 PERFORMANCE CRITERIA

The major goal of the final approach mode is to deliver the aircraft to the flare initiation point with proper position and attitude for a satisfactory flare and touchdown. (Since the flare maneuver involves only the longitudinal system, final approach for the lateral system can be assumed to continue to decrab initiation). Constraints include "acceptable" flight performance during final approach in terms of control and attitude activity, and a satisfactory attitude and position at some particular "decision altitude" prior to flare initiation where the pilot makes a positive decision to either continue or abort the approach.

5.2.1 Control and Attitude Activity

Control and attitude activity is necessary to path maintenance in the presence of turbulence or non-steady winds. However, extra activity induced either by the noise on the MLS signal or as a result of its non-continuous nature is undesirable from both the pilot's and the passengers' points of view. It is usually necessary to give up some measure of "wind proofing" (path following ability) in order to assure adequate "noise proofing". Important variables include:

a. Roll angle, ϕ

b. Roll rate, p

c. Aileron deflection, δ_a

d. Rudder deflection, δ_r

e. Pitch angle, θ

f. Pitch rate, q

g. Vertical acceleration, a_n

h. Elevator deflection, δ_e

[Control deflections are important only in the sense that they are coupled to the pilot's controls. If autopilot generated control commands were decoupled from the pilot's "stick" then these variables need not be limited during final approach except by actual physical limitations, fatigue properties, etc. of the mechanisms].

In the absence of firm fixed maxima to attach to these variables it remains possible to state desirable qualitative performance characteristics:

a. For a given turbulence level, activity should remain as low as possible while maintaining a satisfactory path in space.

b. The rms control and attitude activity should be relatively constant throughout the approach for constant turbulence.

c. The level of activity should correspond to the level of turbulence; i.e., for low or no-wind conditions noise sensitivity must also be low.

5.2.2 Decision Altitude

At decision height the pilot must evaluate performance to that moment and either commit the aircraft to land or execute a missed approach. In addition to a general satisfaction with final approach control and attitude activity levels, he must also consider:

a. Lateral Path error, y
b. Vertical (Longitudinal) Path Error, z
c. Airspeed deviation, u

Decision height varies with visibility condition but its lower bound is on the order of 100 feet.

In order to evaluate performance in these variables, the pilot must be presented with measurements of their magnitudes; he must be presented with measurements of their magnitudes; he must also have an accurate indication of arrival at decision altitude. This implies a dual set of requirements; the first involves the actual aircraft performance, the second the pilot's ability to

measure this performance at the proper point. Measurement ability from the pilot's point of view has not been dealt with in detail. It involves an entirely different set of filters than those for control of the aircraft. In general, measurements for evaluation purposes can use much longer averaging times than those for control purposes, since the variables being measured (position) have correlation times on the order of many seconds and do not require the lead (high frequency) compensation necessary for adequate control. Measurement and averaging techniques suitable for the pilot's use include, for example, the alpha-beta tracker, a dual second order digital filter designed to measure position and velocity estimation.

The net result, in the form of an educated assumption, is that the pilot will be able to measure the position and velocity and various sample weighting schemes for position and velocity estimation.

(This assumption may break down in the presence of certain multipath noise where errors may also have correlation time on the order of seconds.)

Airspeed variations have also not been dealt with in this study; a perfect auto throttle has been assumed which makes the aircraft track gusts perfectly and presents a worst case in vertical position control.

As indications of acceptable limits on the two remaining decision height variables, the Category II specifications are quoted:

Lateral path error	$\pm$ 72 ft. max.
Glideslope Deviation	$\pm$ 12 ft. max.

at 100 ft. altitude (A 12 ft. glideslope error on a 3° glideslope is equivalent to a 240 ft. longitudinal error).

5.2.3 Flare Initiation

After the decision to land has been made, the point of flare initiation provides the transition from final approach to the actual landing phase of flight. As will be discussed in Section 6.0, the ability to measure critical variables at this point and suitably adjust the parameters of the flare law is one of the limiting factors in performing a successful flare maneuver. Given that decision altitude statistics are satisfactory at this point, the statistics of path following and velocity errors at flare will also be satisfactory, if this is so, there is no condition for which suitable flare law parameters cannot be chosen to provide (in the absence of other disturbances) a near perfect touchdown velocity and position. Therefore, no explicit performance criteria will be developed for flare initiation.

5.3 BASIC DATA-RESULTS OF FILTER OPTIMIZATION

In this section, the basic data from the optimization procedure is presented. From Section 2.0 it is recalled that this data is in the form of a combination of minimum path deviation and minimum control activity for a particular data rate, beam noise magnitude and wind gust magnitude. Also presented for the same conditions are data on other important variables. The control system variables include only the parameters of the digital filter.

The data presented in general is subject to more complex interpretation than is given in this section. Its implication in terms of the filtering techniques and explanations for the shapes and relationships of many of the curves have been left out to avoid digression from the major issue - that of sensitivity to noise and data rate. The material discussed in detail in this and succeeding sections has been selected as pertinent to this end.

5.3.1 Lateral System Data

5.3.1.1 Data Rate as the Parameter - Figure 5-4 plots minimum values of path dispersion, σ_y versus aileron activity, $\sigma_{\dot{\delta}a}$ for data rates of 1, 2, 5, 10 and 40 for wind gust intensity (σ_v) of 10 fps, rms and white beam noise (σ_n) of 5.84 ft. rms. (5.84 ft. corresponds to 0.02° rms, 15,000 ft. from the antenna.) The points on each curve represent data for various weighting factors for the two variables in the optimization penalty function. The "region of interest" occurs around the "knee" of the curve; to the upper left the sacrifice in path following ability does not correspond to significant decreases in aileron activity; to the lower right the converse is true. Not surprisingly, there is a definite relationship between the characteristics of this curve and the dynamic characteristics of the path following loop. Figure 5-5 shows examples of transient responses to a step of lateral displacement for three separate cases corresponding to the three areas of Figure 5-4. The optimum filter for the high control activity case produces a relatively fast, slightly underdamped path following response [Figure 5-5a] while that for high lateral dispersion produces a response about half as fast [Figure 5-5c]. The system of Figure 5-5a will provide better response in turbulence but will tend to be sensitive to noise, while that of Figure 5-5c will exhibit a relative insensitivity to noise at the expense of slow correction of gust induced errors.

Within the region of interest of Figure 5-4 the following observations apply:

a. Performance is relatively insensitive to data rate; the maximum increase in lateral deviation for a given aileron activity from 40s/s to 2s/s is approximately 10%

b. There is verly little sensitivity above 5s/s, although there is no doubt that performance can be marginally improved by increasing data rate.

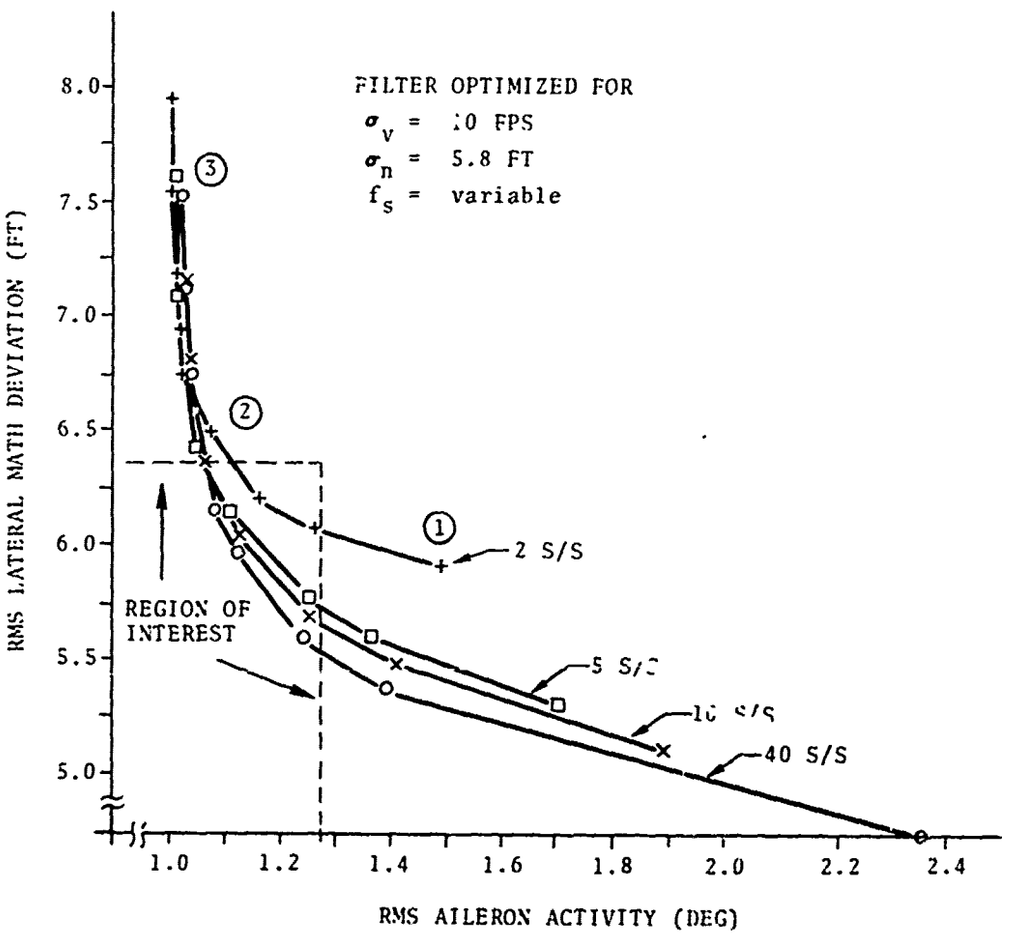

Figure 5-4. Optimum Performance in Path Dispersion Activity Versus Data Rate Aileron

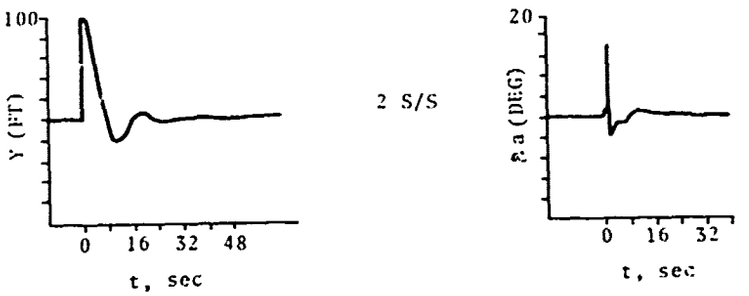

(a) Transient Response Corresponding to Point 1 of Figure 5-4

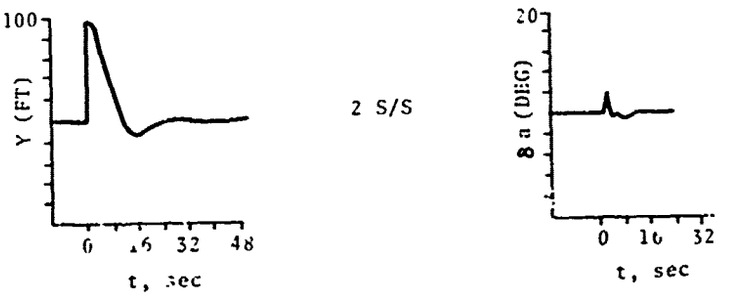

(b) Transient Response Corresponding to Point 2 of Figure 5-4

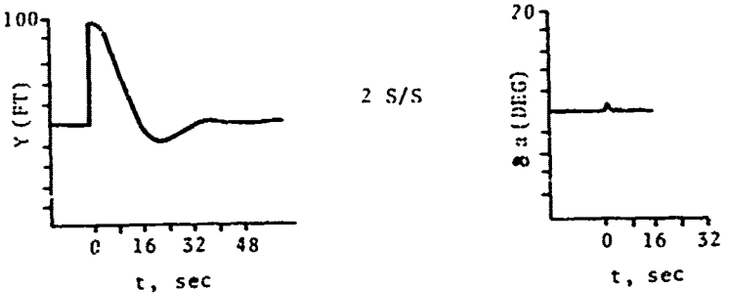

(c) Transient Response Corresponding to Point 3 of Figure 5-4.

Figure 5-5. Transient Response for Various Weighting Factors

Other lateral variables whose rms values show any variation with data rate are lateral velocity $\sigma_{\dot{y}}$, roll angle, σ_{ϕ} and roll rate, σ_{p}. These are plotted against aileron activity in Figure 5-6 for various data rates; the region of interest in Figure 5-4 has been mapped onto these plots also. Again, variations within the region of interest for these variables is on the order of only ten to fifteen percent for data rates from 2 to 40 samples per second.

5.3.1.2 Noise as the Parameter - A data rate of five samples per second was chosen to investigate performance sensitivity to noise. This data, presented in Figures 5-7 and 5-8, may be interpreted two ways: first, it represents the best performance in worst case turbulence 10 ft/sec rms) with the noise value stated in feet; second, if it is assumed that the azimuth error is a constant angular error of a given magnitude, then the performance curves represent that at a given distance from the transmitting antenna (with .02 degrees rms noise, the results shown in Figures 5-7 and 5-8 apply to distances of 8,250 to 33,000 ft. from the azimuth antenna).

Figure 5-7 shows that lateral path deviation tends to be significantly more sensitive to noise than to data rate. Figure 5-8 plots the other three lateral variables. The result here indicates that filtering added in the higher noise cases tend to reduce roll, roll rate, and lateral rate dispersion, but at the expense of increases in lateral position dispersion.

5.3.2 Vertical System Data

During final approach for the vertical system, the autothrottle is assumed to be controlling airspeed perfectly; the vertical control system, which is required to maintain a ground-referenced flight path is therefore presented with somewhat of a worst case situation, i.e., ground speed variations equal to the longitudinal gust components.

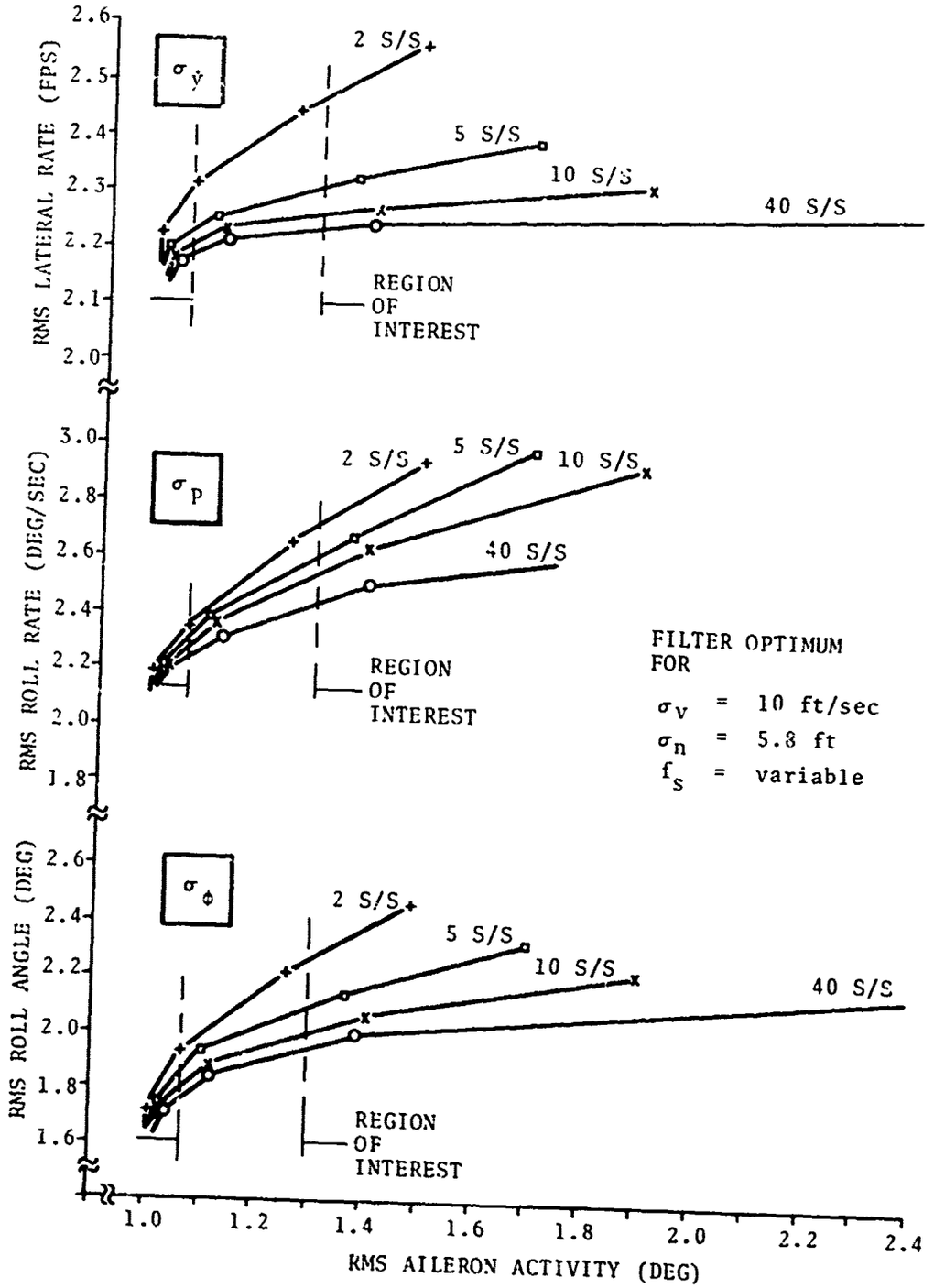

Figure 5-6. Sensitivity of Non-Optimized Variables to Data Rate

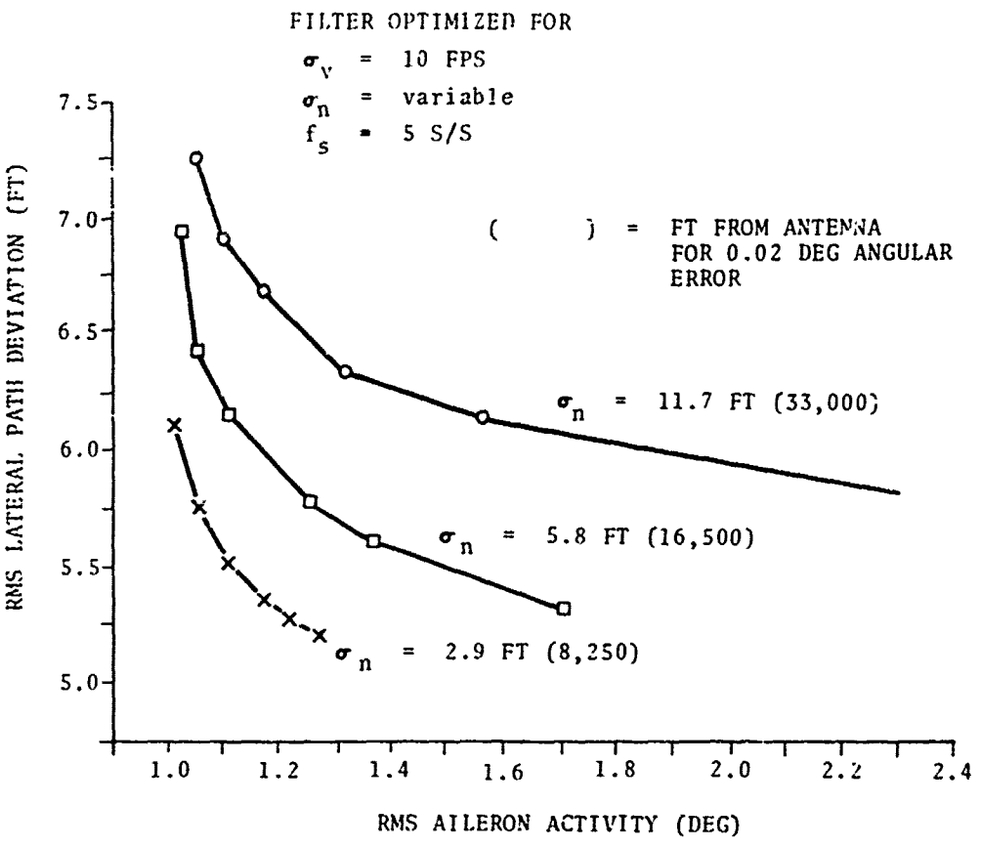

Figure 5-7. Sensitivity of Optimum Path Dispersion Aileron Activity to Noise

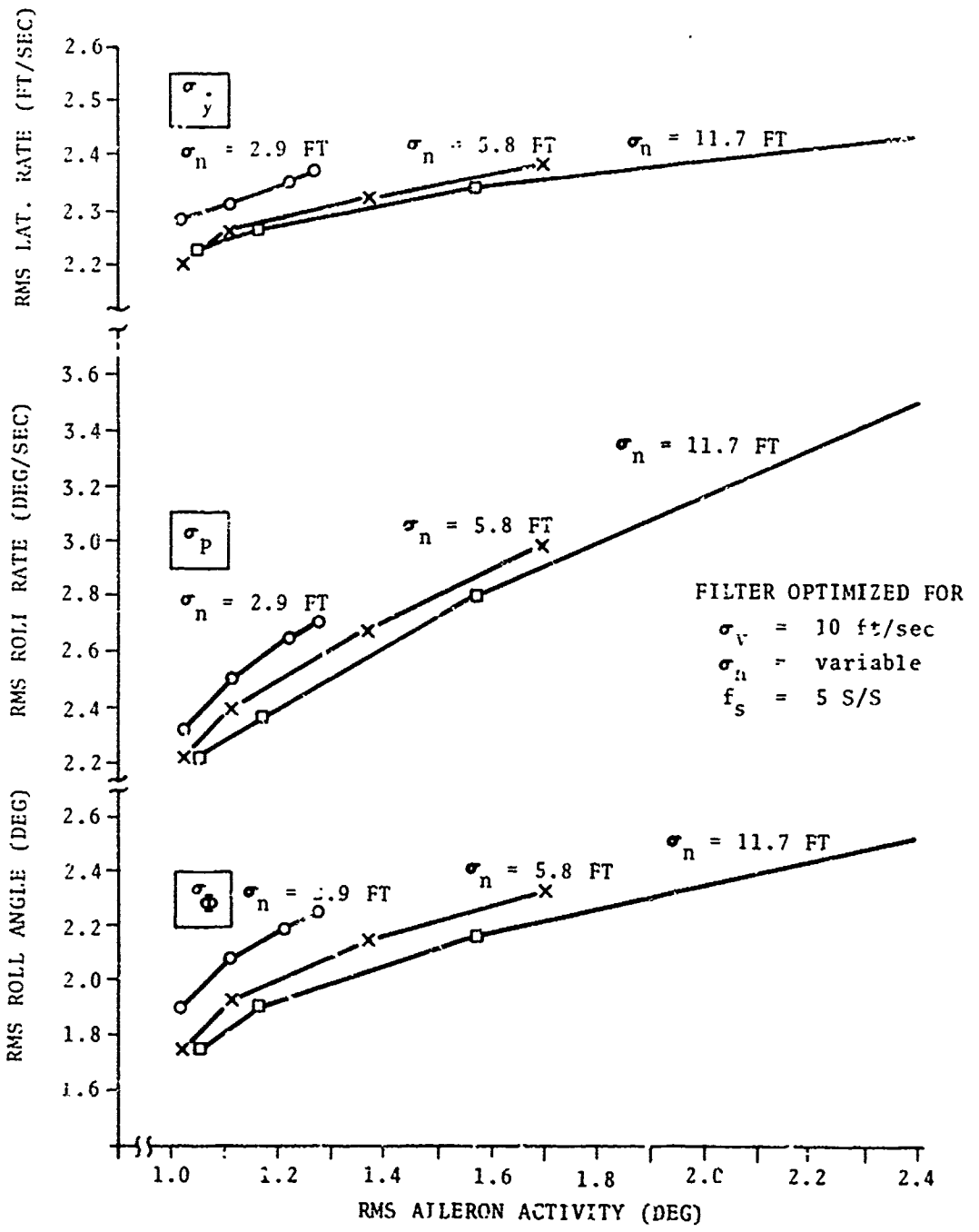

Figure 5-8. Sensitivity of Non Optimum Variable to Noise

5.3.2.1 Data Rate as the Parameter - Figure 5-9 presents minimum path dispersion versus elevator activity for data rates of 2, 5, 10, 15 and 40 per second for wind gust-intensity of 5 fps vertical (σ_w) and 10 fps longitudinal (σ_u). The beam noise, σ_n, is taken as 3.5 ft., equivalent to .033 degrees at 1n. mile (250 ft. alt.) from glidepath intercept point (GPIP).

As can be seen, there is significant relative variation in minimum path deviation over the range of data rates, as much as 40% elevator activity seems relatively independent of data rate, however. The region of interest appears to be restricted to elevator activity values between 2.5 and 3.0 deg. rms; below 2.5, minor decreases in elevator activity are costly in terms of path dispersion, while above 3.0 large increases in elevator activity are required for minor improvements in path following ability.

Other variables which show some sensitivity to data rate include altitude rate ($\dot{Z}$) and pitch rate (q). These are presented as Figure 5-10.

5.3.2.2 Noise as the Parameter - Figures 5-11 and 5-12 show the sensitivity of the vertical path deviation, altitude rate, and pitch rate, to beam noise in the presence of worst case turbulence at five samples per second. It should be recalled that the curves of Figure 5-11 represent data with the filter optimized for the particular conditions stated. As in the lateral system case, there is considerably greater sensitivity to noise than to data rate. (The noise sensitivity is undoubtedly also a function of data rate; results not shown here bear this out).

5.4 PERFORMANCE EVALUATION

Each of the points on each of the curves of Figures 5-4, 5-7, 5-9 and 5-11 represents a possible different choice for filter configuration. It remains to narrow the region of possible choices by selecting performance which best meets the criteria of Section 5.2. Since the level of noise is variable (decreasing) during final approach it is also necessary to consider the effects of

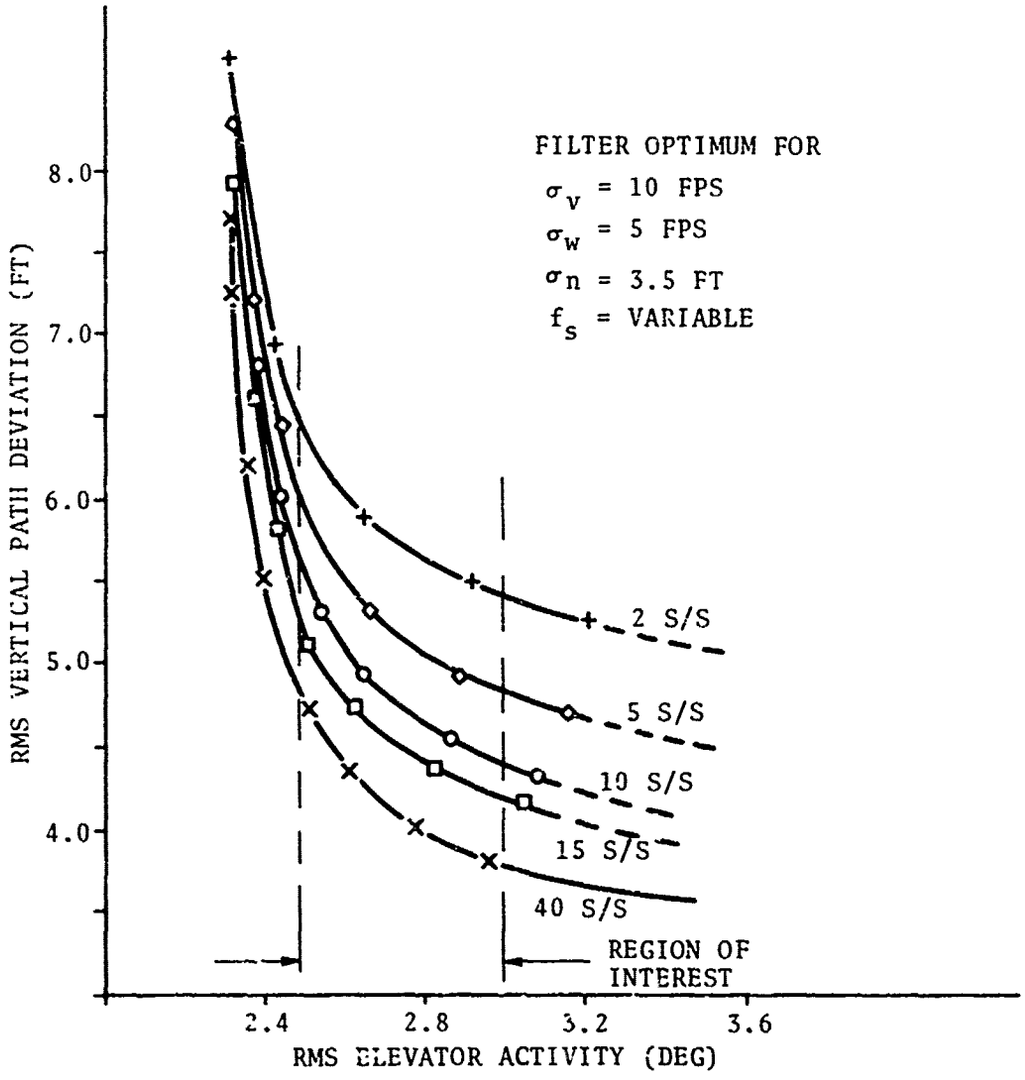

Figure 5-9. Sensitivity of Optimum Glidescope Deviation, Elevator Activity to Data Rate

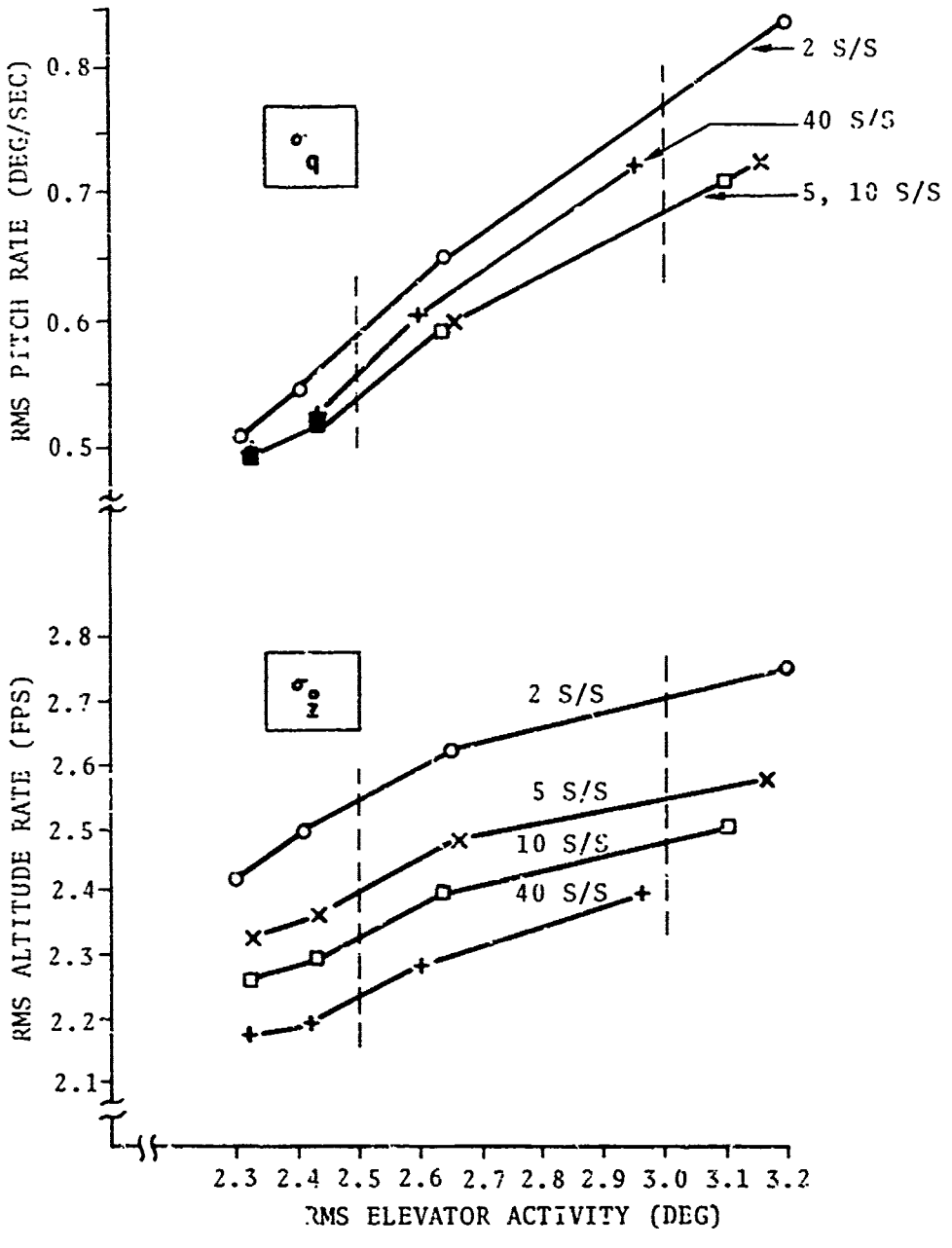

Figure 5-10. Sensitivity of Non Optimum Variables to Data Rate

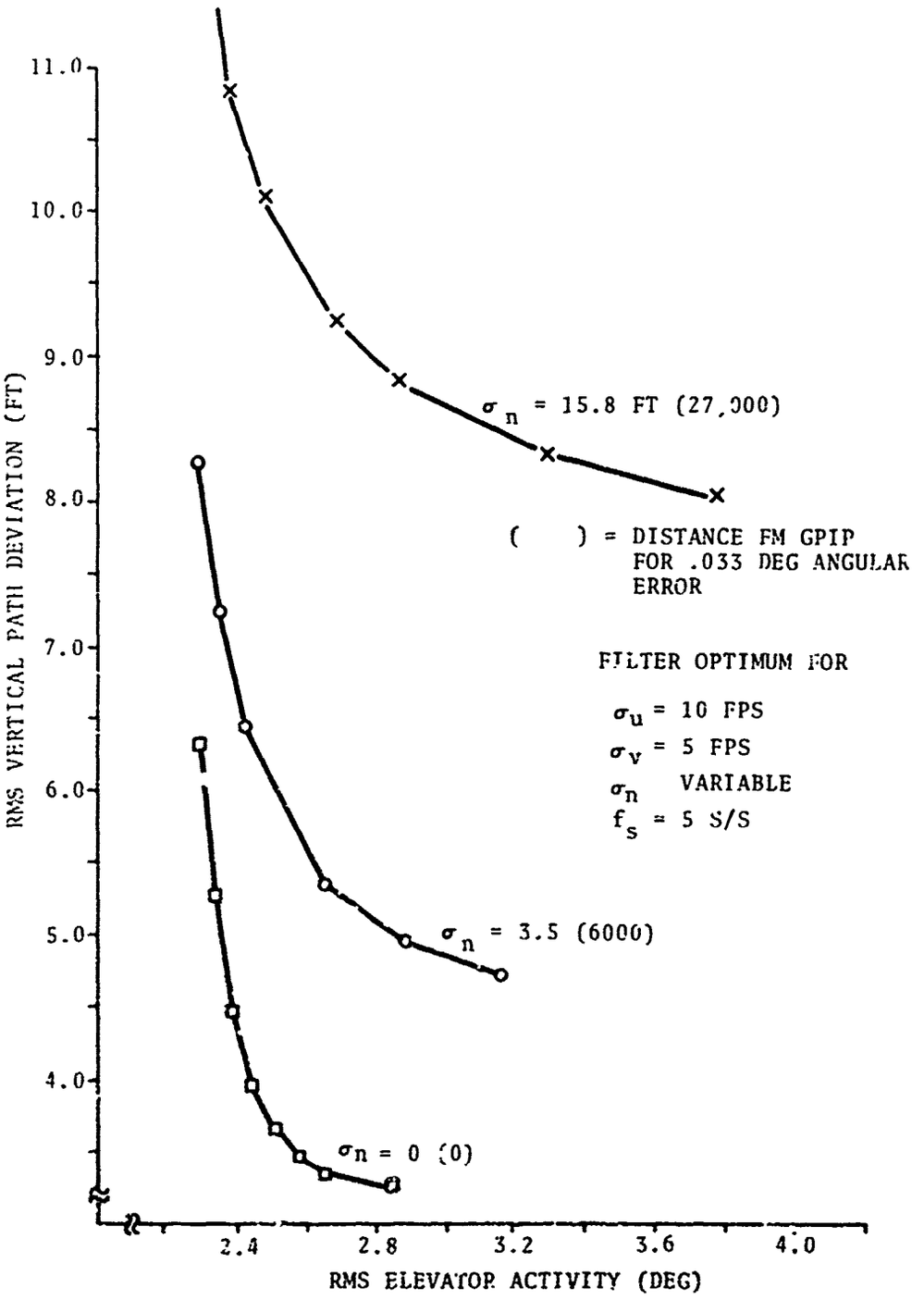

Figure 5-11. Sensitivity of Optimum Glidescope Deviation, Elevator Activity to Noise

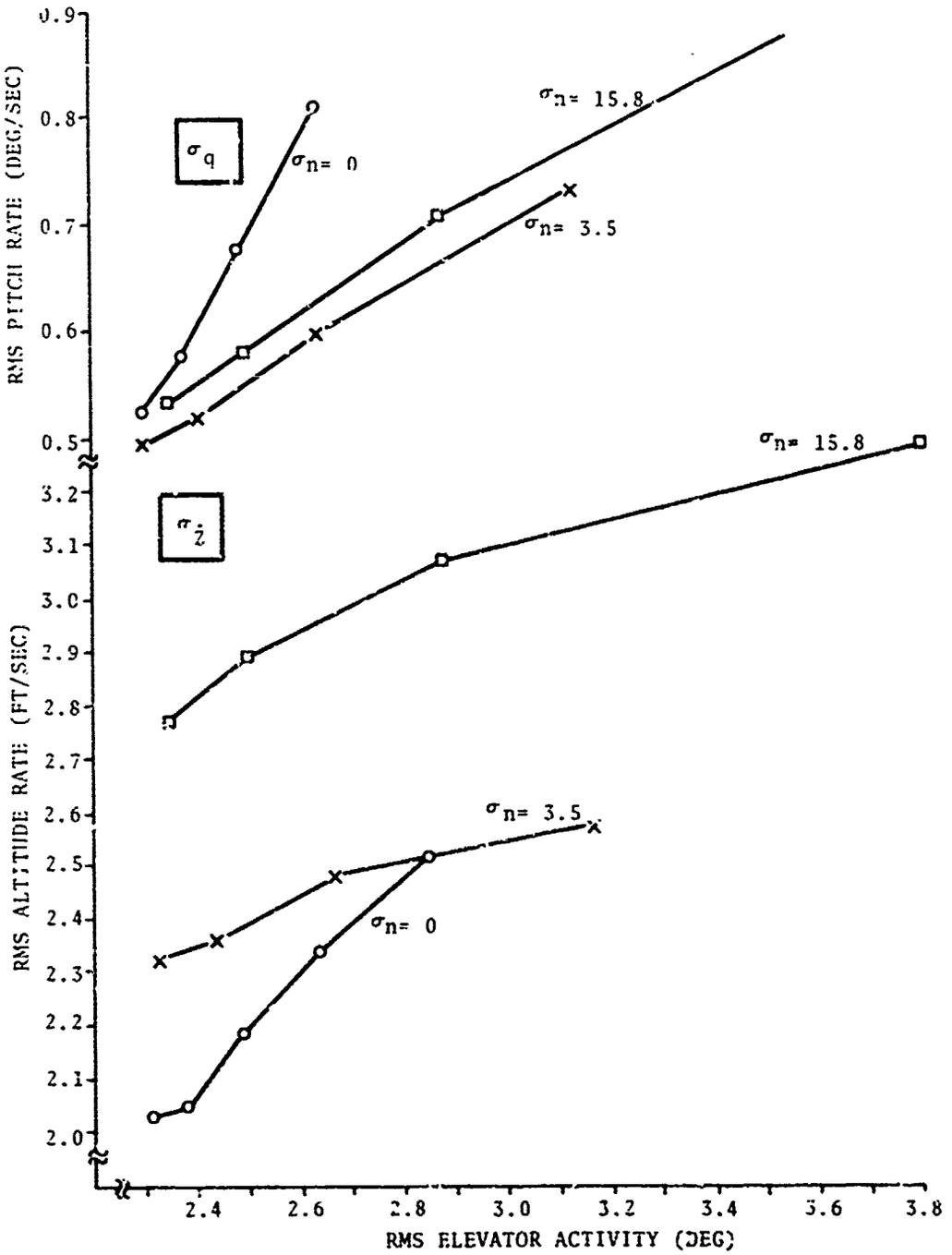

Figure 5-12. Sensitivity of Non-Optimized Variables to Noise

scheduling the filter parameters as a function of range. Worst case turbulence also cannot be assumed to be a universal condition and filters optimized for this condition may exhibit poor performance in low turbulence. How poor this is, and what is necessary to correct it will also be discussed.

5.4.1 The Lateral System

It is apparent from Figures 5-4 and 5-7 that the lateral dimension of the decision altitude "window" is a full order of magnitude larger than expected rms path deviations even with worst case wind, regardless of noise magnitude or data rate. It can therefore be eliminated as a constraint and attention directed towards satisfying minimum activity criteria.

Let's first assume that an ideal condition exists in terms of the ability to schedule filter parameters as a function of the magnitudes of the linear noise and the turbulence in which case optimum performance is achieved throughout final approach. Then for the worst case turbulence the parameters may be chosen to give constant aileron activity. For instance, with an rms aileron activity of 1.2 degrees, performance in lateral path dispersion, lateral rate, roll and roll rate may be taken directly from Figures 5-7 and 5-8. The results are shown in Figure 5-13 for five samples a second. Performance variations with data rates of 2 to 40 are also shown for a single noise value. The abscissa of Figure 5-13 is calibrated both in rms feet of noise and equivalent distance from azimuth antenna for an angular error of .02 degrees. It is clear that with appropriate filter gain scheduling the sensitivity of performance to noise and data rate is reduced to the level of inconsequence. Some further comments also apply:

a. Increasing allowable angular noise tends to expand the equivalent distance scale, however, from the trends of the curves shown, it appears that doubling or tripling allowable angular noise will have no serious consequences.

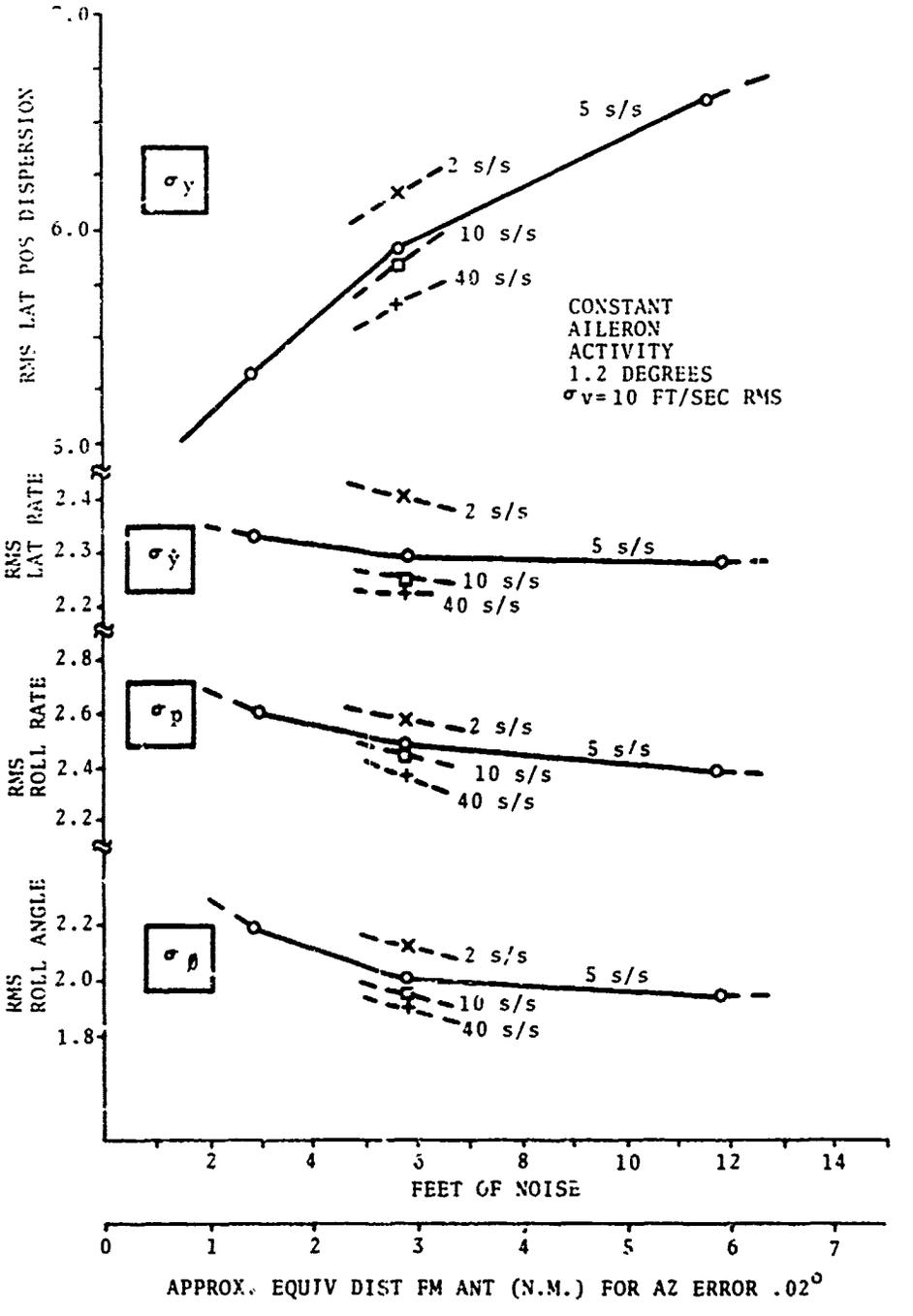

Figure 5-13. Lateral System Performance Versus Distance from Azimuth Antenna

b. With lesser values of rms turbulence, rms activity and path deviations will decrease proportionately (assuming filter parameter scheduling as a function of turbulence).

5.4.1.1 Other Options - It may not be strictly fair to assume that all this filter parameter scheduling as a function of condition is either necessary or feasible; it is not likely that all aircraft will be so equipped in any event. This section therefore will examine some of the options which form partial solution to the MLS filtering problem Optimum performance can be compared with sub-optimum performance when a filter designed for particular conditions is used in other conditions. As a first compromise, it seems reasonable to choose the filter designed for high wind and high noise to be used throughout final approach regardless of wind or range. It is easy to determine the effects of this compromise on the curves of Figure 5-13. Rms lateral position dispersion will not decrease as significantly as the approach continues, however, the upper bound is still the design value. Further, the aileron activity will not remain constant but will decrease slightly as approach proceeds; the other curves of Figure 5-13 will tend to flatten out also. For instance, a system designed for a wind of 10 ft/sec rms and a noise of 42 ft. (20NM for .02 deg. rms azimuth error) will yield results shown in Figure 5-14 for lateral dispersion and aileron activity as a function of noise and range; also shown for comparison are results with proper filter scheduling. Comparison of the two curves indicates that in this case the penalty paid for not scheduling is small when compared with the Category II decision height criterion. It remains to determine performance of the fixed filter in reduced turbulence. As the example for this case, the extreme, or no wind condition was chosen. Figure 5-15 demonstrates that the filter designed for maximum wind produces three times as much aileron activity as the filter optimized for no wind, while providing a slightly lower sensitivity to path following errors. Performance in aileron activity with non-optimum filter may be unsatisfactory beyond 10 nautical miles indicating the possible necessity for some form of

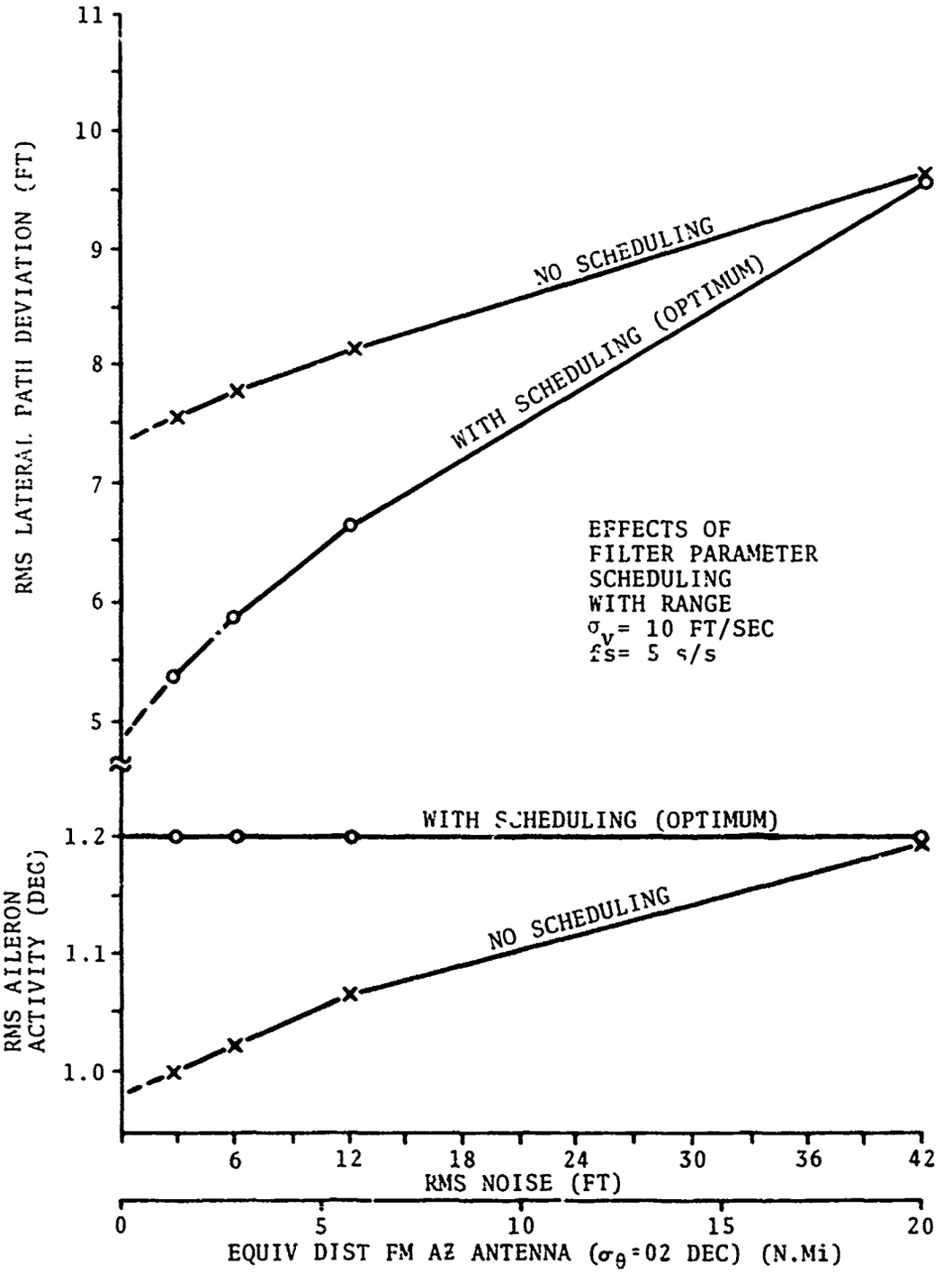

Figure 5-14. Effect of Filter Parameter Scheduling with Channel Distance-Lateral

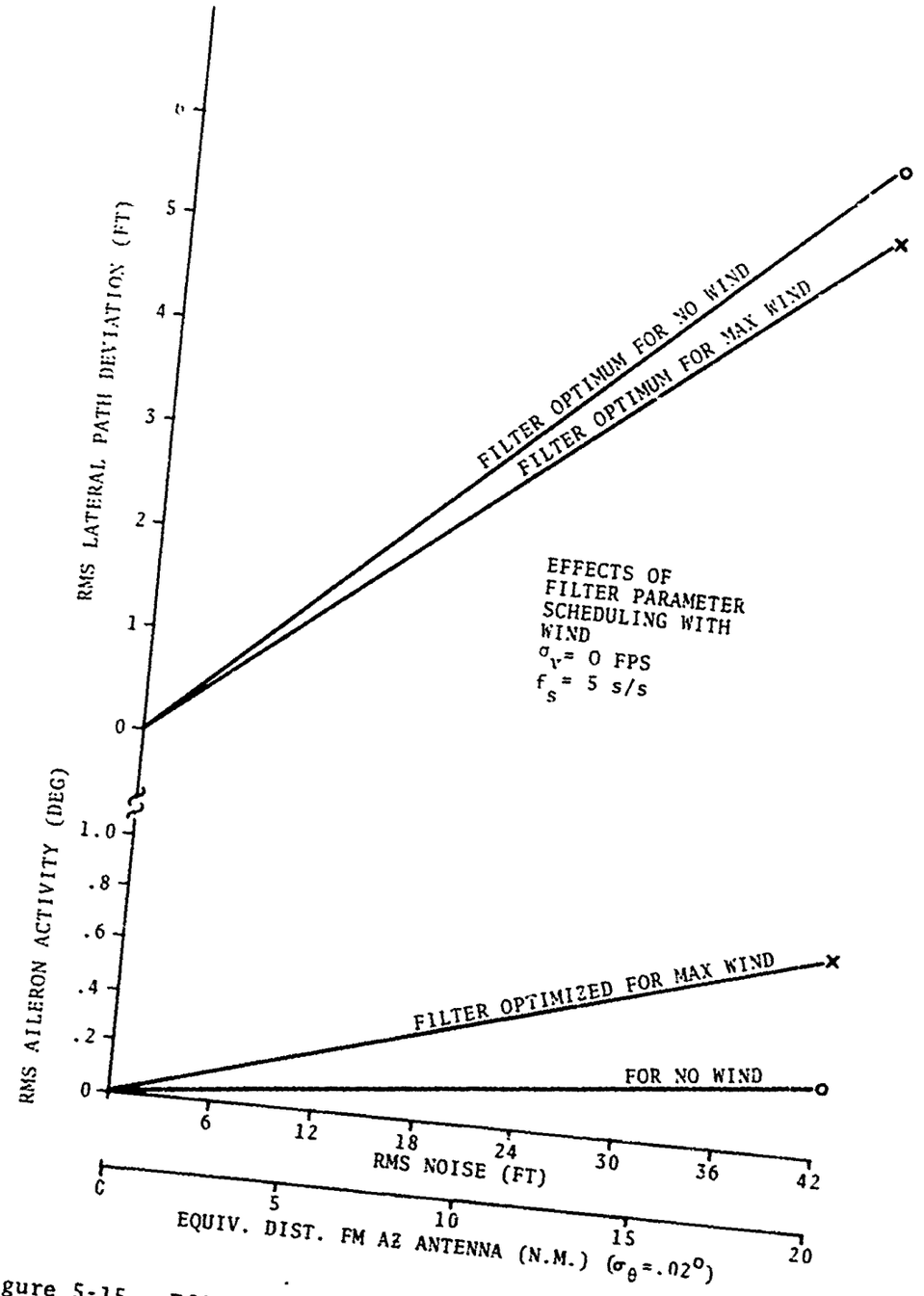

Figure 5-15. Effect of Filter Parameter Scheduling with Wind-Lateral Channel

parameter scheduling with expected wind. The other solution to reducing no wind activity is to accept higher path dispersions with high levels of turbulence. For the lateral system this is not critical and can be accomplished by moving filter parameter choices "up" the optimization curves of Figure 5-4 or 5-7.

5.4.1.2 Conclusions for the Lateral System - It seems evident from the data presented in this section that lateral system sensitivities to noise and data rate can be adequately designed out of the final approach system by intelligent choice of first order filter parameters.

The only exception to this involves the complication of adding an adjustment capability for estimated wind. In the event that noises higher than .02 deg. rms are encountered on the azimuth antenna, this becomes almost a necessity on windless days. (RTCA configurations, B, D, and E may have as much as .06 deg. rms "noise" according to Reference 2).

Satisfactory performance can be achieved with data rates as low as two samples per second providing that adequate care is taken in the selection of the filter parameters.

There is no doubt, however, that the higher data rates and lower noises give the filter designer more latitude and error margin in setting filter parameters, require lessiin the way of active parameter scheduling in flight, and provide generally more desirable performance characteristics.

5.4.2 The Vertical Control System

The results of Figures 5-9 through 5-12 are not as easily interpreted as those for the lateral system, however, let's proceed in a similar manner, choosing constant control activity throughout approach and observing variations in path to dispersion and pitch rate activity. This is done in Figures 5-16 through 5-18 for two values of elevator activity: 2.5 and 3.0 degrees rms. Figure 5-16 plots glideslope deviation as a function of range (or noise) for four data rates. Except possibly in the

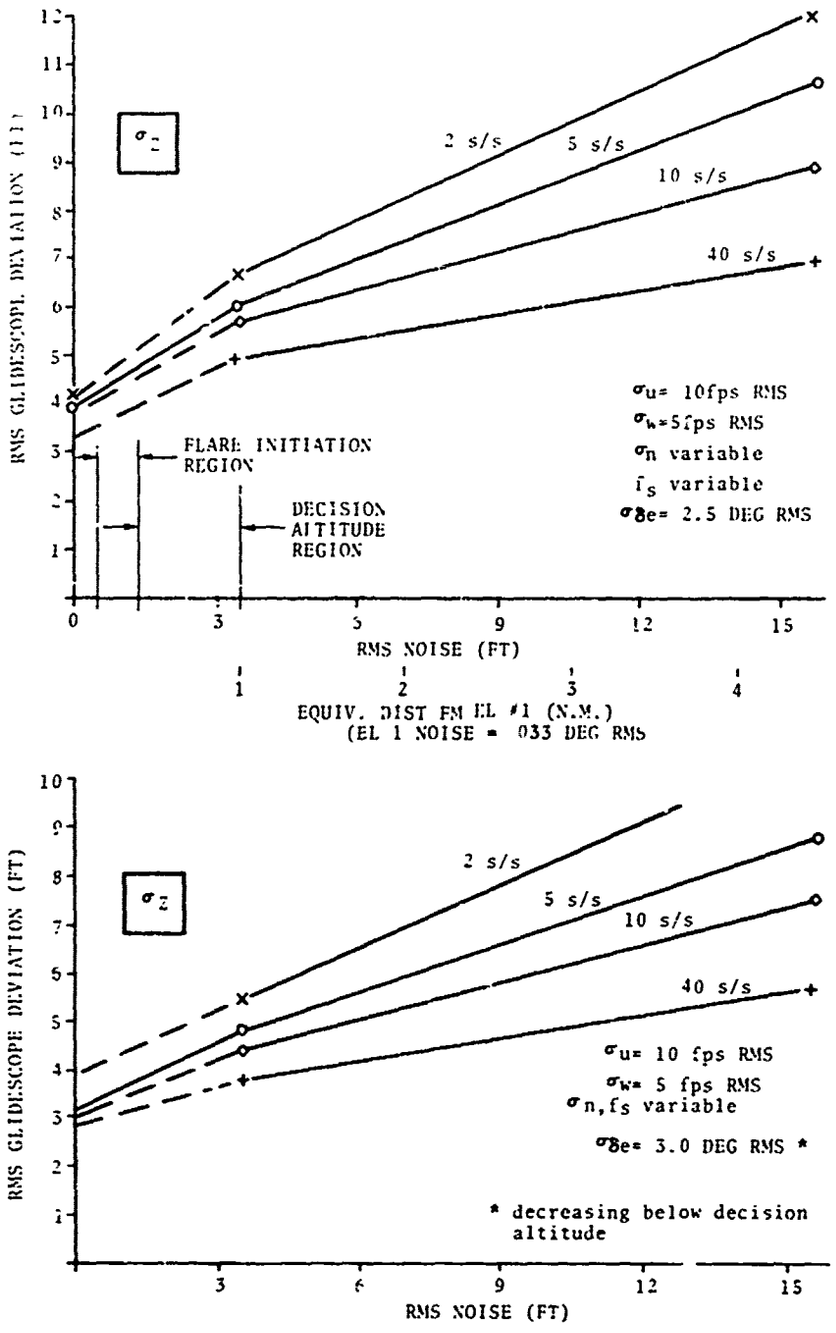

Figure 5-16. Glideslope Deviation Versus Distance from EL 1

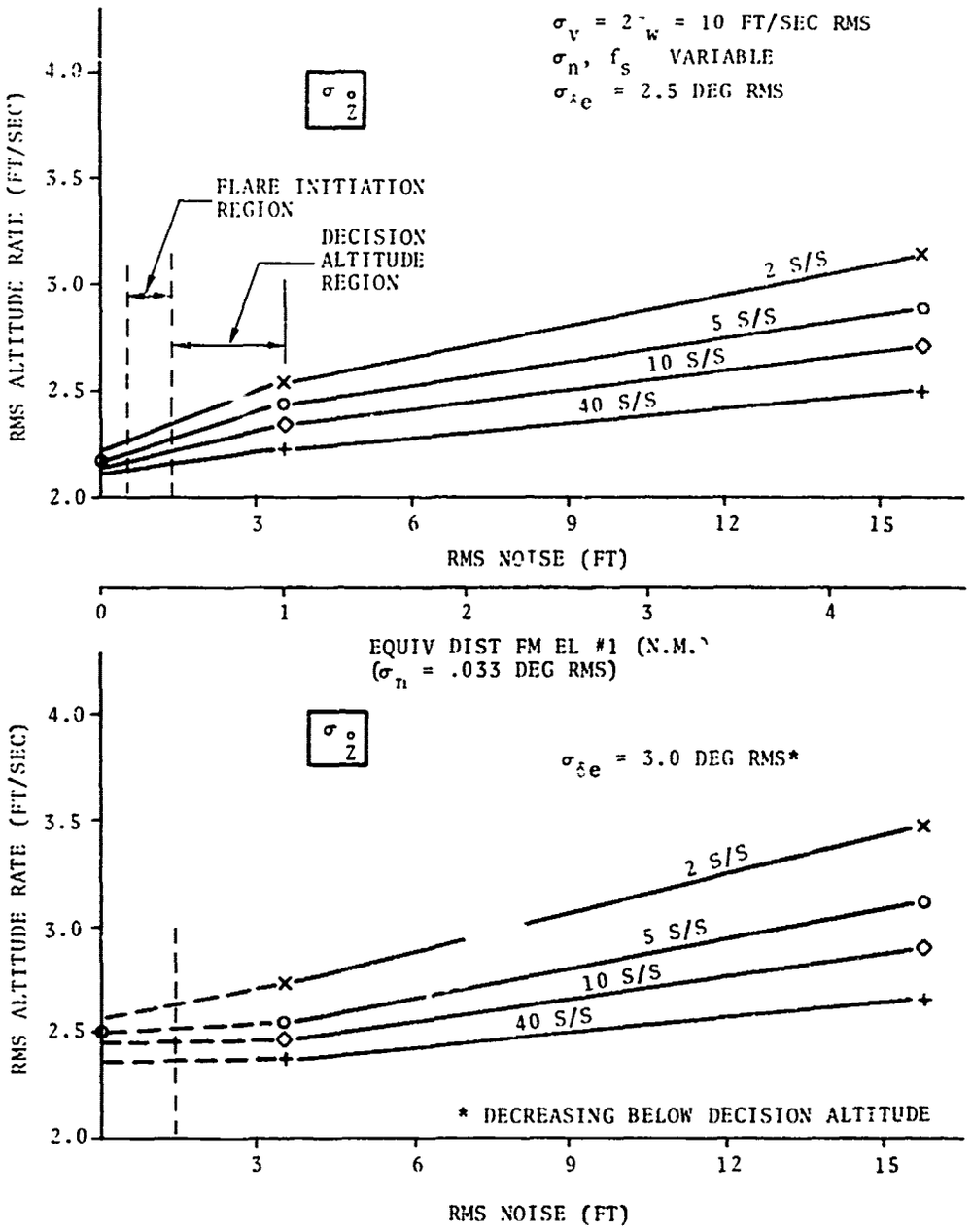

Figure 5-17. Altitude Rate Dispersion Versus Distance from EL#1

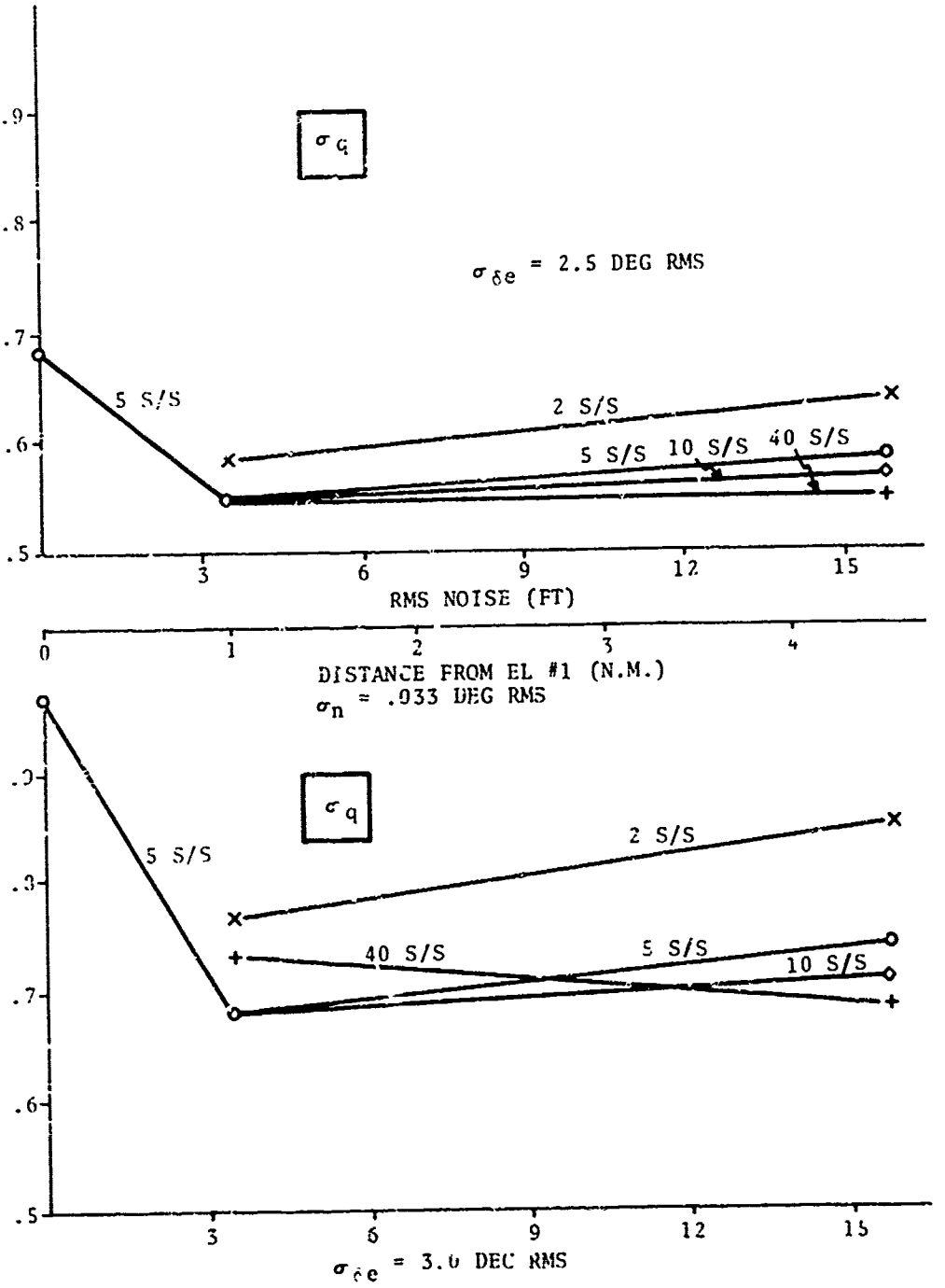

Figure 5-18. Pitch Rate Dispersion Versus Distance from EL#1

decision altitude region, the performance differences are minimal. In comparison with the Category II "window" dimension, ± 12 ft., the dispersions in the decision altitude region represent values in the range of 4σ (3 ft. rms at 40s/s, three degrees elevator activity, lower bound) to 1.8σ (6.6 ft. rms at 2s/s, 2.5 degrees elevator, upperbound). In terms of probability of not making the window this range represents seven in 10,000 to seven in 100. For the maximum wind condition for which this data applies a 93% probability of successful approach is probably acceptably high. An average value (5s/s, 2.5 deg. rms elevator, mid range) is closer to 97% under these conditions. Figure 5-19 presents this data from a different point of view, namely given at 100 ft. decision height, what are maximum noise - minimum data rates which will allow either a 95% or 99% level of success in meeting the 12 foot criteria? Four curves are shown for various levels of elevator activity, glideslope, and probabilities of success. It is clear from this set of curves that the choice of maximum noise or minimum data rate is still not obvious, and is thoroughly dependent upon variations in assumptions and criteria.

Pitch rate and altitude rate activity as depicted in Figures 5-17 and 5-18 show minimal sensitivities to data rate and noise when optimum filtering and constant elevator activity are imposed. These curves also provide no basis for firm decisions on data rate and noise.

5.4.2.1 Filter Parameter Scheduling - The effects of deleting parameter scheduling with range (or noise) will be similar to those for the lateral system. A fixed filter picked to minimize noise induced activity during the early portion of approach will show increased glideslope dispersion near decision height, while one picked to minimize decision height dispersion will allow possible unacceptable levels of control and attitude activity during early approach.

The effects of using a filter designed for maximum wind in a no wind condition are perhaps more pronounced for the vertical control system. As shown in Figure 5-20, even with range

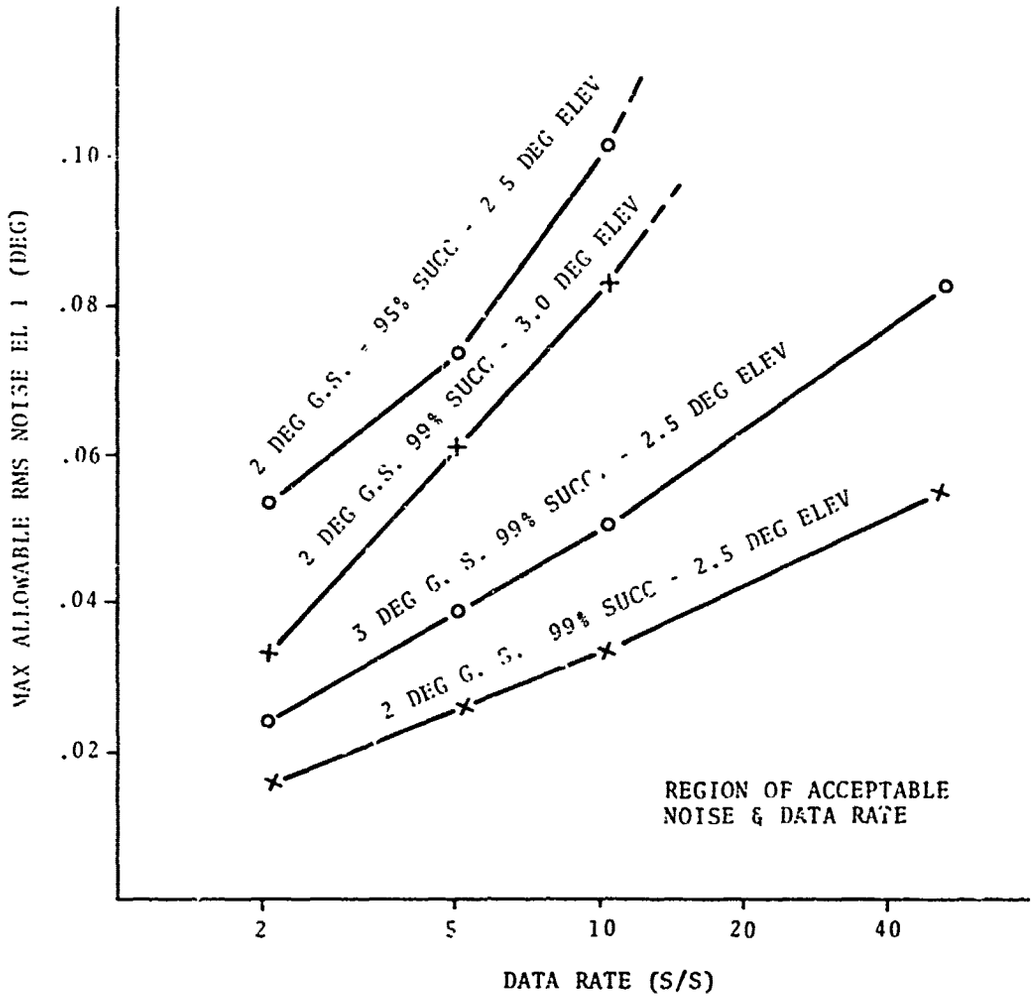

Figure 5-19. Beam Noise, Data Rate Tradeoff Elevation #1, for Various Conditions

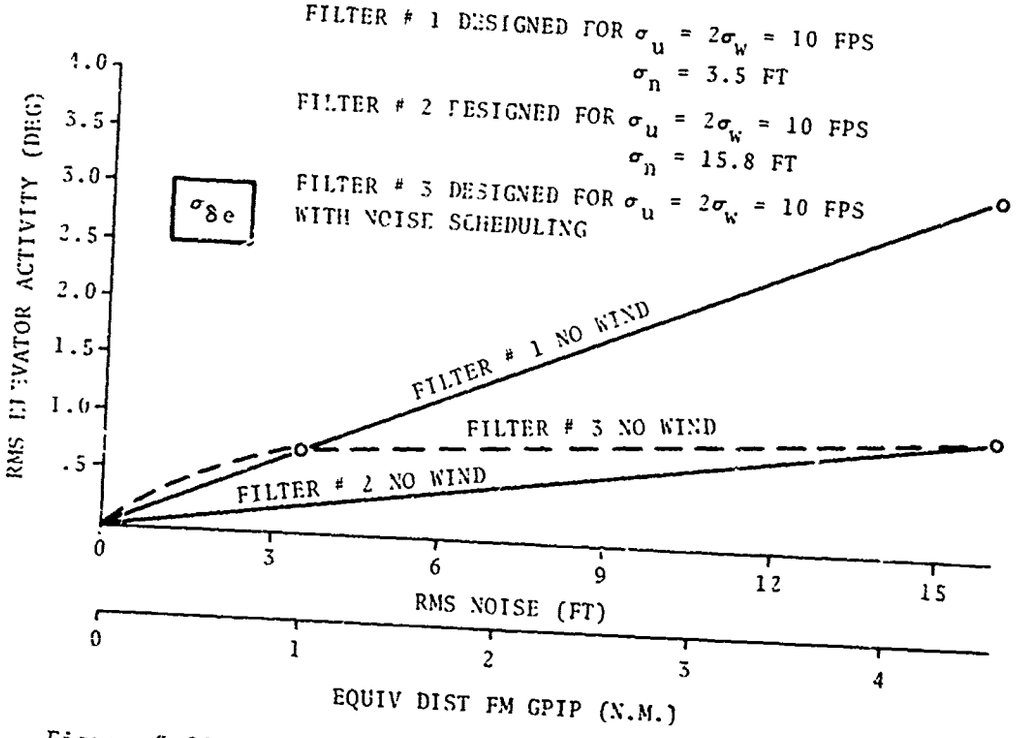

Figure 5-20. Effect of Filter Parameter Scheduling Vertical Channel

scheduling (filter #3) there is an almost constant one degree rms elevator activity level, unacceptably high for calm air.

The dual requirement for decision altitude performance in wind and low noise induced activity with low wind, for this system, makes parameter scheduling with wind and noise advisable if one is to achieve acceptable performance in both conditions.

5.4.2.2 The Importance of a Normal Accelerometer - All the data thus far presented for the vertical control system has been generated using a normal accelerometer as the primary rate and acceleration sensing device. Only very low frequency vertical velocity information was required from the MLS (below .015 rad/sec). In order to demonstrate the importance of a good high frequency source of information to supplement MLS derived velocity information, a limited set of data was generated without the benefit of

normal accelerometer velocity (by setting $K_{\ddot{h}}$ of Figure 4.3 to zero). Filter optimization conducted with maximum wind and 3.5 feet of noise for data rates of 40 and 10s/s yielded results which can be compared with the data of Figure 5-16. Figure 5-21 presents this comparison. The two points shown clearly indicate the indispensability of high frequency information for control purposes. Performance degradation without it is roughly equivalent to performance with five to six times as much noise or performance with data rates reduced by factors of 20 to 50. At 10s/s, instead of 99% success rate at decision height (see Figure 5-19), the success rate drops to 85 to 90% in maximum wind conditions

5.4.2.3 Conclusions for the Vertical System - Again for the vertical system, it is clear from the data presented that sensitivities to noise and data rate can be adequately designed out of the final approach system by intelligent coupler/autopilot design. It is also clear that performance is considerably more sensitive to coupler/autopilot/control system configuration than it is to data rate or elevator noise.

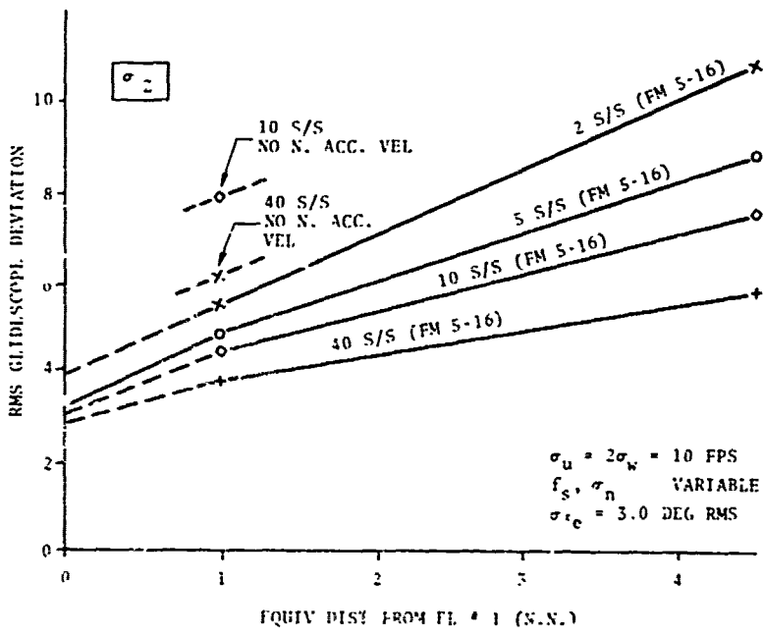

Figure 5-21. Rms Glidescope Deviation Versus Distance from EL#1 - With and Without Normal Accelerometer

5.5 CONCLUSIONS - MLS SIGNAL REQUIREMENTS FOR FINAL APPROACH

The ultimate questions to which the data of this section must be applied simply stated are:

a. What are minimum acceptable data rates for the MLS Azimuth and Elevation #1 functions?

b. What is the maximum allowable noise and its permissible characteristics for satisfactory final approach performance.

Unfortunately, the ultimate answers cannot be determined by performance analysis alone. There is no doubt that every factor in performance evaluation is affected by data rate increases or as noise decreases. The unknowns, of course, are the real benefits of improved performance versus the cost of higher data rates and lower noise. Even if firm limits for performance can be set (e.g., a probability of meeting the Category II window with certain control activity levels), there remains the tradeoff between ground based complexity and airborne system sophistication.

For instance, today's ILS ground stations are qualified for Category I, Category II, Category III, etc. conditions, yet there are some aircraft that are technically capable of making Category III landings at a Category I facility and some which could not make a Category I approach on a Category III beam. Therefore, it can be concluded that the ILS categorization and specifications presume performance characteristics of some "reference" airplane on final approach.

The definition of this "reference" airplane does not exist explicitly, either for ILS or MLS. This leaves a great deal of room for assumptions in performance analysis. Should the MLS be specified on the basis of Cessna 150 performance with a simple receiver and cross pointer display or on the basis of L-1011 performance with $500,000 worth of inertially augumented digital autopilot? Obviously, neither of these but some minimum configured craft in the spectrum between. Nor is the reference craft the

same for every visibility condition - that Cessna 150 under manual control could be qualified for Category I or Category II approaches but probably not for Category III (c).

In the absence of clearly defined ground rules such as these, and adequate assessments of capabilities versus cost and technical difficulty, the best that can be done with performance analysis is to provide data on the sensitivities of important performance characteristics to major system parameters and attempt to conclude from this the relative importance of the various parameters.

In terms of effectiveness of performance improvement alone, ignoring all other considerations, it is clear from the results of this section that the importance of various measures can be ranked, based on path following ability in turbulence as follows:

a. Addition of body mounted accelerometers.

b. Provision for suitable coupler filters with scheduling for wind and noise.

c. Decrease in angular noise of the Elevation #1 function.

d. Increase in data rate of the Elevation #1 function.

e. Decrease in angular noise of the Azimuth function.

f. Increase in data rate of the Azimuth function.

The implications of this ordering are unmistakable: the design of the airborne system is significantly more important to performance during final approach than the characteristics of the ground system. Previous work, reported in Reference 3, on conventional aircraft with no coupler modification to account for the switch from ILS to MLS, tends to reinforce this viewpoint. Because of the lack of proper filtering, these aircraft are very sensitive to MLS noise and maintenance of acceptable control activity levels for final approach for them will tend to set a maximum limit on allowable noise. However, a two or three position switch for filter scheduling based on estimated wind condi-

tions, built into the cheapest of the MLS receivers would alleviate this problem to a great extent, increasing the limit on allowable noise by a factor of two or three.

With all of the foregoing qualifications in mind, the following are proposed as safe minimum data rates and maximum white noise. Table 5-1 assumes no effort to smooth or filter data based on estimated turbulence. Table 5-2 assumes that such a filter is at least crudely implemented for every receiver.

TABLE 5-1. DATA RATE AND NOISE REQUIREMENTS - FINAL APPROACH - MINIMUM CONFIGURATION AIRCRAFT

	Minimum Data Rate	Maximum White Noise
Azimuth	2	.023 deg rms
Elevation #1	5	.033 deg rms

TABLE 5-2. DATA RATE AND NOISE REQUIREMENTS - FINAL APPROACH - COARSE WIND-SELECTABLE FILTERING

	Minimum Data Rate	Maximum White Noise
Azimuth	2	.1 deg rms
Elevation #1	5	.1 deg rms

It is also possible to provide some measure of tradeoff between noise and data rate. The majority of data in this report and in Reference 3 indicates that equivalent performance in path following ability and satisfaction of acceptable flight criteria is obtained if the data rate is quadrupled for every doubling of the noise. In Table 5-1 for instance, if it were found that the minimum feasible azimuth noise were .05 degrees rms instead of .023, then the data rate would have to be moved from two to eight samples per second to achieve similar performance.

Before closing this section, it is necessary to reiterate emphatically that the benefits of higher data rates and lower noise are indisputable and that, regardless of assumptions concerning airborne equipment, better than minimum signal characteristics will provide better than minimum performance. The final decision must await careful cost-benefit analysis.

5.5.1 Requirements for Lower Configurations

In discussion to this point Category II and Category III facilities have been assumed. What are signal requirements for lesser facilities such as the RTCA configurations B and D? Since the primary noise limitation evolves from maintaining acceptable control activity during approach, any degradation in noise specifications will adversely affect the performance of minimum configuration aircraft to the point of unacceptability; the same arguments apply for data rate consideration. Therefore, Tables 5-1 and 5-2 are deemed applicable to all configurations.

6.0 REQUIREMENTS FOR FLARE

The flare, or flareout, maneuver forms the transition from final approach configuration to landing configuration; dynamically, the primary goal of flare is to reduce aircraft sink rate from its value on the glideslope (6 to 15 ft/sec) to one suitable for landing (1.5 to 2.5 ft/sec). Other constraints on the maneuver include maintaining a proper landing attitude and avoiding large accelerations. Any flare control law must also avoid issuing increased sink rate or negative pitch commands during flare. Current jet transport CTOL flare maneuvers are initiated about 50 ft. wheel height and take between seven and 15 seconds to complete.

6.1 FLARE LAWS AND GEOMETRY

The flare law provides the guidance signal to the aircraft autopilot; it generates commands based on the current altitude and/or range of the aircraft to appropriately control the transition in altitude rate. The most common form commands altitude rate as a function of altitude according to Equation 6-1.

$$-\dot{h}_c(t) = Kh(t) - \dot{h}_{td} \qquad (6\text{-}1)$$

subject to initial conditions:

$$-\dot{h}_c(t_i) = -\dot{h}(t_i) = Kh(t_i) - \dot{h}_{td}$$

$\dot{h}_c(t)$ = commanded altitude rate

$\dot{h}(t)$ = actual altitude rate

$\dot{h}_{td}$ = desired altitude rate at touchdown

$h(t)$ = altitude

t_i = flare initiation time

This is the so-called exponential flare law; assuming that the aircraft follows perfectly and that no other disturbances are encountered, altitude and altitude rate are exponential functions of time and range as shown in Figure 6-1. Under the conditions of Equation 6-1, control of the aircraft is exercised in only one dimension, the vertical, and does not explicitly regulate longitudinal touchdown position. There are other one-dimensional flare laws based on commanding pitch or pitch rate, but their object is the same, assuring that sink rate at touchdown is acceptable.

6.1.1 Two Dimensional Flare Laws

It has been suggested at various times in postulating the role of MLS in flare control, that it will allow two dimensional control, through a segmented glideslope, e.g., 3° on EL1, 0.5° on EL2, as shown in Figure 6-2. There are multiple problems with such a strategy:

a. Touchdown position and time depend on airborne antenna height with respect to EL2 height.

b. The nominal touchdown point is almost laterally adjacent to the EL2 antenna and assuming coverage is required to touchdown, EL2 coverage must be very wide angle (or possibly with offset centering).

c. The two segment approach requires flying a fixed path in space, which may lead to dangerous pitch down commands at very low altitudes.

d. The transition from one path to another is not straightforward.

It is possible to exercise some control over longitudinal touchdown point using the exponential flare law and adjusting flare altitude, $h(t_i)$, and gain, K, based on initial condition evaluation. The product $Kh(t_i)$ is fixed by the initial condition on Equation 6.1 to avoid step commands in altitude rate at flare initiation, but within this limitation, K and $h(t_i)$ can take on a wide range of values. From Appendix C it is seen that given an

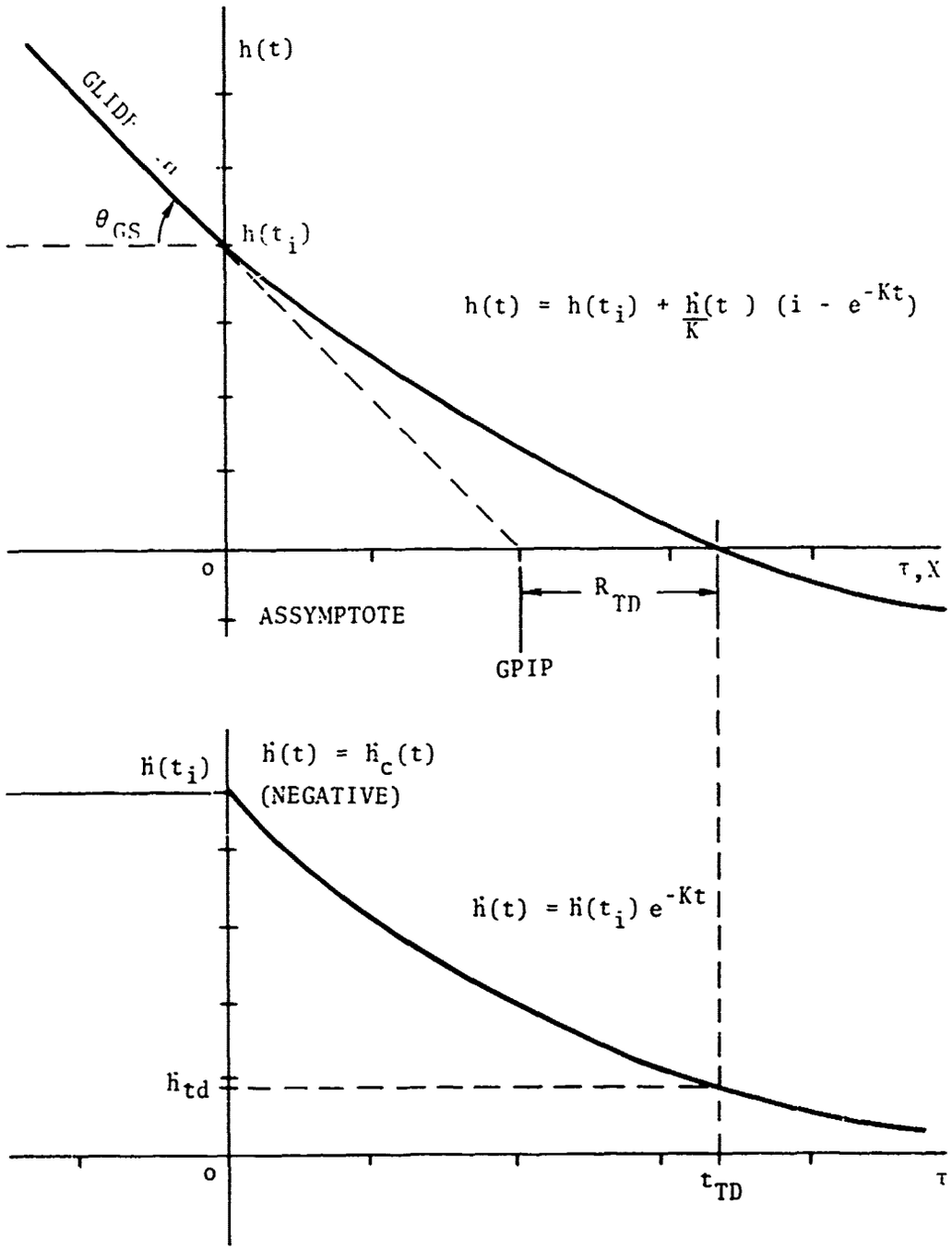

Figure 6-1. Ideal Flare Maneuver

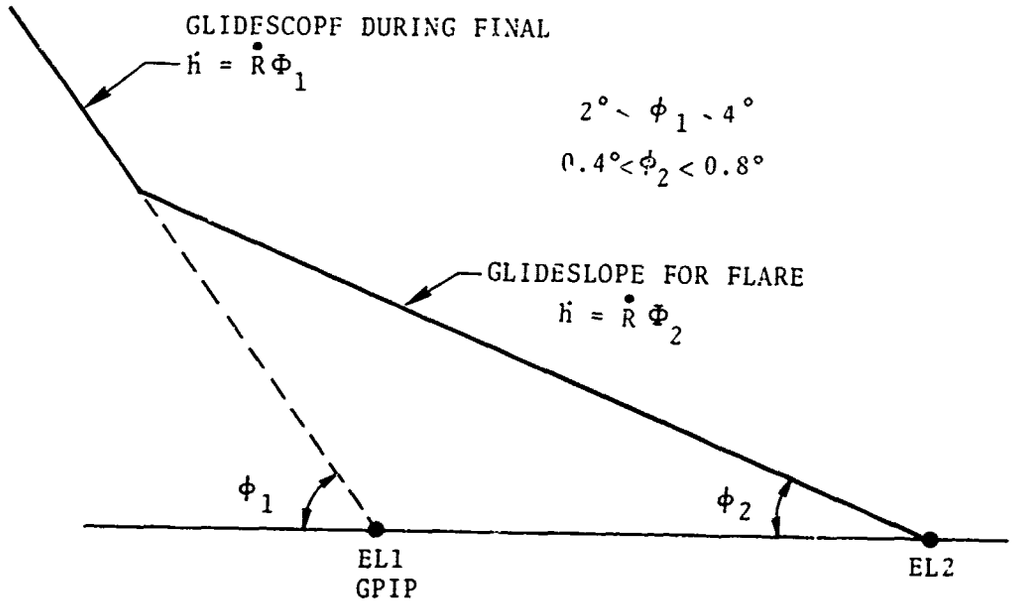

Figure 6-2. Ideal Segmented Glideslope in Lieu of Flare.

initial altitude rate and a desired final altitude rate and touchdown position it is possible to choose an initiation altitude ($h(t_i)$) and exponential time constant (1/K) such that the desired conditions are met in the absence of disturbances during the maneuver. The equations for h and K are given in Equation 6-2 below.

$$h(t_i) = \frac{R_{td}\ \phi_1\ (t)}{\left|\frac{\dot{R}\ \phi_1\ (t)}{\dot{h}(t) - \dot{h}_{td}}\right| \text{Log}_e \frac{\dot{h}(t)}{\dot{h}_{td}} - 1}$$

$$K = \frac{\dot{R}\phi_1(t)\ \text{Log}_e \frac{\dot{h}(t)}{\dot{h}_{td}} + [\dot{h}(t) - \dot{h}_{td}]}{R_{td}\ \phi_1\ (t)}$$

R_{td} = range from GPIP to desired touchdown

$\dot{R}$ = range rate or ground speed (assumed constant)

$\dot{h}(t)$ = measured current altitude rate

$\phi_1(t)$ = measured current EL1 angle

$\dot{h}_{td}$ = desired final altitude rate.

In practice, one would periodically compute anticipated flare altitude during the last few moments of final approach based on current estimates of $\dot{R}$, $\dot{h}(t)$ and $\phi_1(t)$. Flare is then initiated when measured altitude is equal to computed flare altitude. This is not a trivial task; it requires significant computational capability, frequent updates and well designed smoothing and prediction filters for estimates of both anticipated flare altitude and current measured altitude. It does not account for disturbances encountered during flare.

No flare law can exercise control during flare against the possibility of a long landing without violating the ground rule prohibiting pitch down commands. Once a disturbance causes the aircraft to be above its nominal flare path, there is no alternative under this ground rule except to continue on a new path, parallel to the nominal and to accept resultant longitudinal dispersion. In other words, the commanded sink rate should never be greater than that indicated by Equation 6-1., regardless of longitudinal position. The only acceptable method of two dimensional control therefore, involves choosing flare law parameters as judiciously as possible prior to initiation, and maintaining tight closed loop control on altitude rate performance in the presence of turbulence and shear.

6.1.2 Siting Geometry for Flare

It is generally assumed that the EL1 antenna is located a few hundred feet off the runway centerline, about 1000 feet from the threshold. Any EL1 referenced angle has its vertex at the Glide Path Intercept Point (GPIP). The constraints on the placement of EL2 are conflicting. If EL2 is a primary landing aid, then

signal availability must be insured at touchdown for long landing as bad as the 5 or 6 sigma probability level. The further from nominal touchdown the antenna is placed, however, the worse the linear error at nominal touchdown for a given angular error at nominal touchdown for a given angular error or noise level. The distance from the GPIP to nominal touchdown for the ideal exponential flare from 50 ft. altitude is shown in Figure 6-3 as a function of ground speed and glideslope. If allowance is made for a worst case 5 second time dispersion at 300 ft/sec (1500 ft) groundspeed plus the distance from GPIP to nominal touchdown (Figure 6-3) of 1000 ft., then EL2 coverage must be available to 2500 ft. beyond the GPIP. Any closer causes the risk of flying out of the coverage before touchdown to increase. Figure 6-4 shows the resultant geometry and plots distance from flare initiation to EL2 as a function of glideslope and flare altitude.

6.2 AUTOPILOT FOR FLAREOUT

Figure 6-5 diagrams the components of the autopilot used for flare in this sutdy. The primary difference between this and a more conventional design is the use of MLS derived altitude and altitude rate in lieu of altimeter and altitude rate sensor. The normal accelerometer provides high frequency rate information (above .02 rad/sec) through the complementary filter. The presence or absence of the accelerometer is one of the variables in the performance analysis.

6.3 PERFORMANCE CRITERIA AND EVALUATION

The ultimate criteria on performance during flare consists of assuring proper attitude, position and velocity at touchdown position is also important. Performance evaluation and results discussed in this chapter will concentrate on these two variables. In addition, to the flare law parameters, the following disturbances or errors affect the abilityyto control sink rate and touchdown position:

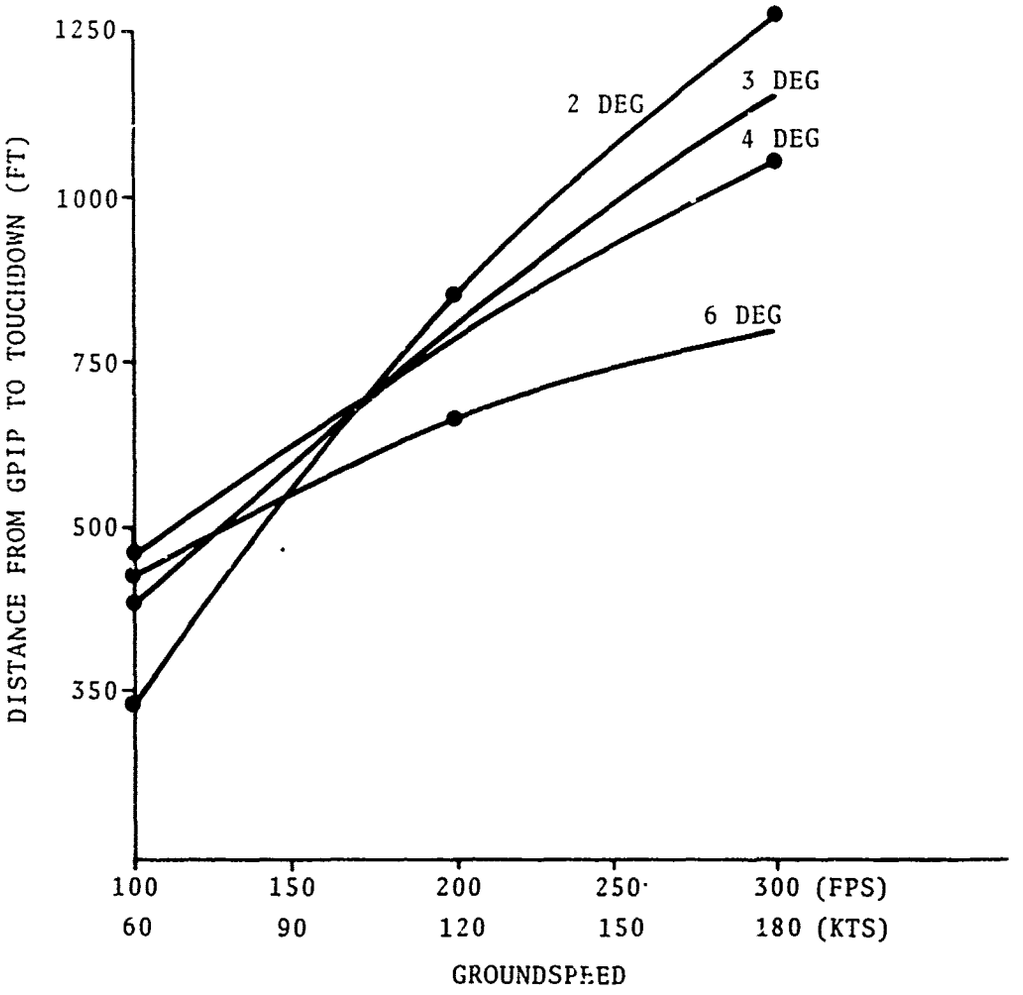

Figure 6-3. Nominal Distance GPIP to TD vs Ground Speed & Glideslope.

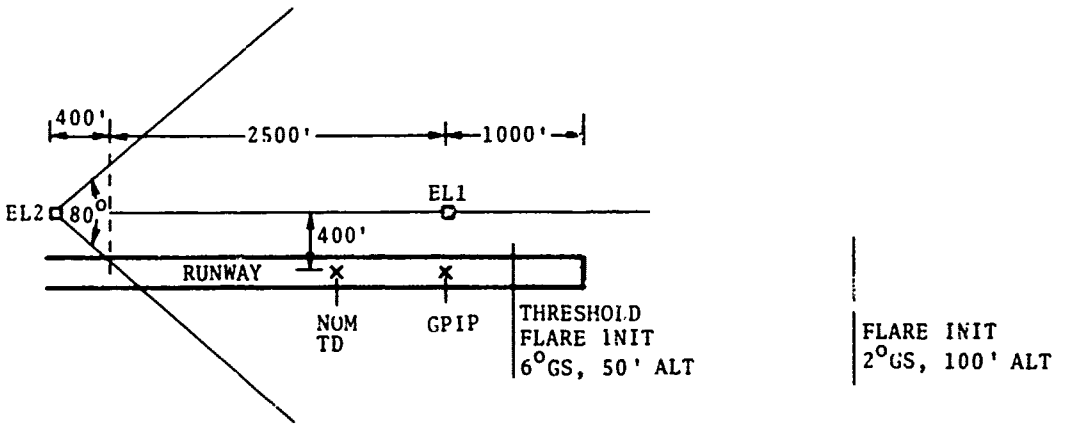

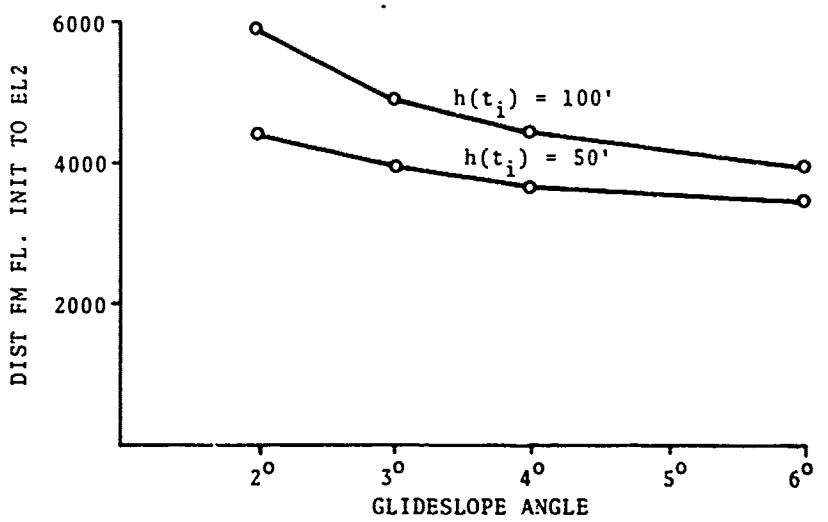

Figure 6-4. Geometry of EL2 Placement

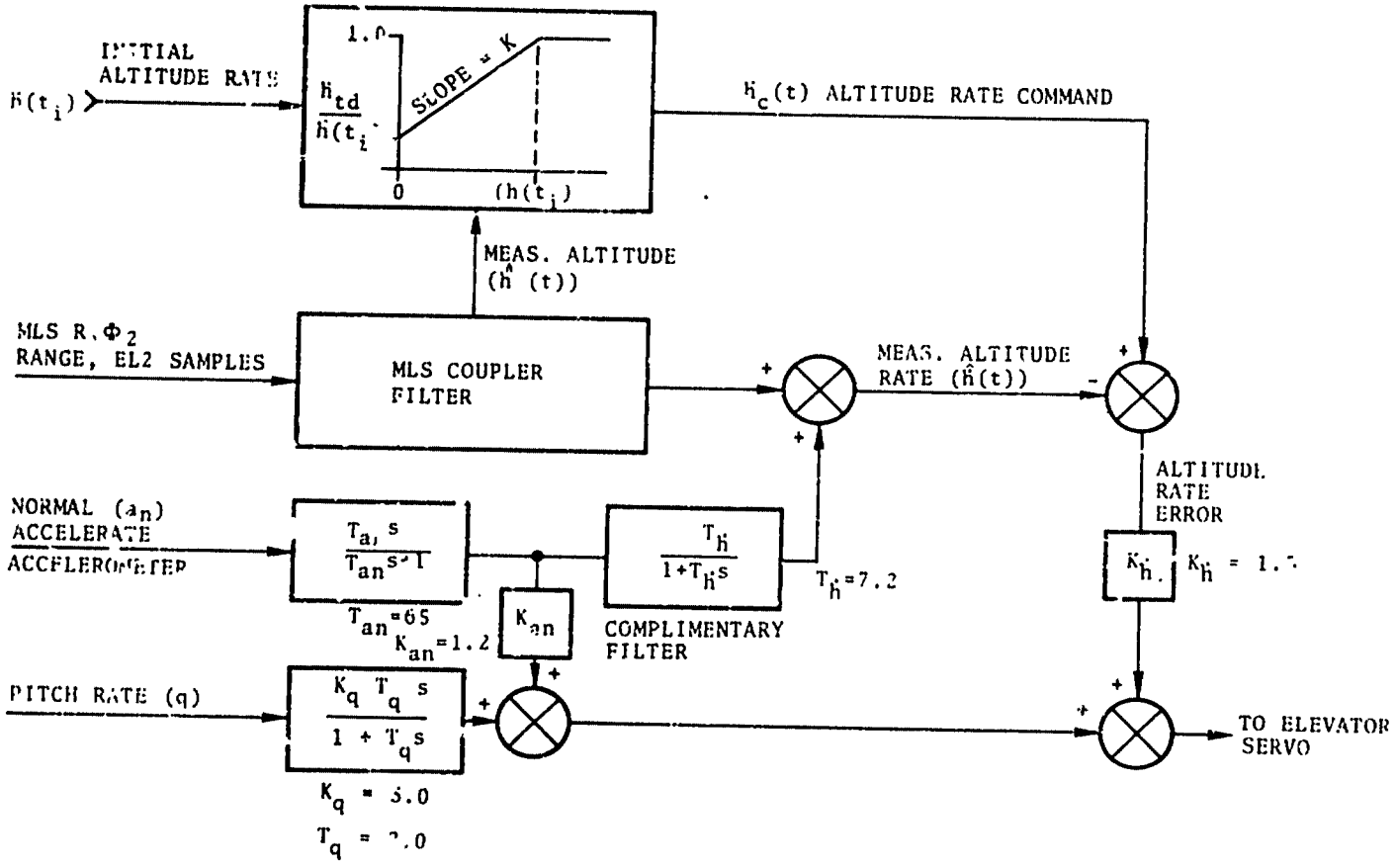

Figure 6-5. Flare Autopilot

a. Initial condition errors

b. Initial measurement errors

c. Wind gusts

d. Measurement noise

e. Control system lag

f. Wind shear

It will be assumed that the effects of these six items can be treated independently. Although not strictly correct due to the nonlinear influence of ground effect, the assumption will allow a reasonably simple treatment and a determination of the relative importance with respect to touchdown performance and its sensitivity to data rate, noise and control system configuration.

6.3.1 Initial Condition and Initial Measurement Errors

Two initial condition errors may be important to the success of the flare maneuvers: initial altitude rate and glideslope deviation at flare initiation. Deviations in initial altitude rate are compensated for in the flare law of Equation 6.1 by suitably adjusting the product $Kh(t_i)$. If this complexity is not undertaken however, there will be a step command in altitude rate at flare initiation. The subsequent transient will result in acquisition of the nominal exponential trajectory prior to touchdown; however, the trajectory will be displaced longitudinally resulting in short landings for higher than nominal altitude rate and long landings for lower than nominal. This is illustrated in Figure 6-6. The magnitudes of the errors are dependent upon control system characteristic and characteristics of the nominal flare maneuvers. Uncompensated glideslope deviation at flare initiation produces a deterministic effect on longitudinal touchdown position as a function of ground speed and initial altitude rate. According to equation 6.3

$$\delta R_{td} = \dot{R}\delta z_{fl}/\dot{z}_{fl} \simeq z_{fl}/\phi_1 \qquad (6.3)$$

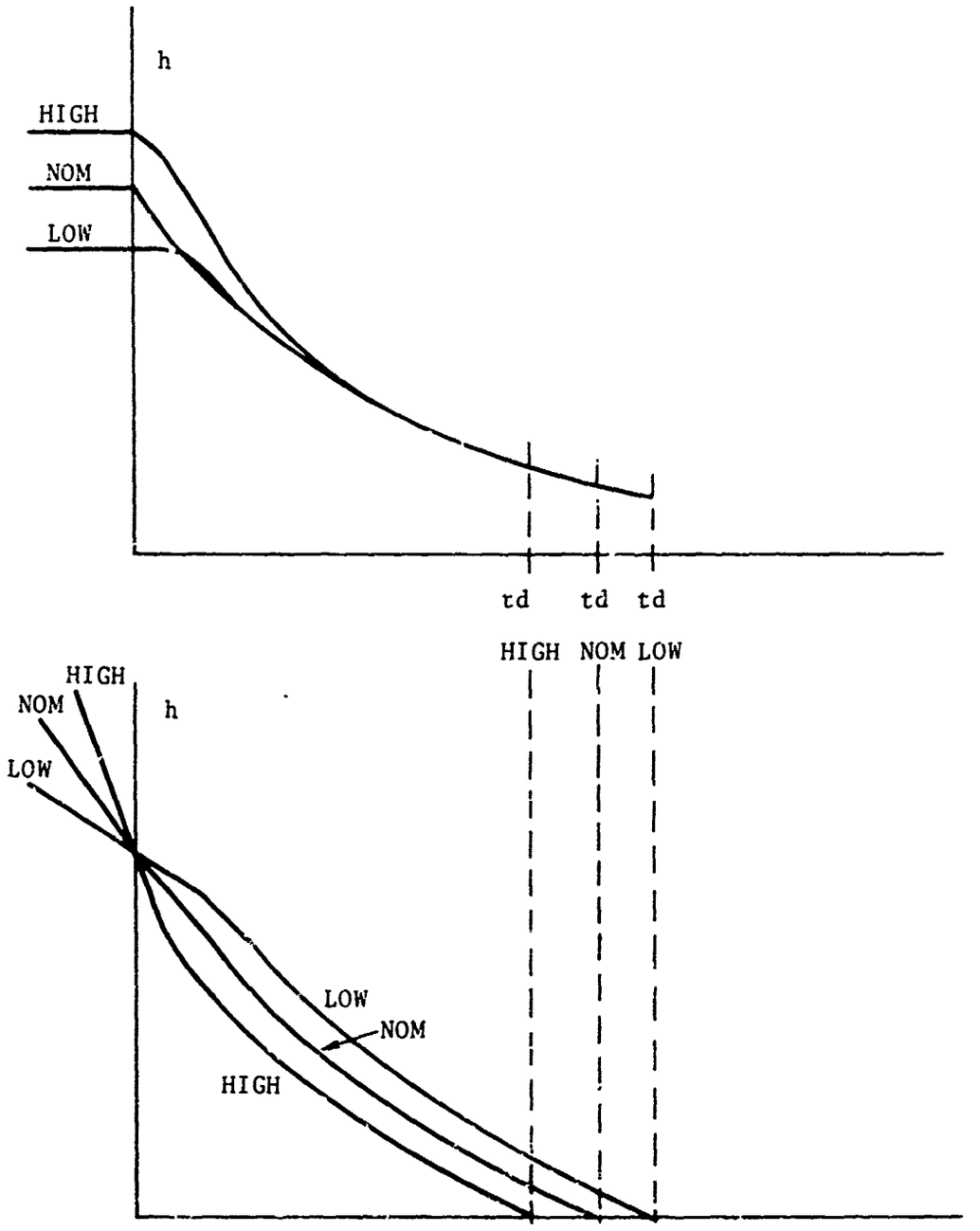

Figure 6-6. Effects of Initial Deviation in Altitude Rate

$\dot{R}$ = ground speed (ft/sec)

δz_{fl} = glideslope deviation at flare (ft)

$\dot{z}_{fl}$ = altitude rate at flate (ft/sec)

ϕ_l = glideslope angle (rad)

For example, a five foot glideslope deviation on a 3 degreee glideslope produces an error in touchdown position of about 100 ft. This effect can be compensated for by setting flare parameters according to Equations 6.1 and 6.2.

Using the adaptive flare laws of Equations 6.1 and 6.2 presumes the ability to adequately measure the parameters required to properly set $h(t_i)$ and K. These parameters include ground speed altitude, altitude rate and ELI angle. Design of measurement techniques and calculation of sensitivities to measurement errors for the various control laws has not been undetaken in this study. There is no doubt that this represents an important area of investigation both for determination of performance sensitivity of flare parameters and for assessing the effectiveness of the more complex adaptive flare laws. With respect to data rate and noise requirements, however, the rationale of Section 5.2.2 is also applied here: The ability to measure and predict based on sampled data where the output is the evaluation of a single set of parameters should prove significantly less a problem than using the same data to provide adequate control. Effective control of a complex system requires significant lead compensation or high frequency information in order to overcome its inherent lag. It's a tautology to state that the control system must sense or "know" it has an error before it can compensate for it, that its ability to measure is better than its ability to control. For strictly measurement purposes, therefore, more filtering and smoothing are possible, decreasing the effects of measurement noise on the quality of the measurement.

While thus acknowledging the existence of the problem, this study has assumed that measurement techniques are indeed available which can be suitably applied in order to reduce the effects of measurement errors to second order. Further it would seem that such

measurements could be achieved through the use of DME and EL1 alone.

6.3.2 Measurement Noise and Wind Turbulence

In considereing random disturbances, a procedure similar to that of Section 5.0 was undertaken. An optimum filter was selected for each set of conditions under consideration; the filter was optimized with respect to altitude rate dispersion and control activity. The primary variable for this portion of the study in addition to data rate and noise, was degree of utilization of normal accelerometer data, in an attempt to determine which information is critical to performance during flare. A full set of data considering all combinations of all options has not been generated; however, data from selected sets of conditions has led to the ability to form several important conclusions. The list of options considered is presented as Table 6-1.

TABLE 6-1. CONFIGURATIONS CONSIDERED FOR FLARE PERFORMANCE ANALYSIS

D.R.	NOISE	POSITION	VELOCITY	ACCELERATION
1. 10 s/s	1 f	EL2	EL2 + N. Acc	N. Acc.
2. 10 s/s	1 ft	EL2	EL2	None
3. 10 s/s	2 ft	EL2	EL2	None
4. 2 s/s	1 ft	EL2	EL2	None
5. 2 s/s	2 ft	EL2	EL2	None
6. 10 s/s	1 ft	EL2	EL2	N. Acc
7. 10 s/s	1 ft	EL2	EL2 + N. Acc	None
8. 10 s/s	1 ft	EL2	EL2	EL2

Under the column labeled noise, 1 ft. rms represents .035 deg. rms 1500 ft from the EL2 antenna (appropriate nominal touchdown point); 2 ft. rms represents either .07 deg. rms at the same point or .035 deg. rms at 3000 ft. from EL2 (approximate flare initiation point). The sources of control system information for position, velocity and acceleration are listed in columns with those respective headings. Two options are considered for velocity information: the combined output of low frequency EL2 information and

high frequency integrated normal accelerometer (NAcc) information; and velocity derived only from the first difference of the EL2 data. Three options for acceleration data were considered: acceleration from the NAcc; no acceleration information; and acceleration data derived only from the second difference of EL2 position samples. (The presence of DME data to convert EL2 angular information to linear information is assumed; DME errors and characteristics have not been considered however, since they will only contribute second order effects; see Section 5.1). Option 1 represents a baseline case with "best" acceleration and velocity information as generated from the normal accelerometer. Options 2 through 5 consider data rate and noise variations with velocity information derived solely from the MLS Range and EL2, and no acceleration information. Option 6 adds acceleration information from the normal accelerometer but continues to rely on MLS for velocity. Option 7 uses no acceleration information but derives velocity primarily from the accelerometer (Nos. 6 and 7 are not realistic configurations but demonstrate the relative importance of good acceleration or velocity information). Option 8 again uses only MLS for velocity and provides an acceleration signal also derived solely from MLS.

The performance in altutude rate for these eight cases is shown in Figure 6-7, plotted against elevator activity. (It must be recalled here that these data are not statistically valid in an absolute sense since they do not include ground effect).

The following comparative statements apply:

a. Attitude rate dispersion is relatively insensitive to data rate (compare 2 with 4 and 3 with 5)

b. Altitude rate dispersion is relatively insensitive to noise (compare 2 with 3 and 4 with 5)

c. Altitude rate dispersion is significantly decreased when acceleration information from the normal accelerometer is available (compare 1 and 6 with 2 and 8)

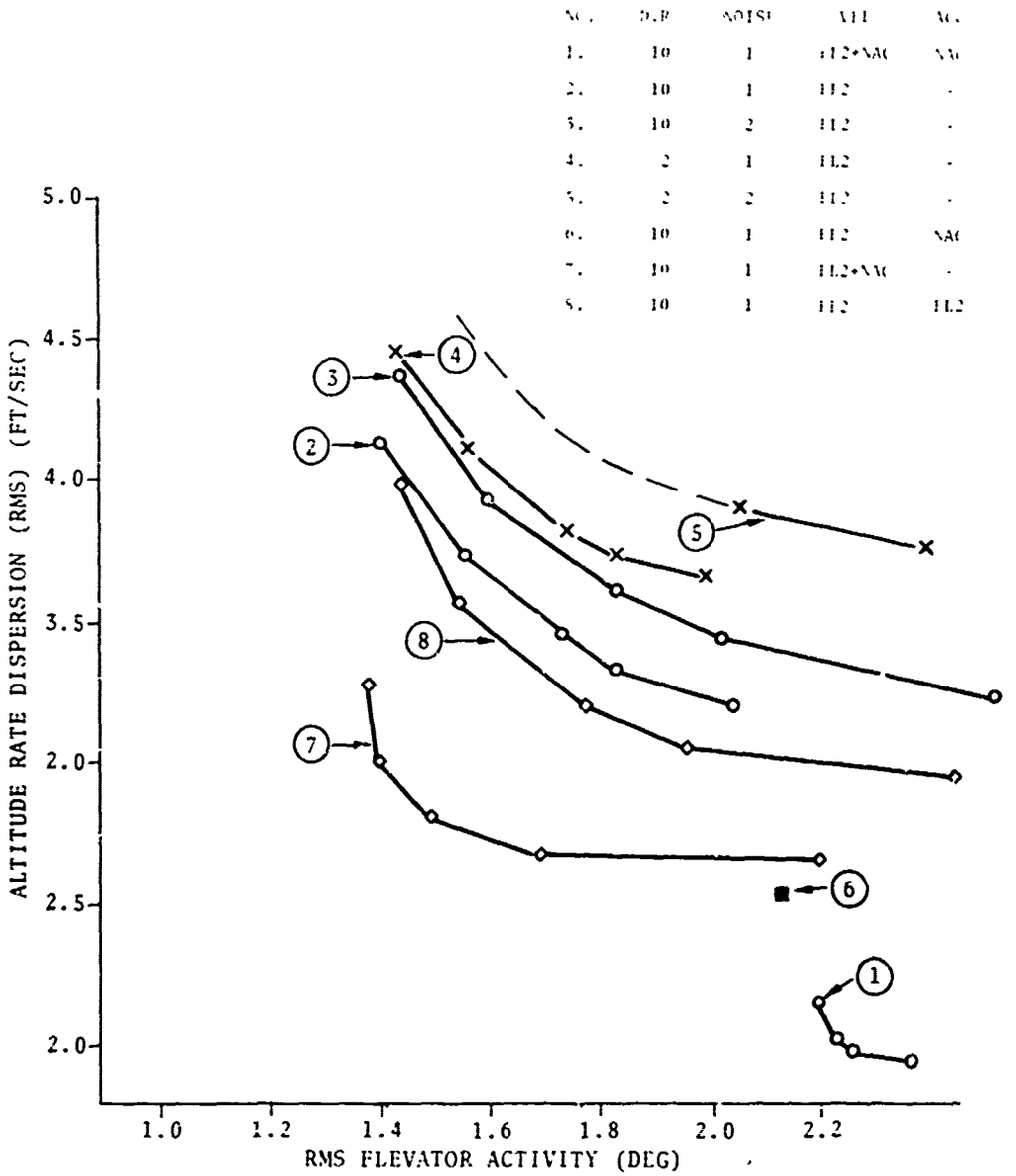

Figure 6-7. Altitude Rate Dispersion with Optimum Filter for Various Flare Configurations.

d. Some improvement is achieved using good high frequency velocity information in the absence of an acceleration signal (compare 7 with 2)

An understanding of the rationale behind these data is essential to further interpretation and generalization. The spread of these curves indicates primarily one thing: the capability of each control configuration to anticipate and correct for turbulence induced deviations from the nominal altitude rate profile. The higher the order of the information sensed in terms of spectral content, the better that deviations can be anticipated; for instance, acceleration is the rate of change of velocity, therefore, a direct knowledge of acceleration is essentially an indication of the current trend of velocity; if this trend is in an undesireable direction, correction can begin prior to actually detecting a velocity deviation, making for a tighter velocity control loop.

The source of the higher order information (acceleration, velocity) has much do do with its effectiveness. In the case of the normal accelerometer, the acceleration signal is directly generated and can be easily integrated for high frequency velocity information. With MLS, which provides only position information, the signal must be effectively differentiated twice to obtain acceleration. In the absence of any noise on the position samples this requires only that the data rate be high enough such that it encompasses the spectrum of the acceleration information. If the signal is noisy, further complications develop. The act of differencing or differentiating successively multiplies the noise level by the sampling frequency. (e.g., if position noise is 1 ft. rms for 10 s/s position information, it is 10 ft/sec rms for derived velocity and 100 ft/sec^2 rms for derived acceleration; although, spectral content varies, there may still be significant noise within the frequency band of interest. When a filter which includes derived rate or acceleration is implemented and optimized in the presence of noise, then the parameters adjust themselves such that only low frequency information is passed, essentially negating the effect or the attempted derivation in the first place. This is illustrated by comparison of curve 8 (derived velocity, derived acceleration) with curve 2 (derived velocity, no acceleration);

there is little substantive difference in these two curves. However, when MLS derived velocity with acceleration from the N. Acc is used, the point labeled 6 results (a single optimization was performed for condition six).

One further manipulation of the data of Figure 6-7 serves to illuminate the relative differences in performance of the various configurations. If it is assumed that the dispersions in altitude rate achieved in case 1 were maximum allowable for safety, then the other cases could be brought down to this level by restricting the maximum allowable wind to some lower levels. Such an exercise produces estimates of allowable worst case winds as shown in Table 6-2.

TABLE 6-2. EQUIVALENT MAXIMUM ALLOWABLE HEADWIND FOR SAFE TOUCHDOWN

CASE	D.R.	NOISE	VEL	ACC	MAX WIND
1	10	-	EL2 & N. Acc	N. Acc	25.0 kt.
2	10	-	EL2	-	14.9
3	10	2	EL2	-	14.2
4	2	1	EL2	-	13.3
5	2	2	EL2	-	12.8
7	10	1	EL2 & N. Acc	-	17.8
8	10	1	EL2	EL2	15.6

Under these assumptions the best that could be achieved in the absence of a normal accelerometer lies between 7 and 8 - a limiting head-wind of 16 or 17 knots. According to the FAA advisory circular 20-57A (reference 6) this wind is exceeded about 8 percent of the time, while the reference wind, 25 knots, is exceeded only 1 percent of the time. The aircraft with no acceleration information would be prohibited from landing eight times more frequently than a similar aircraft with acceleration data.

6.3.3 Control System Lags and Wind Shear

The effects of these two disturbances have not been considered explicitly in this study. However, the results of the foregoing sections provide sufficient insight to allow conclusions to be drawn with respect to them.

Control system lag in the absence of ther disturbances will result in a deterministic effect which essentially causes the true altitude rate to lag commanded altitude rate. Altitude rate at touchdown will therfore be higher than nominal. This effect can easily be calibrated out, however, by adjusting the flare parameters. Dynamic lag, on the other hand is precisely that which was under examination in the last section; the filtering required under varying conditions varies the control loop response time; high altitude rate dispersion is indicative of greater lags, sloppier control loops, and a less responsive system.

Wind Shear can be considered a special case of wind turbulence. The mechanism by which it affects the aircraft is the same. There is no reason to believe that performance under shear condition is not affected by data rate, noise, and control system configuration in an analogous manner. Therefore, conclusions to be drawn with respect to performance in turbulence can also be applied by implication to performance in shear.

6.4 CONCLUSIONS

The primary conclusion toward which the work of this chapter is directed is that a normal accelerometer or other inertial source of acceleration information is required for adequate performance during flare. A flare control system without it performs poorly in turbulence and may be severely limited in allowable operational environment. If this conclusion is accepted then there is every advantage to deriving velocity information from the accelerometer also. The only information required of EL2 then is altitude for gain scheduling and low frequency velocity data. However, this information could also be provided with either a barometric or radio altimeter which is calibrated during final approach using DME,

EL1, and normal accelerometer data. The calibration is easily accomplished by integrating the difference between computed altitude and altitude rate given by the altimeter. This effectively corrects the output of the altimeter to ground and inertial referenced quantities and requires the altimeter to operate stably on its own, providing corrected altitude and low frequency altitude rate data, for a period of less than 15 seconds.

What then is the role of EL2? From a flight performance point of view it appears that EL2 is the proverbial fifth wheel. It has no function which cannot be provided adequately by other currently available on-board sensors. Its only possible role is one of redundancy and reliability but its benefits in this role have yet to be clearly studied.

It would seem that a reassessment of the requirements for EL2 should be undertaken along these lines; its effectiveness as sole primary landing guidance aid for flare is definitely limited.

7.0 OTHER AREAS OF INVESTIGATION

7.1 AZIMUTH SIGNAL REQUIREMENTS FOR ROLLOUT GUIDANCE

A rollout control system was designed for the CV-880 as described in Appendix D. A limited number of exercises with respect to data rate and noise were conducted. As originally suspected, it was found that rollout performance should not have a limiting influence on MLS azimuth signal characteristics.

The control system uses rudder steering from touchdown (groundspeed 225 fps) to a point at which airspeed decreases to 120 fps; nosewheel steering is then phased in and contiues to stop. For the purposes of the simulation deceleration was considered constant.

The use of DME to assist in high speed turnoffs was not considered.

The results of simulation runs for the following sets of conditions are presented:

- Figure 7-1. Response to initial position offset at touchdown:
  Data Rate = 40s/s 2s/s;
  Noise = none
- Figure 7-2. Response to MLS Noise No Wind;
  Data Rate = 40s/s, 1s/s
  Noise = .023 deg rms
- Figure 7-3. Response to Crab Angle at touchdown (4 deg);
  Data Rate = 40s/s, 1s/s;
  Noise = none
- Figure 7-4. Response to Crosswind Gusts (5 fps rms);
  Data Rate = 40s/s, 1s/s;
  Noise = none

In contrast to work on final approach and flare, no attempt was made during the design to specifically consider effects of data rate and noise. As a result, the control activity at lower data rates exhibits undesirable oscillations in most cases. From

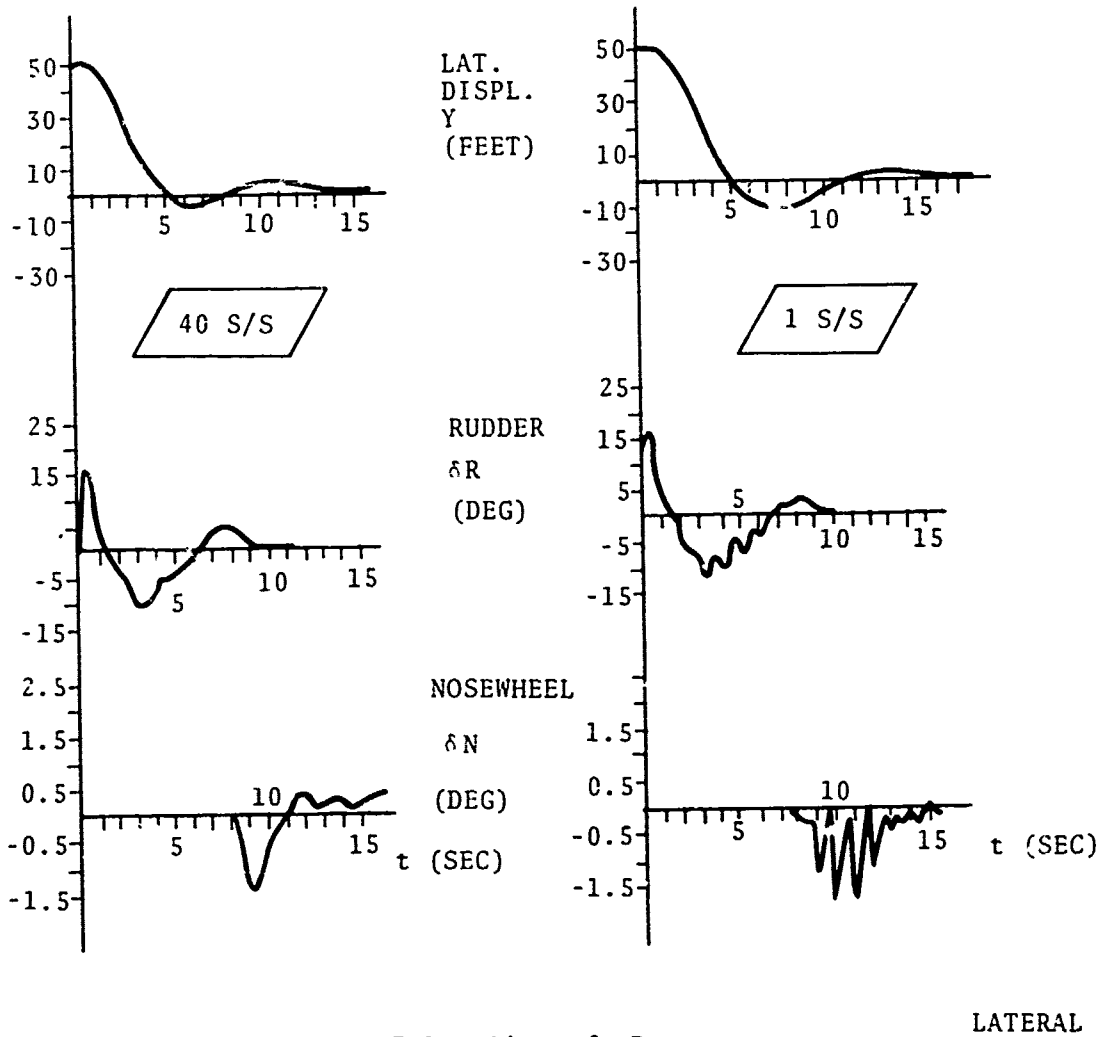

Figure 7-1: Aircraft Response to Offset at Touchdown

Figure 7-1. Aircraft Response to Offset at Touchdown

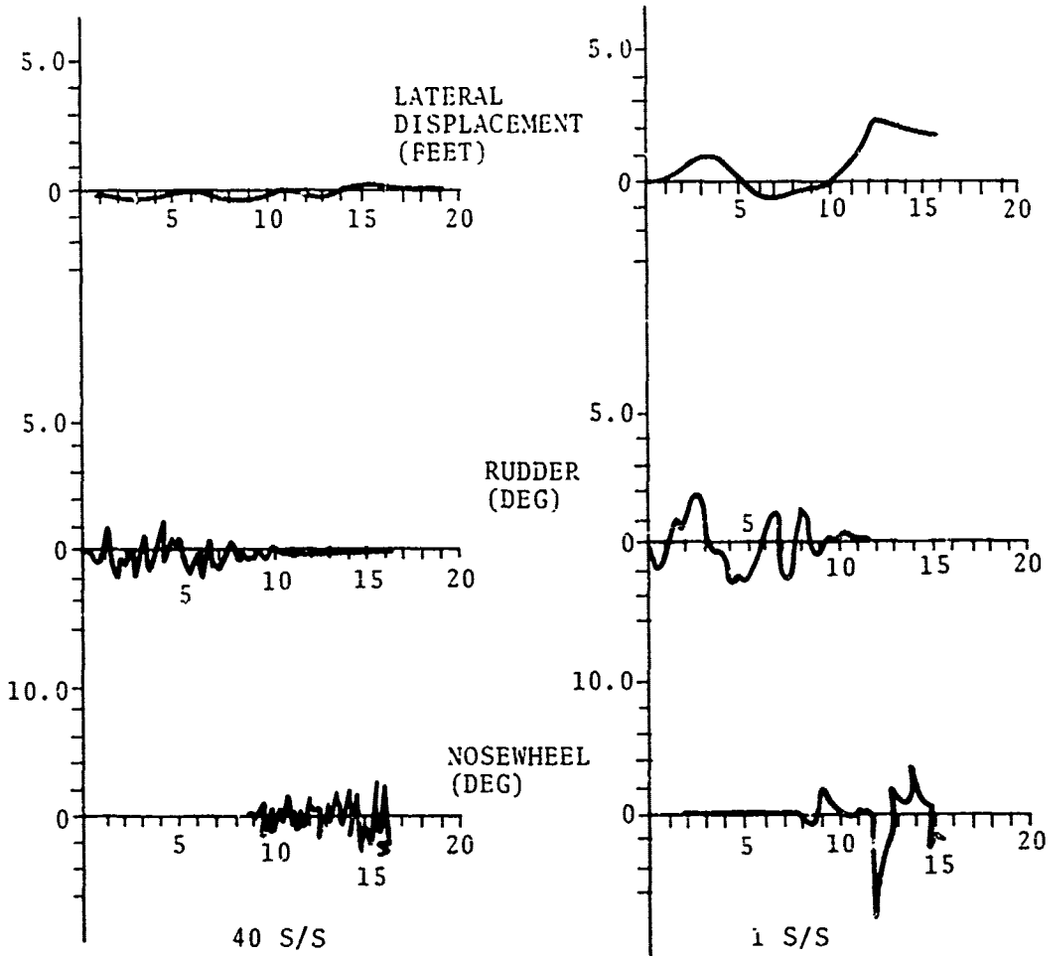

Az .023

Figure 7-2. Response to ILS Noise Az Noise = .023 deg rms
Initial Range 1000 ft. from Antenna.

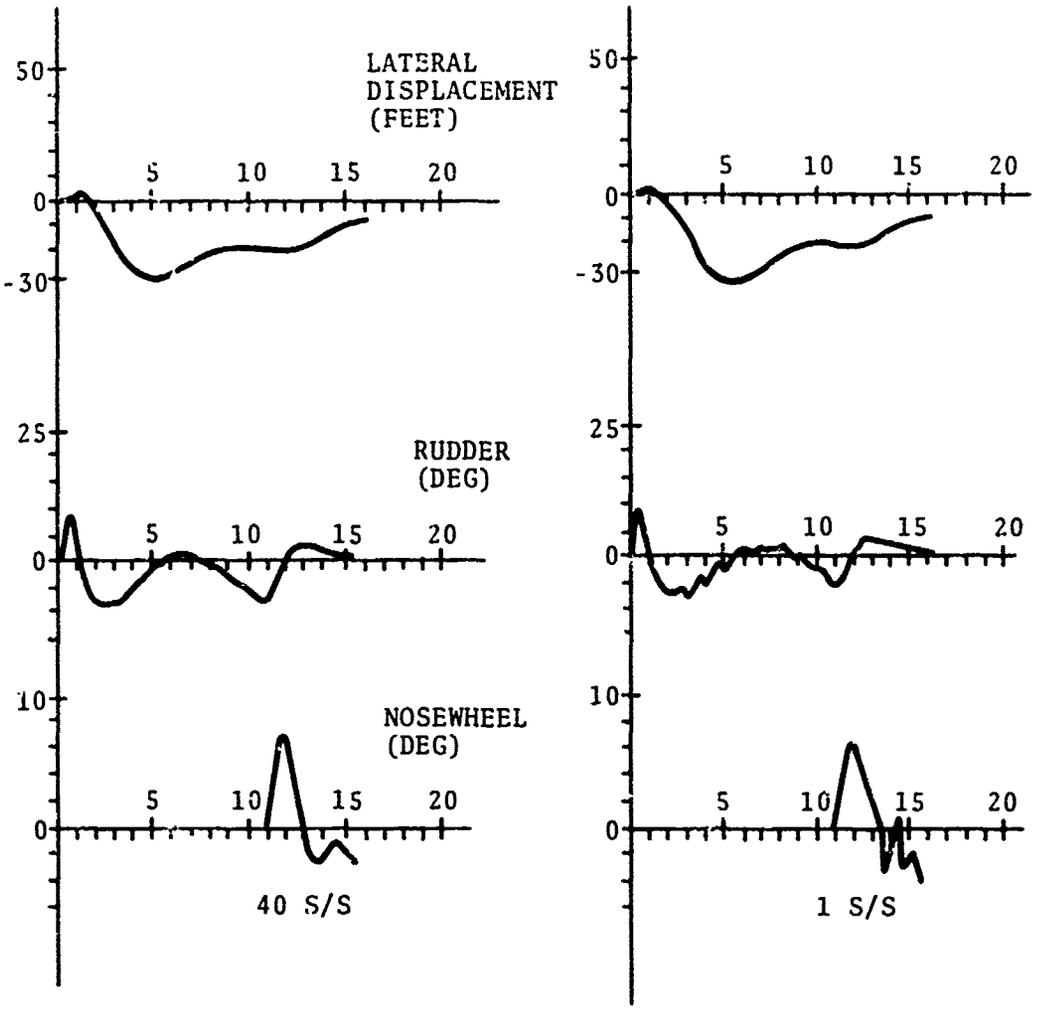

Figure 7-3. Response to Crab Angle at Touchdown ψ_o=4deg

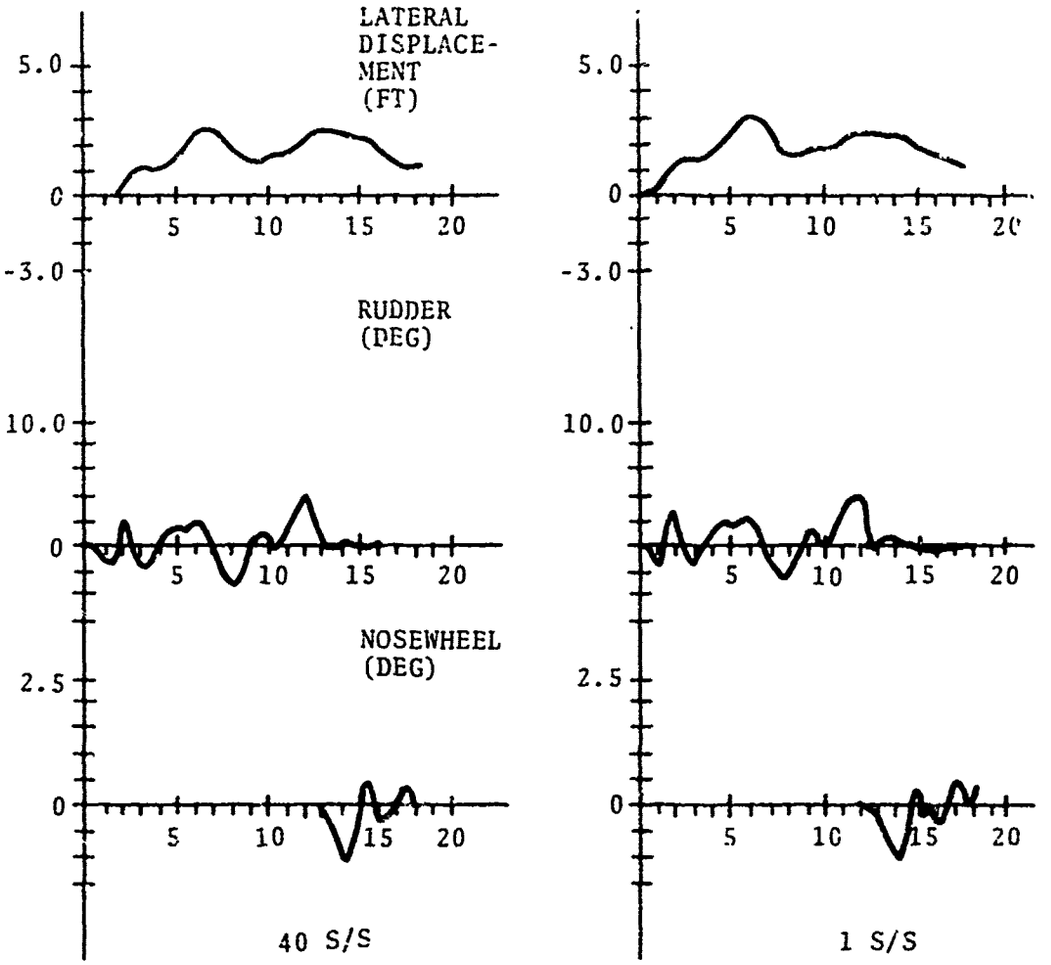

Figure 7-4. Response to Crosswind Gusts During Rollout [Gust Intensity = 5 fps rms]

Figure 7-1 it is also seen that the 1 s/s response is somewhat slower than that at 40 s/s.

Responses to MLS and aerodynamic noises (Figures 7-2, 7-4) show little sensitivity to data rate except again in the control activity area. The absolute magnitude of centerline deviations is also small.

There is no doubt that filtering must be carefully selected for rollout with data rate and noise values explicitly considered. However, the results presented here indicate that no serious problems will be encountered for an reasonable value of data rate or noise.

7.2 OTHER STUDIES - PLANNED AND IN PROGRESS

To date TSC efforts have been directed towards detailed study of requirements for the landing phase of flight, final approach through touchdown primarily in the areas of data rate and noise, for conventional aircraft.

The following activities, intended to illuminate and provide insight into other possible uses of MLS in the terminal area and to isolate important MLS characteristics for these uses, are planned or in progress, with completion scheduled for January 1973:

a. Extend data rate and beam noise studies to include performance during curved approach. Determine under varying assumptions the ability of an aircraft to fly time constrained curved approaches in the terminal area as a function of MLS signal characteristics (coverage is not a parameter of this task.

b. Using currently experimental ARTS III metering and sequencing procedures as a model, show sensitivity of performance in the terminal area to MLS azimuth coverage with dispersion in time of arrival at runway threshold as a figure of merit. Three levels of sophistication in usage of MLS by the airborne user will be examined.

1. MLS used only to generate heading and ground speed data.

2. MLS used in a 3D area navigation role, with on-board computed flight paths between waypoints.

3. MLS used in a 4D guidance scheme - paths designed with real-time constraints.

(Accuracy and data rate are not parameters of this task).

c. Using available computer programs which generate terminal area noise profiles, show the effect of varying approach paths in reducing noise in selected areas. Assuming MLS coverage is required over the area of possible approach paths, interpolate results to show benefits in terms of possible noise reduction as a function of MLS coverage.

d. With minimal amounts of actual simulation, attempt to generalize the results generated to date on data rate and accuracy requirements for CTOL to STOL and VTOL operations, based on familiarity and working knowledge of STOL and VTOL control and on the dynamic effects of sampling and noise determined previously.

e. Based on the results of the above and other related work, recommend and justify modification to currently assumed system concepts and requirements.

8.0 SUMMARY

This report discusses the results of analysis conducted during FY 1972 directed towards determining Microwave Landing System signal requirements for conventional aircraft. The phases of flight considered include straight-in final approach, flareout, and roll-out.

A limited number of detailed problems in performance analysis have been considered. Data from computer simulation, covariance propagation and system optimization, with a careful selection of variables has provided the means for generalizing from the results of these specific experiments to more comprehensive functional, data rate, noise, and control system requirements for automatic landing.

The general conclusions resulting from this effort can be summarized as follows:

1. Regardless of aircraft configuration, when MLS is used for automatic control, higher data rates and lower noise levels will always provide better performance in path following ability and effectiveness of control surface activity.
2. Performance exhibits more basic sensitivity to airborne control system and filter configuration than to data rate and noise.
3. Performance analysis alone provides insufficient justification for choosing minimum suitable sampling rates or maximum allowable noise levels. Economic/technical feasibility tradeoffs must be included with performance figures of merit, especially in the area of airborne vs. ground based capabilities.
4. The major disturbing force associated with landing is turbulence and wind shear. The measure of a control system's effectiveness is its ability to anticipate and

counteract wind induced displacements. Acceleration data is required for effective control in turbulence. NLS information, in the form of sampled, noisy position data, cannot adequately provide this. For effective control in turbulence accelerometer(s) are required.

5. If too much high frequency information is demanded of MLS data, noise induced control and attitude activity become unacceptable in moderate or light wind conditions.

6. Airborne gain scheduling, as a function of range from transmitting antenna and of estimated turbulence, is recommended with any control configuration in order to most effectively suppress the signal noise while maintaining path following capability.

7. The higher the data rate (and/or the lower the noise), the greater the flexibility available to the airborne system designer.

8. Noise produces more undesireable performance characteristics for conventionally equipped aircraft (those without specially designed MLS coupler-processors) than for those with advanced configurations; maximum allowable noise is limited by the assumption that these aircraft must use MLS data with no significant modifications.

9. With every indication that minimum configuration aircraft will have the most problem with low data rate and high noise, there appears to be no justification for decreased sample rates or increased noise for ground stations of less than maximum conditions.

8.1 CONCLUSIONS FOR FINAL APPROACH

If forced to choose minimum data rate maximum noise for the Azimuth and Elevation #1 functicns based on requirements for final approach, the value shown below would result.

Function	Maximum Data Rate	Maximum Noise	Maximum Noise*
Azimuth	2s/s	0.023 deg rms	0.1 deg rms
Elevation #1	5s/s	0.033 deg rms	0.1 deg rms

*Maximum noise if all receivers equipped with coarse wind-selectable filters

It should be reiterated, however, that higher data rates and lower noise will provide for better performance and more system design latitude, with a result and favorable impact on safety margins.

8.2 CONCLUSIONS FOR FLARE

Elevation #2 is ill-suited to serve as sole primary guidance and control data source for the flare maneuver in turbulence. A normal accelerometer is required for wind suppression; velocity data is also available from the normal accelerometer. Precision altitude for flare initiation and correction of barometric or radio altimeter is available from DME and Elevation #1. The role of the elevation #2 function in the MLS scenario should be seriously reconsidered.

8.3 CONCLUSIONS FOR ROLLOUT. (AZIMUTH GUIDANCE)

If the azimuth signal is present and of quality similar to that during final approach, then no serious difficulties will be encountered in designing rollout control.

9.0 REFERENCES

1. National Plan for Development of the Microwave Landing System, July 1971, NTIS No AD733268.

2. A New Guidance System for Approach and Landing, DO-148, Radi Technical Commission for Aeronautics (SC-117), December 18, 1970.

3. Lanman, M. H., An Investigation of Microwave Landing Guidance System Signal Requirements for Conventionally Equipped Civilian Aircraft, DOT-TSC-FAA-71-24, (FAA-RD-71-86) June 1971.

4. Bryson, A. E., and Ho, Yu-Chi, Applied Optimal Control, Blaisdell Co., 1969.

5. Desai, M., Mackinnon, D., Madden, P., Optimal and Suboptimal Flight Path Control in the Terminal Area Using Radio-Inertial Measurements, MIT Draper Lab Report R-666, July 1970.

6. Automatic Landing Systems (ALS), Advisory Circular 20-57A, 12 January 1971, Federal Aviation Administration.

APPENDIX A

STOCHASTIC FLIGHT CONTROL SYSTEM DESIGN BY PARAMETER OPTIMIZATION

A.1 INTRODUCTION

The design of a flight control system for an aircraft needs to take into consideration a large number of factors such as the nature of the flight-path environment and that of the feedback signals available from a variety of sensors, a variety of effectors available for control, etc. Moreover, for an MLS based control system, the availability of the position signals in sampled form adds an important dimension to the design problem. Conventional cut-and-try design methods do not offer a clear and comprehensive procedure which will take into account considerations such as those listed above, nor provide a ready index to judge the performance of the system so designed. Moreover, an extremely tedious design process would be needed for a comprehensive performance analysis of an MLS based flight control system. Optimal Control theory for the feedback control in presence of uncertainty overcomes some of the limitations of conventional design procedures, with the optimization yielding an optimal filter-controller for a given performance criteria. However, this optimization procedure involves lengthy, cumbersome and difficult numerical computations. A fixed configuration approach for a filter-controller structure utilizing parameter optimization techniques circumvents this difficulty. A comprehensive performance analysis of the control system for a given configuration, effector size and type, and control energy limit can be carried out by suitably scanning the performance index used in the optimization.

The following sections introduce the methods for determining the behaviour of a physical system subject to stochastic disturbances, formulate a parameter optimization problem and investigate the necessary conditions for the existance of an optimum solution.

A.2 RESPONSE OF A LINEAR SYSTEM TO STOCHASTIC INPUTS

Consider a discrete system mode:

$$x(i+1) = \Phi x(i) = \Gamma u(i) \quad * \qquad \text{(A-1)}$$

where

x = n x 1 vector describing the state of the system

Φ = n x n matrix describing the influence of the state at instant i on the transition to instant i+1.

u = m x 1 vector describing the process noise assumed to be a Gaussian white random sequence with zero mean and correlation matrix Q.

Γ = n x m matrix describing the effect of the process noise on the system.

The average behaviour of the above system in presence of process noise is described by the following matrix difference equation:

$$X(i+1) = \Phi\, X(i)\, \Phi' + \Gamma Q\, \Gamma' \qquad \text{(A-2)}$$

$$X(0) = X_o$$

where X is the covariance matrix of x with

$X = E(xx')$ where E is the expectation operator.

Of primary interest in control system investigations are time-invariant or stationary systems.** The matrix X will attain a steady state as $i \to \infty$ in case of a time-invariant (i.e. Φ and Γ are constant) asymptotically stable system and a constant correlation matrix Q with X satisfying

$$\Phi X \Phi' + \Gamma Q \Gamma' = X. \qquad \text{(A-3)}$$

The process is then said to be statistically stationary in the limit as $i \to \infty$.

The solution of (A-3) is conveniently obtained by transformation to a set of ordinary linear algebraic equations which are then solved using any one of a multitude of numerical techniques.

---

*Appendix B describes the development of a discrete model for an aircraft system incorporating a fixed configuration digital filter-controller.

**Such an assumption is valid over a small range of vehicle velocities. Each speed regime must be investigated separately and control system parameters suitably established.

Since X represents the average behaviour of the system in presence of noise, it provides a basis for formulating an optimization problem which leads to the minimization of system response to stochastic disturbances.

A.3 STOCHASTIC RESPONSE MINIMIZATION

We shall define the performance index, J, as a linear combination of the elements of the covariance matrix X with

$$J = \sum_{i=1}^{n} \sum_{j=1}^{n} \alpha_{ij} X_{ij} \qquad \text{(A-4)}$$

The elements α_{ij} are selected to reflect the goal of the design. For example, the association of non-zero values of α_{ij} with thed trajectory error and the effector activity results in a solution which minimizes the mean-square value of the trajectory error subject to a penalty on effector activity.

For analytical purposes (A.4) is conveniently expressed in an equivalent form:

$$J = \text{Trace } CX$$

where

$$\text{Trace } CX = \sum_{i=1}^{n} (CX)_{ii}$$

and $$c_{ij} = \alpha_{ji}$$

Now for a stationary and stable system, a parameter optimization problem can be defined as follows.

Problem Definition

Find a set of parameters, p, which minimizes the performance index

$$J = \text{Trace } CX, \qquad C>0 \qquad \text{(A-5)}$$

subject to the constraints

$$\Phi X \Phi' + \Gamma Q \Gamma' - X=0 \qquad \text{(A-6)}$$

where

p = 1 x 1 vector of adjustable paramenters. Both matrices Φ and Γ are assumed to be functions of parameter p.

Solution

The minimization of (A-5) subject to the constraints (A-6) can be easily handled by adjoining the constraints to the performance index by a Lagrange Multiplier Matrix P, yielding an augmented performance index J, with

$$\bar{J} = \text{Trace}\left[CX + P\left(\Phi X \Phi' + \Gamma Q \Gamma' - X\right)\right] \qquad \text{(A-7)}$$

N Now consider perturbations δ_{pi} in the values of p_i. The change in the performance index can be written as

$$\delta J = \text{Trace}\left[\delta P\left\{\Phi X \Phi' + \Gamma Q \Gamma' - X\right\} + \delta x\left\{C + \Phi' P \Phi - P\right\} + \sum_{i=1}^{1} 2P\left\{\frac{\delta \Phi}{\delta p_i} X \Phi' + \frac{\delta \Gamma}{\delta p_i} Q \Gamma'\right\} \delta p_i\right]$$

neglecting 2nd order terms in δp_i (A-8)

Choosing in (A-8)

$$C + \Phi' P \Phi - P = 0 \qquad \text{(A-9)}$$

we have:

$$\delta \bar{J} = \delta p' \frac{\delta J}{\delta p} \qquad \text{(A-10)}$$

where

$\frac{\delta J}{\delta p}$ = 1 x 1 gradient vector with each element $\frac{\delta J}{\delta p_i}$ defined as:

$$\frac{\delta J}{\delta p_i} = \text{Trace}\left[2P\left\{\frac{\delta \Phi}{\delta p_i} X \Phi' + \frac{\delta \Gamma}{\delta p_i} Q \Gamma'\right\}\right] \qquad \text{(A-11)}$$

Equation (A-10) yields readily the following necessary condition for $\tilde{J}$ to be at a local optimum. Viz.

$$\frac{\delta \tilde{J}}{\delta p} = 0 \qquad \text{(A-12)}$$

Thus, the necessary conditions for a minimum are:

$$X = \Phi X \Phi' + \Gamma Q \Gamma' \qquad \text{(A-13)}$$

$$P = \Phi' P \Phi + C \qquad \text{(A-14)}$$

$$J_p = 0 \qquad \text{(A-15)}$$

A.4 NUMERICAL METHODS

A large number of iterative mathematical algorithms have been developed for generating solutions to the problem defined in the previous section. The most useful algorithms utilize the value of J and the gradient with respect to p, J_p, to construct a sequence of parameter vectors which converge to an optimal solution. A comprehensive description of the numerical optimization algorithms is contained in Chapter 4 of Ref. 1.

Reference

(1) Mukund Desai, Duncan MacKinnon and Paul Madden, Optimal and Suboptimal Flight Path Control in the Terminal Area Using Radio-Inertial Measurements.

R-666, C.S. Draper Laboratory, M.I.T., July 1970

APPENDIX B

DISCRETE AIRCRAFT AND FLIGHT CONTROL SYSTEM MODEL

BY MUKUND DESAI

B.1 INTRODUCTION

The following sections deal with the development of a discrete model for the dynamics of an aircraft system and the flight control system which includes a digital filter-controller system. This discrete model is used in the stochasitc flight control system design using parameter optimization described in Appendix A.

B.2 THE AIRCRAFT SYSTEM

The aircraft flight control system dynamics with a fixed-configuration digital filter-controller can be represented by the following linear system of equations:

Aircraft Control System

$$x_1 = Ax_1 + Bu^* + G_1 w_1 \qquad \text{(B-1a)}$$

Signal

$$y(i) = Hx_1(i) + w_2(i) \qquad \text{(B-1b)}$$

Digital Filter-Controller

$$x_2(i+1) = \Phi_2 x_2(i) + \Gamma_2 y(i) \qquad \text{(B-1c)}$$

Control

$$u(i) = \bar{\Psi}_1 x_2(i) + \bar{\Gamma}_2 y(i) \qquad \text{(B-1d)}$$

where

x_1 = Aircraft - control system state

x_2 = Digital filter-controller state

$-(i) = -(t_1)$

t_i = Sampling instants i = 0,1,2...

$= t_{i-1} + T$

T = Sampling interval

u^* = Output of a zero-order hold operating on control u(i)

w_i = White Gaussian noise with $E[w_1] = 0$ and $E[w_1(t)w_1(\tau)] = Q_1 \delta(t-\tau)$

w_2 = White Gaussian random sequence with $E(w_2) = 0$ and

$E[w_2(i)w_2'(j)] = W_2\delta_{ij}$

$\delta_{ij} = 1$ if $i = j$

$= 0$ if $i \neq j$

Figure B-1 shows a schematic representation of the aircraft system.

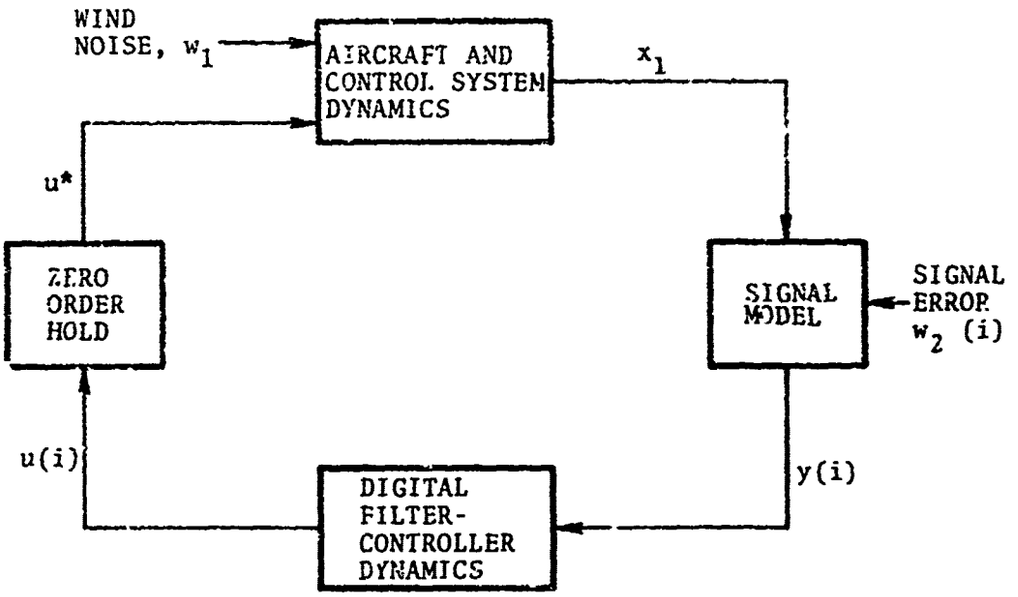

Figure B-1. Aircraft - Control System Dynamics

It is easy to work with a discrete model rather than a continuous-discrete aircraft model as represented by equations B-1. The following section develops the discrete model.

B.3 DISCRETE MODEL

At the sampling instant, t_{i+1}, we have from eq - B-1a:

$$x_1(i+1) = \Phi_1(i+1,i)\, x_1(i) + \Gamma_1(i+1,i)\, u(i) + w_1(i+1,i) \quad \text{(B-2)}$$

where

$$\frac{d\Phi_1}{dt}(t, t_i) = A\Phi_1(t, t_i) \tag{B-3}$$

$$\Phi_1(t_1, t_i) = I \tag{B-4}$$

$$\Gamma_1(t, t_i) = \int_{t_i}^{t} \Phi_1(t, \tau)\, B\,(\tau)\, d\tau \tag{B-5}$$

$$w_1(i+1, i) = \int_{t_i}^{i+1} \Phi_1(t_{i+1}, \tau) G_1\, w_1(\tau) d\tau \tag{B-6}$$

Equations B-1b, B-1c, B-1d and B-2 can be combined to yield:

$$x(i+1) = \Phi x(i) + \Gamma w(i) \tag{B-7}$$

where

$$x = \left|\begin{array}{c} x_1 \\ \hline x_2 \end{array}\right| \tag{B-8}$$

$$\Phi = \left|\begin{array}{c|c} \Phi_1 + \Gamma_1 \Psi_2 H & \Gamma_1 \Psi_1 \\ \hline \Gamma_2 H & \Phi_2 \end{array}\right| \tag{B-9}$$

$$\Gamma = \left|\begin{array}{c|c} I & \Gamma_1 \Psi_2 \\ \hline 0 & \Gamma_2 \end{array}\right| \tag{B-10}$$

$$w(i) = \begin{array}{l} w_1(i+1, i) \\ \\ w_2(i) \end{array} \tag{B-11}$$

It may be easily verified that w(i) is a white Gaussain random sequence with the statistics

$$E[w(i)] = 0$$

and $E[w(i)w'(j)] = Q\delta_{ij}$

with $Q = \begin{matrix} W_i(i+1) & 0 \\ 0 & W_2 \end{matrix}$

and

$$\frac{dW_1(t, t_i)}{dt} = AW_1(t, t_i)+W_1(t, t_i)F^T +G_1Q_1G^T \quad \text{(B-12)}$$

$$W_1(t_i, t_i) = 0 \quad \text{(B-13)}$$

Equation B-7 represents the discrete model of the aircraft-control system including the digital filter-controller. It describes the evolution of the aircraft-controller state x and also the effect of the wind noise as well as the noise on the MLS position signal. The average behaviour of the system can be obtained from the following matrix equations:

$$X(i+1) = \Phi X(i)\Phi' + \Gamma Q\Gamma' \quad \text{(B-14)}$$

$$X(0) = X_0$$

APPENDIX C

TWO DIMENSIONAL FLARE CONTROL THROUGH FLARE LAW PARAMETER ADJUSTMENT

BY MAURICE LANMAN

C.1 INTRODUCTION

Design an exponential flare path which results in proper longitudinal touchdown position and sink rate regardless of initial glideslope, glideslope deviation, or altitude rate. The following assumptions and conditions are applicable:

(1) The aircraft is assumed to follows commanded sink rate perfectly.

(2) No disturbances are encountered during flare.

(3) Flare initiation altitude and the "time constant" at the exponential maneuver provide the adjustment capability.

(4) No step transients in altitude rate at initiation are allowed.

C.2 THE EXPONENTIAL FLARE LAW

$$-\dot{h}_c(t) = Kh(t) - \dot{h}_{td} \qquad (C.1)$$

$-\dot{h}_c(t)$ = commanded sink rate

$1/K$ = = exponential time constant

$h(t)$ = altitude

$-\dot{h}_{td}$ = desired sink rate at touchdown

In order to satisfy condition (4) above, the following initial conditions apply:

$$\dot{h}_c(t_i) = \dot{h}(t_i) = -Kh(t_i) + \dot{h}_{td} \qquad (C.2)$$

$$Kh(t_i) = -(\dot{h}(t_i) - \dot{h}_{td}) \qquad (C.3)$$

t_i = time of flare initiation

$\dot{h}(t_i)$ = actual sink rate at flare initiation

Simplifying notation:

$$Kh_i = -(h_i - \dot{h}_{td}) \qquad (C.4)$$

The homogenous solution to equation (C-1) leads to the following expression for sink rate and altitude as functions of time:

$$\dot{h}(t) = \dot{h}_i e^{-Kt} \qquad (C.5)$$

$$h(t) = \frac{-h(t)+\dot{h}_{td}}{K} \qquad (C.6)$$

The following equations represent the full set of initial and final conditions for a perfect maneuver:

$$\dot{h}_i = h_i \quad \text{(defined)}$$

$$\dot{h}_{td} = \dot{h}_{td} \quad \text{(defined)}$$

$$h_{td} = 0 \quad \text{(defined)}$$

$$h_i = \frac{\dot{h}_i+\dot{h}_{td}}{K} \quad \text{(C.3 or C.6)} \qquad (C.7)$$

$$t_{td}-t_i = T = \frac{1}{K} \log_e \frac{h_i}{h_{td}} \quad \text{(from C-5)} \qquad (C.8)$$

C.3 TWO DIMENSIONAL CONTROL

The approach from here involves choosing a flare time, T, such that, given an average groundspeed, the longitudinal position at touchdown dows not vary. This time is chosen on the basis of groundspeed and glideslope angle. Once T is chosen, K is set such that (C.8) is satisfied, and such that (C.7) is satisfied.

From any point prior to flare (see fig. C.1) the range to touchdown can be approximated as follows:

$$T(t) = \frac{h(t)}{\phi(t)} + R_{td} \qquad (C.9)$$

Assuming a constant groundspeed, $\dot{R}$, [not necessary to the method but simpler to illustrate] throughout, the time to touchdown is given as follows:

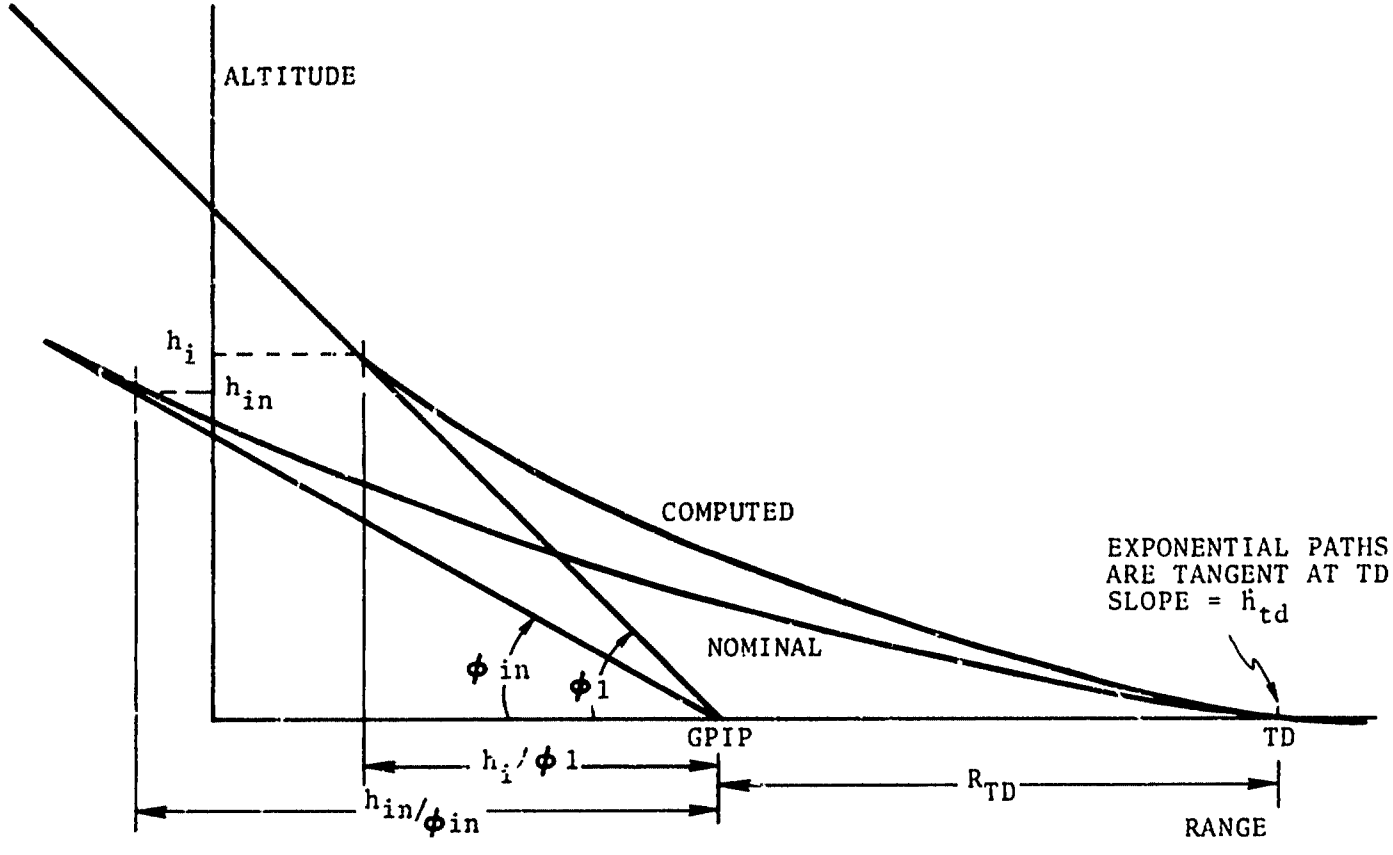

Fgiure C-1. Representation of Variable Parameter Flare.

$$T(t) = \frac{R(t)}{\dot{R}} = \frac{h(t) + R_{td}\,\phi(t)}{\dot{R}\phi(t)} \qquad (C.10)$$

$T(t)$ = current estimated time to touchdown

$\dot{R}$ = ground speed

$\phi(t)$ = current elevation #1 angle

$R(t)$ = current range to touchdown

R_{td} = desired distance from GPIP (El #1) to touchdown

[Note: $\phi(t) = \phi_n(t) + \delta\phi(t)$ where ϕ_n is nominal glideslope and $\delta\phi$ is glideslope deviation]

Equating T(t) in C.10 with T in C.8 leads to the following equation involving continuous estimation of K:

$$K(t)h(t) + K(t)R_{td}\phi(t) = \dot{R}\phi(t)\,\log_e \frac{h(t)}{h_{td}} \qquad (C.11)$$

The product Kh, however, is regulated according to (C.4)

$$K(t)\,h(t) = -(\dot{h}(t) - \dot{h}_{td}) \qquad (C.12)$$

Combining (C.12) and (C.11):

$$\hat{K}(t) = \frac{R\phi(t)\,\log_e \frac{h(t)}{h_{td}} + (\dot{h}(t) - \dot{h}_{td})}{R_{td}\,\phi(t)} \qquad (C.13)$$

Equation C.13 provides the continuous estimate of K, the exponential flare constant as a function of groundspeed, desired touchdown sink rate and estimates of current altitude rate and current elevation angle.

The current estimate of flare initiation altitude is derived from (C.7) and (C.13)

$$\hat{h}_i(t) = -\frac{(\dot{h}(t) - \dot{h}_{td})}{K(t)} \qquad (C.14)$$

$$= \frac{R_{td}\phi(t)\ [\dot{h}(t) - \dot{h}_{td}]}{\phi(t)\ \log_e \frac{\dot{h}(t)}{\dot{h}_{td}} + [\dot{h}(t)-\dot{h}_{td}]} \qquad (C.15)$$

In actual mechanization, $h_i(t)$ and $K(t)$ would be updated periodically during the final moments at final approach. When actual measured altitude become equal to estimated ideal flare altitude, then flare is initiated and the value of K at that instant is fixed for the remainder of the maneuver.

Figure C.2 shows flare altitude computed from (C.15) as a function of groundspeed and glideslope.

For good performance, accurate measurements of altitude rate, altitude, EL #1 angle, and groundspeed are required. It would also be desireable to provide during final approach, an estimate of time remaining to flare initiation as given by (C.16):

$$(t-\hat{t}_i) = \frac{h(t) - \hat{h}_i(t)}{-\dot{h}(t)}$$

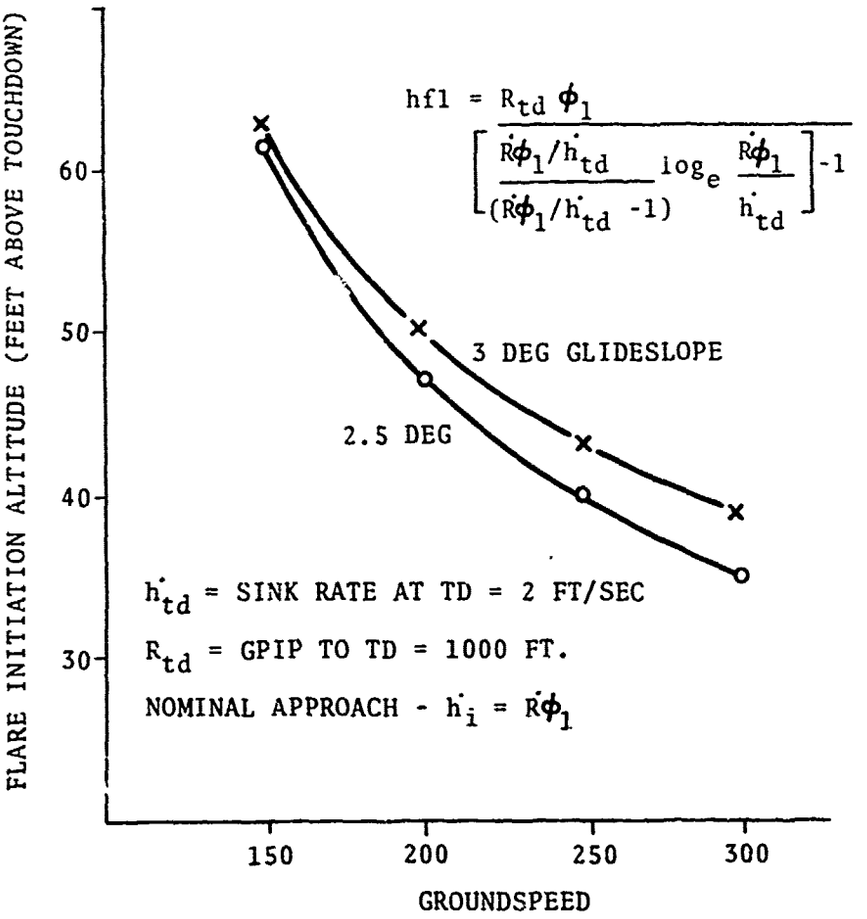

Figure C-2. Flare Initiation Altitude vs Groundspeed
2D Flare-Nominal Approach.

APPENDIX D

CV-880 ROLLOUT MODEL & CONTROL SYSTEM

BY PAUL MADDEN

FROM MIT/CSDL MEMO A41 OF
NOV 5, 1972

D.1 INTRODUCTION

The following sections delineate the vehicle math model and control system which has been integrated into the CV880 digital simulation to extend the capabilities of the latter to include the landing and roll-out phase of flight.

D.2 GENERAL DESCRIPTION OF THE CV880 LANDING GEAR AND ROLL-OUT CONTROL

The CV880 landing gear consists of two main gear units, each consisting of a four-wheel truck, located slightly behind the aircraft center of gravity, and a nose gear unit of two wheels. Braking is provided on both main and nose gears and anti-skid systems are incorporated on all units.

Nose wheel steering is directed from the rudder pedals (limited travel) as well as from a separate wheel control (or tiller) that provides for larger angles of travel or is automatically commanded by the roll-out system. The latter incorporates variable gains to compensate for changes in rudder and nose wheel effectiveness with airspeed and groundspeed, respectively, and range from the localizer antenna.

D.2.1 Basis for Aircraft Model and Control System During Roll-out

1. Nose and wing main gear forces computed independently; asymmetric landings are thereby accommodated.
2. All forces contributed by the landing gear are resolved into stability axes for compatibility with the existing simulation equations of motion.
3. The landing maneuver is divided into two phases:
   (i) main gear touchdown to nose gear touchdown, and
   (ii) the three-point roll-out phase.
4. Nose wheel steering is incorporated and is commanded by the roll-out control system. The nose wheel is locked until airspeed drops to 70 kts (120 fps) at which point rudder control becomes ineffective and is slowed-out while simultaneously nose wheel steering is slowed-in.

5. Maximum braking is assumed during the roll-out phase on nose and main gear units.

6. Small angle approximations are assumed in evaluation of strut compression and compression rate from the aircraft state and in the resolution of the gear forces into stability axes.

D.3 TIRE AND OLEO DEFLECTION

Tire and oleo deflection are determined from a knowledge of the aircraft state. The location of the aircraft center of gravity above the runway, the nose and main gear coordinates, and the aircraft body axis pitch and roll angle are required.

D.3.1 Equations for Oleo Strut Compression and Compression Rate

D.3.1.1 Body Axis Theta

$$\theta_B = \theta_S + \alpha_T \qquad (D.1)$$

D.3.1.2 Total (Tire + Strut) Displacement

$$z_i = z_{max} - (z_{cg} + x_i\theta_B - y_i\phi_B) \qquad (D.2)$$

where z is the height of the extended gear (no load) below the aircraft cg

z_{cg} is the height of the aircraft cg above the runway

x_i is the longitudinal body axis coordinate of the landing gear units (+ve forward of cg)

y_i is the lateral body axis coordinate of the gear (+ve to starboard)

i = 1 right main gear
= 2 left main gear
= 3 nose gear.

D.3.1.3 Strut Compression Rate

$$z_i = -z_{cg} - x_i\theta_B + y_i\phi_B \qquad (D.3)$$

D.3.1.4 Displacement wrt Stability Axes

$$z_i = z_{cg} + x_i\theta_S - y_i\phi_S \qquad (D.4)$$

D.4 MAIN AND NOSE GEAR REACTION LOADS

Initial gear loads are determined by the tire deflection. The oleo strut is pre-loaded so that no strut compression takes place until the strut reaction exceeds the preload; therefore, all deflection is initially tire deflection until the pre-load is exceeded.

D.4.1 Equations Governing Gear Reaction Loads

D.4.1.1 Tire Load-Deflection Law

$$VFP \triangleq F_z/(p + 0.08p_r)w(wd)^{1/2} \qquad (D.5)$$

where

$$\delta/w = \begin{cases} 0.75(VFP) & VFP \leq 0.1 \\ 0.03 + 0.42\ (VFP) & VFP > 0.1 \end{cases}$$

for TYPE VII tires and

where

F_z is the strut reaction load (lbs.)

p is the tire pressure (psi)

p_r is the rated tire pressure

w is the tire width (in.)

d is the tire diameter (in.)

δ is the tire deflection (in.)

D.4.1.2 Oleo Spring and Damping Force - Oleo spring rate and landing gear damping factor are nonlinear functions of the strut compression. In the case of the CV880, the spring rate may be determined from a table of relative strut compression versus strut inflation which is found in the CV880 maintenance manual.[2] S knowledge of piston area is required to transform the table into a load-deflection curve. The compression-inflation curves are displayed in Figure (D.1) and Figure (D.2).

Strut damping factor as a function of strut compression was synthesized from available data for, and dynamic comparison with, the B747 landing gear as described in reference 3. Transient response characteristics of the two systems to an indentical strut displacement initial condition are compared in Fig. (D.3). The weight of the aircraft in each case is representative of a landing flight condition. The damping factor curves are seen in Fig. (D.4).

Initially, the nonlinear spring and damping parameters were approximated by piecewise-linear segments. However, in some simulation situations, it was found that limit cycles developed in the system state. The magnitude of the cycles could be reduced with the choice of a smaller (unacceptable) time step. The limit cycle behaviour was checked by substitution of the discontinuous representation of the landing gear spring and damping characteristics with a third order polynomial.

D.4.1.3 Strut Vertical Force - The landing gear strut reaction force is the sum of the strut spring and damping forces:

$$F_z = F_s + F_d \qquad (D.6)$$

D.4.1.4 Tire Deflection - The tire deflection is determined by the strut reaction force; this follows from equation (D.5). Interdependence of strut reaction force and tire deflection requires that an iterative procedure establish final values of these vari-

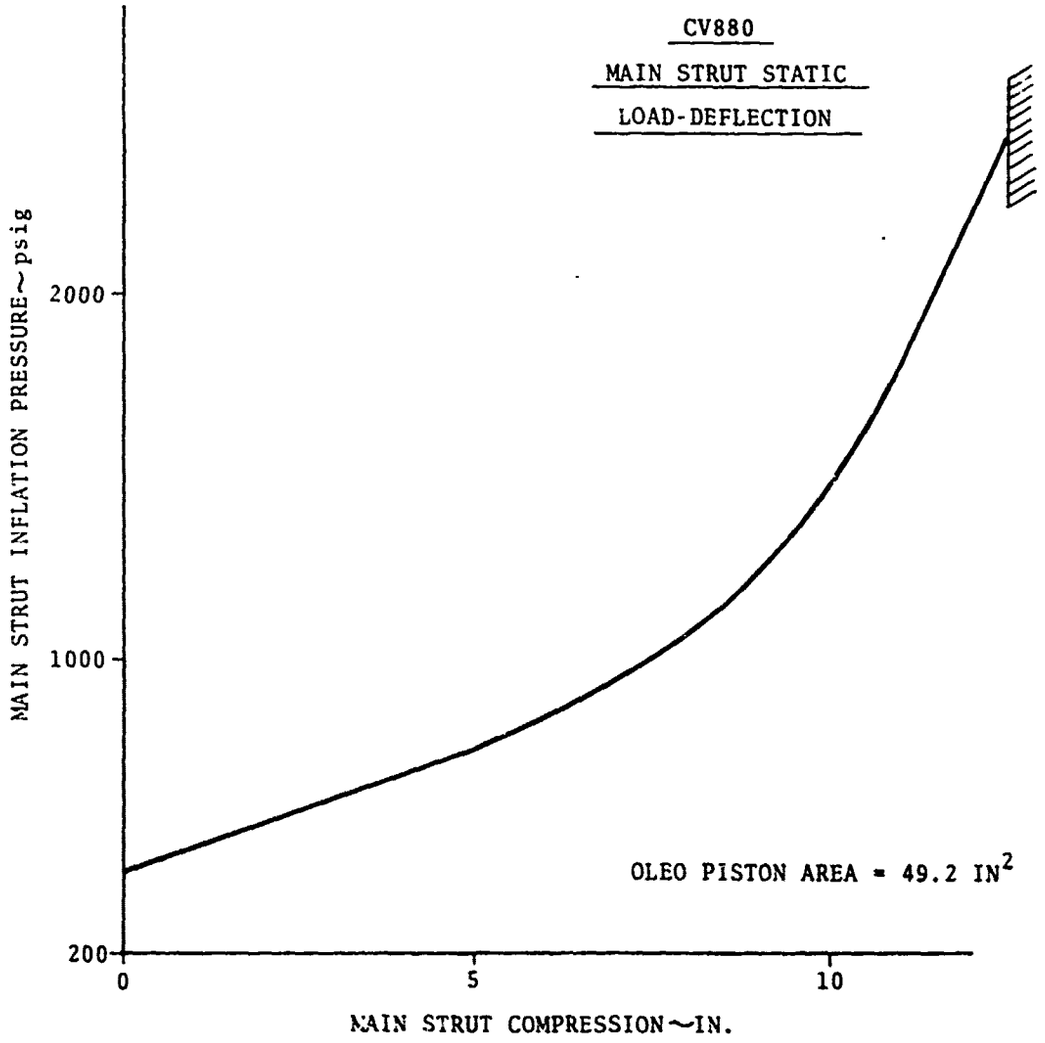

Figure D-1. CV880 Main Gear Spring Characteristic

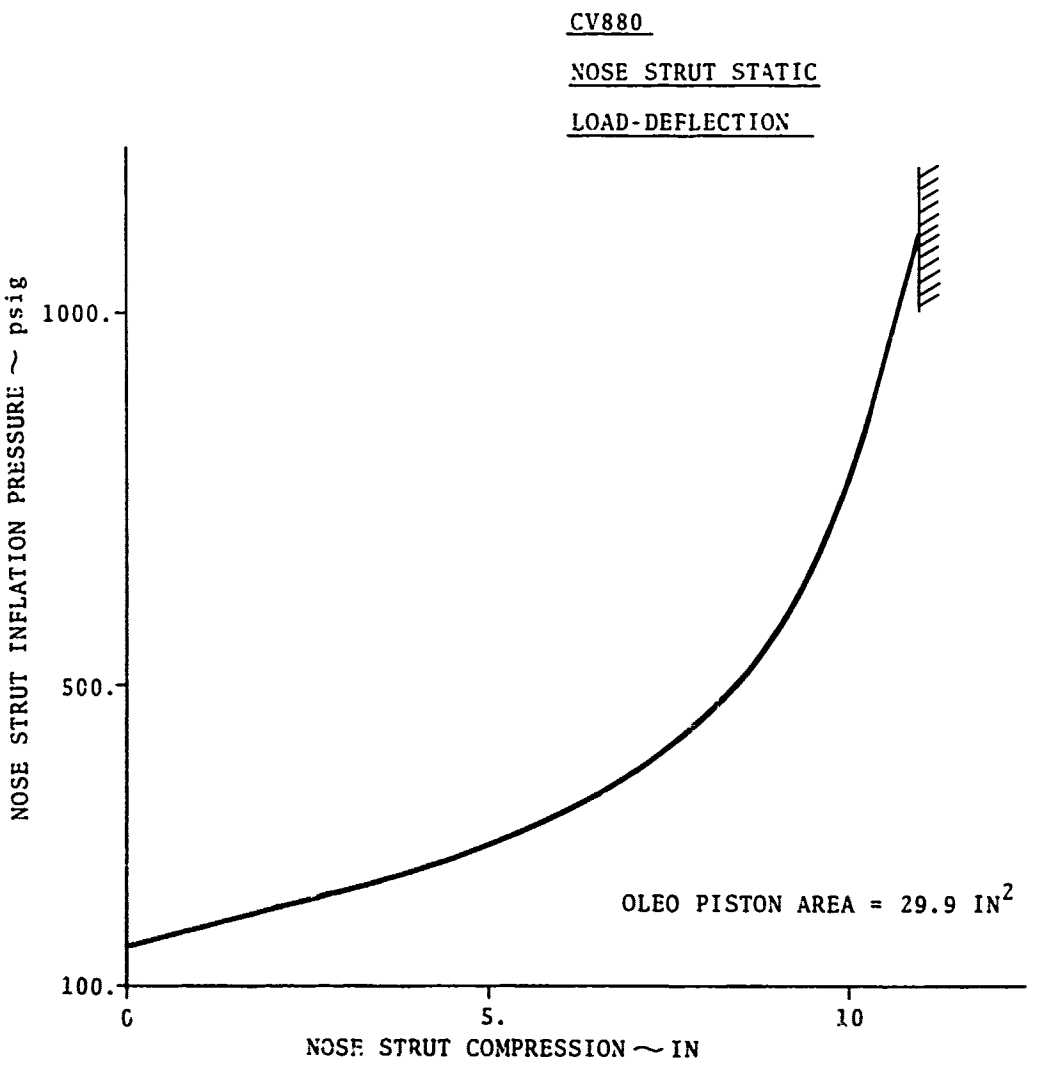

Figure D-2. CV880 Nose Gear Spring Characteristic

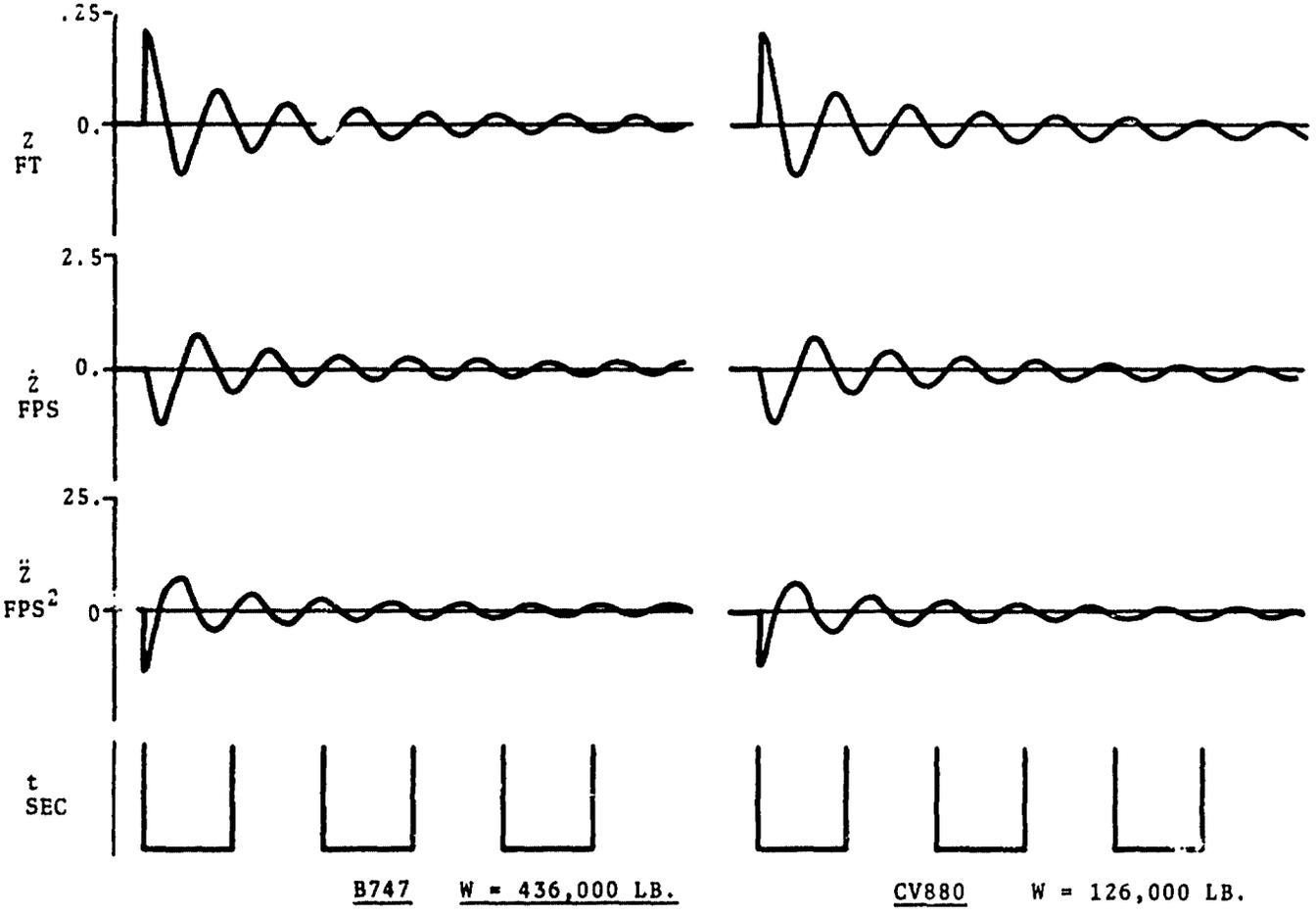

Figure D-3. Transient Response Characteristics of the B747 & CV880 Landing Gear to a Strut Displacement Initial Condition of 2.5 inches.

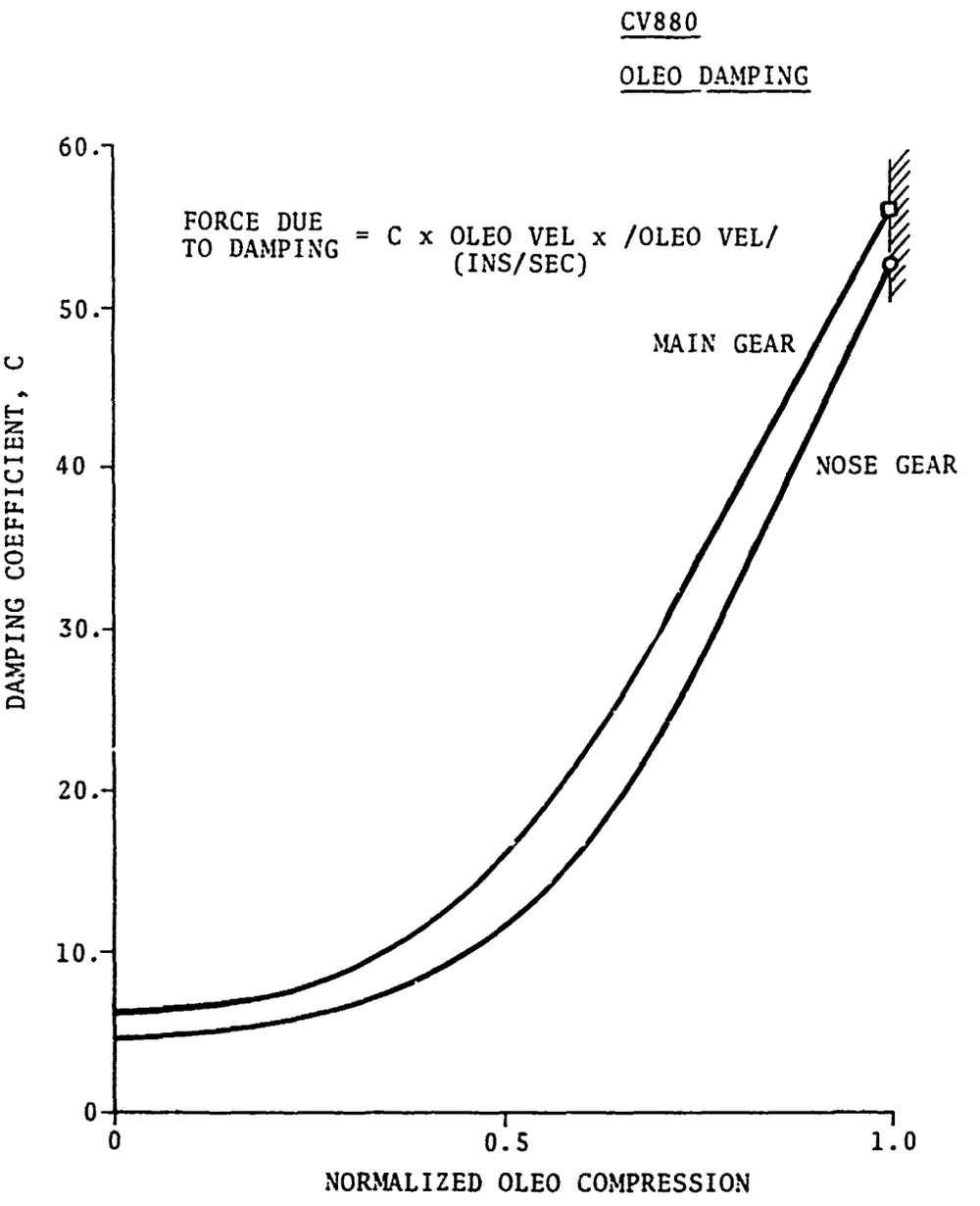

Figure D-4. CV880 Oleo Damping Factor, C.

ables. The interdependence is explained by the fact that the air craft state determines total (tire plus oleo strut) displacement so that evaluation of oleo strut compression requires knowledge of the tire deflection.

The iterative procedure involves equations (D.2), (D.5) and (D.6); iteration proceeds until successive estimates of tire deflection agree within a set tolerance or until the number of iteration cycles exceeds a set limit.

D.5 TIRE NORMAL AND TANGETIAL FORCES

The tire normal and tangetial forces primarily determine the aircraft lateral and longitudinal motion on the ground.

D.5.1 Tire Normal Force

The tire normal force is a function of tire yaw angle and tire cornering power. The latter depends upon tire deflection and specific tire constants.

D.5.1.1 Tire Cornering Power - Tire power is defined[1] as the rate of change of cornering force (force normal to the tire plane) with tire yaw angle λ for $\lambda \to 0$.

$$N \triangleq \frac{dF_n}{d\lambda}_{\lambda \to 0}$$

Cornering power is a function of tire vertical deflection and inflation pressure. Data available for typical aircraft tires indicate that cornering power increases with increasing vertical deflection for small deflections up to a maximum value and then decreases. In addition, cornering power increases approximately linearly with increasing inflation pressure. The following empirical equations describe the fuctional dependence of cornering power on defection and inflation pressure:

$$N = C_c(p + 0.44p_r)w^2 \left[1.2(\delta/d) - 8.8(\delta/d)^2\right]$$

$$\text{for } (\delta/d) \leq 0.0875$$

$$N = C_c(p + 0.44p_r)w^2 \left[0.0674 - 0.34(\delta/d)\right]$$

$$\text{for } \delta/d \geq 0.0875 \qquad \text{(D.7)}$$

For TYPE VII tires, $C_c = 57$ (N, force/rad)

Cornering power must be separately evaluated for right and left main gear tires and the nose gear tires.

D.5.1.2 Tire Yaw Angle - To evaluate tire normal forces, actual yaw angles at the tires must be known. The yaw angle is determined by the aircraft track angle along the runway, the aircraft heading, the aircraft yaw rate (since the wheels are displaced from the aircraft center of gravity) and, in the case of the nose wheel, the steering angle.

If the yaw angle exceeds a limiting value beyond which the cornering force is independent of the yaw angle (constant cornering power), then the yaw angle is set equal to the limiting value.

$$\lambda = \gamma + \psi - \varepsilon \qquad |\lambda| \leq 15 \text{ degrees} \qquad \text{(D.8)}$$

where

λ is the tire yaw angle

γ is the steering angle (nose wheel only)

ψ is the aircraft heading angle

ε is the track angle at the gear stations

Track angle is determined at each gear station, viz.

$$\varepsilon_i = \tan^{-1}(Y_i/X_i) \quad i = 1,2,3$$

where

$$Y_i = Y_E + rx_i \cos\psi - ry_i \sin\psi$$

and X_i X_E

$\dot{Y}_E$ and $\dot{X}_E$ are the lateral and longitudinal components of the velocity at the aircraft cg relative to the runway and r is the yaw rate.

D.5.1.3 Tire Normal Force - The tire normal force is given by

$$F_n = N\lambda \tag{D.9}$$

D.5.2 Tire Tangential Force

Tire tangetial forces arise due to friction at the contact surface of tire and runway. The shear forces that develop depend upon the vertical force on the tire and the coefficient of friction for the particular combination of wheel braking and runway surface characteristics.

D.5.2.1 Coefficient of Friction - It has been demonstrated[4] that the coefficient of friction (with maximum non-skid braking) varies almost linearly with ground speed on a dry surface and similarly on a wet surface except at very low speeds when the coefficient increases rapidly to almost the dry surface value. The value of rollong friction (no braking) is essentially independent of ground speed and runway surface condition. Consequently, the braking and rolling coefficients of friction are given by the following empirical expressions,

$$\mu_B = C_1 + C_2 U$$

$$\mu_R = 0.015 \tag{D.10}$$

where the dry surface values for C_1 and C_2 are[4]

$$C_1 = .53$$

$$C_2 = - .00055$$

and U is the ground speed in feet per second.

D.5.2.2 Tire Tangetial Force - The tire tangetial force is given be

$$F_t = \mu F_z \qquad (D.11)$$

D.6 AIRCRAFT MATH MODEL AND COMPUTATIONAL PROCEDURE

The touchdown and roll-out maneuver is divided into two phases. The first describes aircraft motion from main-gear touchdown to nosewheel contact and the second, the roll-out phase, describes subsequent motion.

During the first phase, usually of short duration, the a craft equations of motion are modeled by the conventional free flight perturbation equations used prior to touchdown with additional terms to account for main-gear tire vertical, tangetial and normal force effects. During this phase, the aerodynamic configuration is not altered from the pre-touchdown state and airspeed does not alter appreciably; consequently, the modified small perturbation equations provide an adequate model.

At the beginning of the roll-out phase, the aircraft aerodynamic configuration is altered considerably with deployment of full spoilers (lift-dumping) and possibly alteration fo flap setting to maximize load on the tires and minimize wind gust effects. Reverse thrust may also be utilized during roll-out. Speed varies from the possible maximum touchdown value to zero. The small perturbation equations cannot be utilized conventionally during this phase.

The roll-out model equations are called from the simulation vehicle model subroutine when the mode switching routine determines that the aircraft has landed. Further mode switching dur g roll-out is effected internally within the roll-out subroutine.

D.7 ROLL-OUT CONTROL SYSTEM

D.7.1 Introduction

The roll-out control system is operative only during the three-point roll-out phase. From main-wheel touchdown to nose-wheel contact, the decrab control system remains effective. The system operates in two modes, the first commanding rudder during the high dynamic pressure period of roll-out and the second commanding nose-wheel steering after rudder control becomes ineffective.

The control system gains in both modes are range independent requiring the use of DME. However, position gain in the rudder command mode is a function of airspeed to reflect the rudder force dependence upon dynamic pressure. Steering command mode position gain is scheduled with groundspeed.

D.7.1.1 Rudder Command Mode - A Schematic of the roll-out control system is seen in Figure D-5, and associated gains in Table D-1.

The variation of position gain with airspeed reflects the decreasing effectiveness of rudder as airspeed falls. However, it is not possible to retain the high spped characteristics of this mode by gain scheduling proportional to inverse dynamic presure because of resultant early rudder saturation for any realistic position error. The current gain scheduling ensures that rudder does not saturate for position errors less than about 50 feet.

At the recommended speed for transition to nose-wheel steering of 120 feet per second,[4] the control system slows-out rudder control with a 1 second time constant while simultaneously introducing nose-wheel steering through a 1 second slow-in.

D.7.1.2 Nose-Wheel Steering Command Mode - The saturation limit for nose-wheel steering angle increases from 10 degrees at transition speed to about 50 degrees at low speed. Gain scheduling in the steering command mode is constructed so that position gain increases with decreasing groundspeed to retain effectiveness of the steering command mode while remaining within the steering-angle saturation limits with realistic position errors.

Gain scheduling in both the rudder and steering mode position loops did not require compensatory scheduling of damping gains.

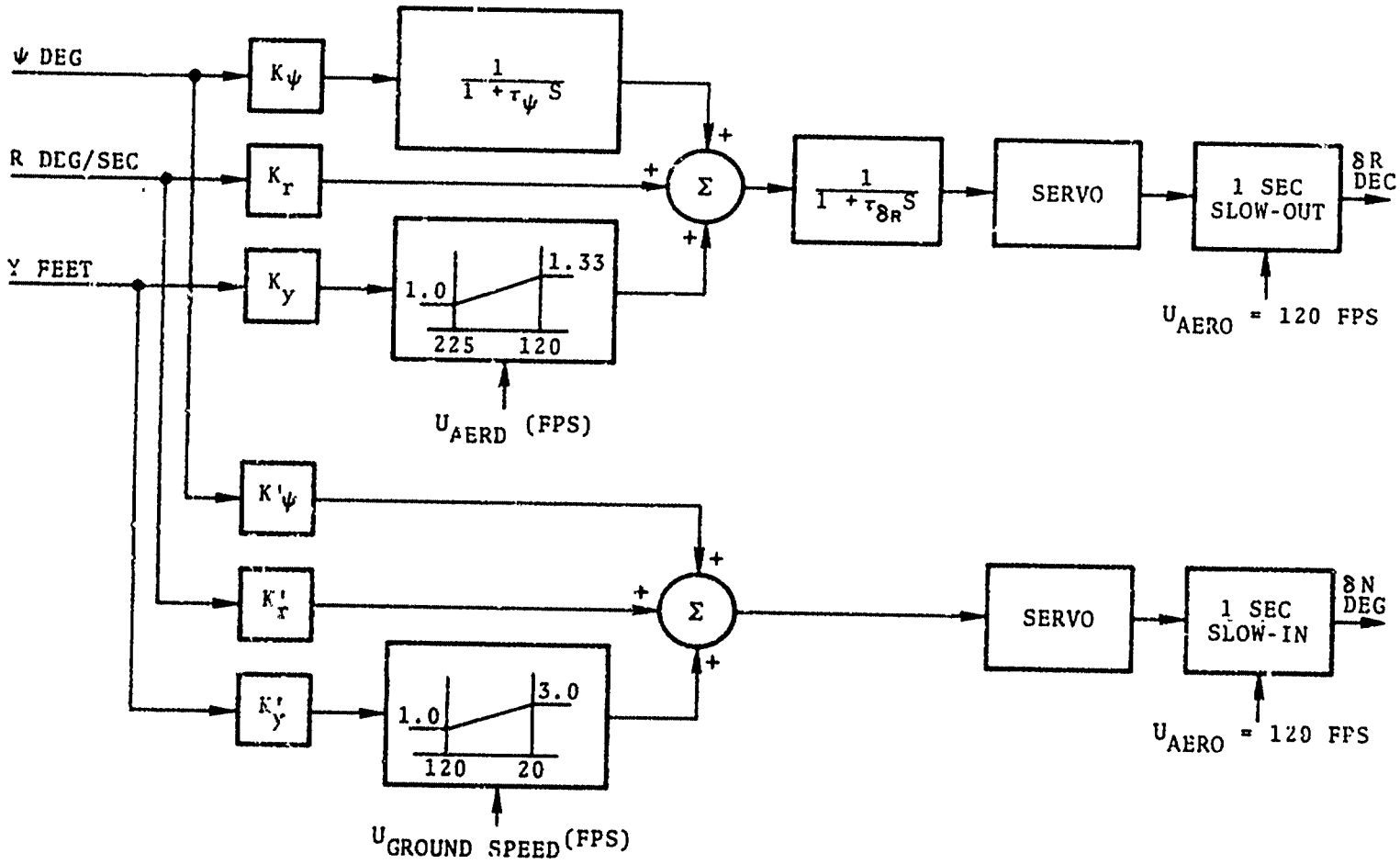

Figure D-5. CV880 Roll-Out Control System Schematic

TABLE D-1. ROLL-OUT CONTROL SYSTEM GAINS AND TIME CONSTANTS

$K_\psi = 7.8$	$\tau_\psi = 0.35$ sec
$K_r = 9.4$	$\tau_{\delta_R} = 0.08$ sec
$K_y = 0.645$	
$K'_\psi = 2.25$	
$K'_r = 2.25$	
$K'_y = 0.43$	

D.8 REFERENCES

1. Smiley, Robert F. and Walter B. Horne, "Mechanical Properties of Pneumatic Tires with Special Reference to Modern Aircraft Tires," NACA TR R-64, 1960.

2. Anon. 'CV880 Maintenance Manual', pp. 6-7 of 32-3-0 Oct. 21/63 and pp. 201-217 of 12-5-0, July 9/62.

3. Hanke, Rodney, C., "Simulation of a Large Jet Transport Aircraft," Vol. 2, NASA CR-1756, March 1971.

4. Anon. "Pavement Grooving and Traction Studies," NASA SP-5073, 1996.